

**For Reference**

---

**NOT TO BE TAKEN FROM THIS ROOM**

EX LIBRIS  
UNIVERSITATIS  
ALBERTAENSIS



**For Reference**

NOT TO BE TAKEN FROM THIS ROOM











THE UNIVERSITY OF ALBERTA

PHYSICAL AND CHEMICAL STUDIES OF THREE  
VARIANTS OF MENO ENCEPHALOMYELITIS VIRUS

by

DOUGLAS G. SCRABA

A THESIS

SUBMITTED TO THE FACULTY OF GRADUATE STUDIES  
IN PARTIAL FULFILMENT OF THE REQUIREMENTS FOR THE DEGREE  
OF DOCTOR OF PHILOSOPHY

DEPARTMENT OF BIOCHEMISTRY

EDMONTON, ALBERTA

SEPTEMBER, 1968



Thesis  
1968 (F)  
62 D.

UNIVERSITY OF ALBERTA  
FACULTY OF GRADUATE STUDIES

The undersigned certify that they have read, and recommend to the Faculty of Graduate Studies for acceptance, a thesis entitled "PHYSICAL AND CHEMICAL STUDIES OF THREE VARIANTS OF MENGO ENCEPHALOMYELITIS VIRUS", submitted by Douglas G. Scraba in partial fulfilment of the requirements for the degree of Doctor of Philosophy.





## ABSTRACT

Three antigenically indistinguishable plaque-type variants of Mengo encephalomyelitis virus, differing markedly in biological properties, have been highly purified and some of their physical and chemical properties studied.

The L-, M-, and S-Mengo virions have identical appearances when examined in the electron microscope, being spherical in shape with diameters of 26.2-27.2 m $\mu$ . They show identical sedimentation rates in sucrose density gradients, and all three have a buoyant density, as determined by isopycnic centrifugation in Cs<sub>2</sub>SO<sub>4</sub>, of 1.331 g/cm<sup>3</sup>. Analytical ultracentrifugation, employing the method of Möller (1964) established that the "molecular" weight of each of the Mengo variants is  $8.3 \pm 0.7 \times 10^6$  daltons. It was not possible to differentiate among the variants on the basis of ultraviolet absorption or optical rotatory dispersion spectra.

Isolated RNA's from L-, M-, and S-Mengo virions were found to be virtually identical in base composition, in "melting" behavior, and in sedimentation and diffusion coefficients. The experimentally determined molecular weight for Mengo viral RNA was shown to be  $1.7 \pm 0.2 \times 10^6$  daltons. Each of the three virions is composed of about 23% RNA and 77% protein by weight.

Isolated proteins from L-, M-, and S-Mengo virions were found to be similar in amino acid composition and in behavior during electrophoresis on polyacrylamide gels. Electrophoresis experiments demonstrated that the Mengo virus capsid is composed of several distinct polypeptides.



Optical rotatory dispersion studies of the three Mengo variants and their corresponding RNA's over the wavelength range 300-210 m $\mu$  revealed no significant differences in the cross-over points, positions of peaks and troughs, and amplitudes among them. This suggests that the manner in which the proteins are arranged to encapsulate the RNA is precise and similar in all three cases. By subtracting the contribution of the RNA from that of the virus, an optical rotatory dispersion curve of the protein in situ was obtained. This curve was characteristic of a polypeptide chain with low  $\alpha$ -helical content.

Differences among the Mengo variants with respect to net surface charge and surface distribution of charged groups were found to exist. These differences made it possible to resolve L-Mengo from either S- or M-Mengo by chromatography on hydroxylapatite. L-Mengo was also distinguished from the other two variants on the basis of its rate of sedimentation in dextran sulfate density gradients and its rate of migration during electrophoresis in agarose gel. Each of the variants exhibited a reproducible and characteristic thermal denaturation (i.e. "melting") curve when heated in 0.1 M potassium phosphate (pH 7.1). Of the three variants, the melting temperature of M-Mengo alone was decreased when the pH of the buffer was lowered to 6.2. There were also striking differences among the three variants in regard to total:infectious particle ratios - with values of approximately 3000:1, 75:1, and 100:1 being obtained for preparations of L-, M-, and S-Mengo, respectively.





## ACKNOWLEDGEMENTS

The author wishes to express his sincere appreciation to his supervisor, Dr. J. S. Colter, for the direction, encouragement, and patience which he extended during the course of this work.

Special thanks are due to Dr. C. M. Kay and his technical associates for their guidance and cooperation in performing the physico-chemical experiments, and to Dr. T. Yamamoto of the Department of Microbiology for taking the electron micrographs.

The author is grateful to Miss P. Hostvedt, Mr. R. Tsujikawa, Mrs. L. Yaremko, Mr. C. Lee, and Mrs. V. Jajczay for competent assistance with the production and purification of viruses.

Drs. J. B. Campbell, L. B. Smillie, B. G. Lane and other members of the Biochemistry Department provided many helpful suggestions and comments.

The work of Mrs. L. Randall in the organization and typing of the final manuscript was appreciated.





## TABLE OF CONTENTS

	<u>Page</u>
Abstract . . . . .	iii
Acknowledgements. . . . .	v
List of Tables . . . . .	ix
List of Illustrations . . . . .	x
List of Abbreviations . . . . .	xiii
INTRODUCTION. . . . .	1
ROUTINE MATERIALS AND METHODS . . . . .	9
CHAPTER 1. The Production and Purification of Viruses	
Introduction . . . . .	14
Procedures and Results	
Growth of viruses in Povitsky bottles . . . . .	14
Growth of viruses in roller bottles . . . . .	16
Partial purification . . . . .	17
Column chromatography . . . . .	17
Efficiency of the purification procedure. . . . .	19
Chromatography on large columns . . . . .	21
Discussion . . . . .	22
CHAPTER 2. Physicochemical Studies of Whole Virions	
Introduction . . . . .	25
Materials and Methods. . . . .	25
Results	
Electron Microscopy - shape and size of the virions . . . . .	26
Equilibrium sedimentation in cesium sulfate density gradients . . . . .	28
Velocity sedimentation in sucrose density gradients . . . . .	29



	<u>Page</u>
Hydrodynamic parameters of the virions	
Sedimentation coefficients. . . . .	30
Diffusion coefficients. . . . .	31
Partial specific volumes. . . . .	31
Molecular (particle) weights. . . . .	33
Discussion . . . . .	33
CHAPTER 3. The RNA and Protein Components of Mengo Virions	
Introduction . . . . .	37
Materials and Methods. . . . .	37
Results and Discussion	
Hydrodynamic properties of the Mengo virus RNA's . . . . .	40
Base compositions of the Mengo virus RNA's. . . . .	41
Amino acid compositions of the viral proteins . . . . .	42
Acrylamide gel electrophoresis of disrupted virions . . . . .	45
Some physical properties of carboxymethylated L-Mengo protein . . . . .	47
Optical properties of the Mengo virions and their RNA's	
Ultraviolet absorption spectra. . . . .	50
Virus extinction coefficients . . . . .	50
Optical rotatory dispersion . . . . .	51
CHAPTER 4. Differences Among L-, M-, and S-Mengo Virions	
Introduction . . . . .	55
Procedures and Results	
The resolution of L-Mengo virus from M- or S-Mengo	
Hydroxylapatite chromatography. . . . .	55
Dextran sulfate density gradient centrifugation. . . . .	56
Agarose gel electrophoresis . . . . .	58



	<u>Page</u>
The absorbance-temperature profiles for the Mengo variants. . . . .	60
The total:infectious particle ratios for the Mengo variants. . . . .	64
Discussion . . . . .	67
SUMMARY AND DISCUSSION. . . . .	70
BIBLIOGRAPHY. . . . .	76
APPENDIX. . . . .	83





# LIST OF TABLES

<u>Table</u>		<u>Facing page</u>
1.1	Virus yields in the presence of "enhancing" agents. . . . .	15
1.2	Partial purification of M-Mengo virus: removal of labelled cellular material . . . .	20
1.3	Final purification of M-Mengo virus by chromatography on hydroxylapatite: removal of labelled cellular material . . . . .	21
2.1	Diameters of Mengo virus particles. . . . .	27
2.2	Hydrodynamic properties of purified variants of Mengo virus. . . . .	30
2.3	Physical properties of Mengo virus. . . . .	34
2.4	Comparison of the physical properties of some picornaviruses . . . . .	35
3.1	Hydrodynamic properties of the Mengo virus ribonucleates . . . . .	40
3.2	Base compositions of ribonucleates isolated from the Mengo virus variants . . . . .	42
3.3	Base composition of ribonucleates isolated from some picornaviruses. . . . .	42
3.4	Amino acid compositions of proteins isolated from the Mengo virus variants. . . .	42
3.5	Amino acid composition of some picornavirus proteins. . . . .	44
3.6	Calculation of the partial specific volume of the protein from S-Mengo virus . . . . .	44
3.7	Optical rotatory dispersion parameters of the Mengo viruses and their RNA components. .	52
4.1	Melting characteristics of the Mengo variants and Mengo RNA. . . . .	61
4.2	Total:infectious particle ratios for the Mengo virus variants. . . . .	65
4.3	Specific infectivities of the Mengo virus variants. . . . .	66
4.4	Burst sizes of the Mengo variants in L-cells .	69



# LIST OF ILLUSTRATIONS

<u>Figure</u>		<u>Facing page</u>
A.1	Plaques produced by the three Mengo virus variants under agar overlay . . . . .	5
1.1	Chromatography of partially purified M-Mengo virus on hydroxylapatite. . . . .	18
1.2	Rechromatography of highly purified M-Mengo virus . . . . .	18
1.3	Chromatography of <sup>3</sup> H-labelled M-Mengo virus . . . . .	19
1.4	Chromatography of partially purified M-Mengo virus: removal of labelled cellular material. . . . .	21
1.5	Ultraviolet absorption spectra of peak fractions from the column chromatography of M-Mengo virus. . . . .	21
1.6	Chromatography of partially purified S-Mengo virus (large column). . . . .	22
1.7	Chromatography of partially purified L-Mengo virus (large column). . . . .	22
2.1	Electron micrograph of L-Mengo virus, shadowed preparation. . . . .	26
2.2	Electron micrograph of L-Mengo virus, negatively stained. . . . .	26
2.3	Equilibrium sedimentation of Mengo virus variants in Cs <sub>2</sub> SO <sub>4</sub> density gradients. . . . .	28
2.4	Sedimentation of Mengo virus variants in pre-formed sucrose density gradients. . . . .	30
2.5	Photographs taken during the sedimentation of M-Mengo virus in the analytical ultracentrifuge . . . . .	30
2.6	Densitometer tracings of photographs of M-Mengo virus taken during a diffusion run in the analytical ultracentrifuge . . . . .	31
2.7	Plot of diffusion data, $1/4y^2[u^{-2}(1-S_w^2t)]$ vs t, for M-Mengo virus . . . . .	31
2.8	Sedimentation of L-, and S-Mengo virions in D <sub>2</sub> O-H <sub>2</sub> O solutions . . . . .	32



<u>Figure</u>		<u>Facing page</u>
3.1	Densitometer tracings of photographs taken during the sedimentation of S-Mengo RNA in the analytical ultracentrifuge. . . . .	40
3.2	The separation of nucleotides obtained by phosphodiesterase hydrolysis of M-Mengo RNA . . . . .	41
3.3	Ultraviolet absorption spectrum of M-Mengo protein . . . . .	43
3.4	Polyacrylamide gel electrophoresis of disrupted Mengo virions . . . . .	47
3.5	Densitometer tracings of the polyacrylamide gels shown in Figure 3.4 for the L-Mengo variant . . . . .	47
3.6	Schlieren photographs taken during the sedimentation of carboxymethylated L-Mengo protein in the analytical ultracentrifuge . . . . .	47
3.7	Densitometer tracing of the stained polyacrylamide gel following electrophoresis of carboxymethylated L-Mengo protein. . . .	49
3.8	Ultraviolet absorption spectra of Mengo virus and viral RNA . . . . .	50
3.9	Optical rotatory dispersion spectra of M-Mengo virus, viral RNA, and viral protein . . . . .	52
4.1	Chromatography of a mixture of partially purified L-Mengo and M-Mengo on hydroxylapatite . . . . .	56
4.2	Chromatography of a mixture of highly purified L-Mengo and S-Mengo on hydroxylapatite . . . . .	56
4.3	Sedimentation of Mengo virus variants in density gradients of dextran sulfate. . . .	57
4.4	Densitometer tracings of stained agarose gels following electrophoresis of L-, M-, and S-Mengo viruses . . . . .	59
4.5	Photographs taken during the sedimentation of L-Mengo RNA in the analytical ultracentrifuge . . . . .	61
4.6	Melting curves for the Mengo virus variants. . . . .	61







<u>Figure</u>		<u>Facing page</u>
4.7	Melting curve for Mengo RNA . . . . .	61
4.8	Comparative melting curves for M-Mengo virus and viral RNA . . . . .	62
4.9	The effect of pH on the melting curve for M-Mengo virus . . . . .	64
4.10	Relationship between absorbance and plaque-forming units for highly purified preparations of L-, M-, and S-Mengo viruses . . . . .	65



## LIST OF ABBREVIATIONS

pfu	plaque-forming unit(s)
LD <sub>50</sub>	50% of lethal dose
PTA	phosphotungstic acid (potassium salt)
RNA	ribonucleate
EDTA	ethylene diamine tetraacetic acid (sodium salt)
TRIS	tris(hydroxymethyl)-amino methane
$S_{20,w}^0$	intrinsic sedimentation coefficient
$D_{20,w}^0$	intrinsic diffusion coefficient
$\bar{v}$	partial specific volume
M	molecular (particle) weight
ORD	optical rotatory dispersion
T <sub>m</sub>	temperature at the midpoint of the hyperchromic change

All temperatures are given in Centigrade  
degrees.



## INTRODUCTION

Mengo encephalomyelitis virus was first isolated in 1946 from the cerebrospinal fluid of a paralyzed captive rhesus monkey. The virus was so named because it was isolated in the Mengo district of Uganda, and because it produced lesions in the central nervous system tissues of infected animals and encephalitic symptoms in man (Dick et al., 1948 a,b). Passage of the virus in mouse brain rendered it highly lethal to these rodents whether administered intracerebrally, intraperitoneally, intranasally, or subcutaneously (Dick, 1948).

Subsequent serological tests (Dick, 1949; Warren et al., 1949) established that Mengo virus was very closely related to the viruses designated Columbia-SK (Jungeblut and Sanders, 1940), MM (Jungeblut and Dalldorf, 1943), and EMC (Helwig and Schmidt, 1945). This "Columbia-SK group" of viruses (Jungeblut, 1958) is immunologically distinct from the mouse-adapted strains of poliomyelitis virus and from Thieler's mouse encephalitis viruses.

At present, the viruses Columbia-SK, MM, EMC, Mengo, and ME (Franklin et al., 1959; Hausen and Schäfer, 1962) are collectively known as the "encephalomyocarditis viruses" (Warren, 1965; Andrewes and Pereira, 1967). These agents are highly infectious for rodents, and are generally propagated in mouse or rat tissues in the laboratory. Recent studies (Ellem and Colter, 1961; Craighead, 1965) have shown that, although closely related, these viruses are not antigenically identical.





In addition to being serologically related, members of the encephalomyocarditis virus group have many physical, chemical and biological characteristics in common. A brief review of some of these characteristics follows.

Although discovered in widely separated areas, and isolated from several different species, members of the encephalomyocarditis group are now regarded as strains of a single RNA-containing virus, classified within the picornavirus category (Andrewes and Pereira, 1967). This virus is spherical in shape, 24-27 m $\mu$  in diameter (Faulkner et al., 1961; Dales and Franklin, 1962; Hausen and Schäfer, 1962), and composed of RNA and protein. Electron micrographs have revealed that the protein capsid of the virion is composed of discrete subunits, probably arranged in icosahedral symmetry (see, e.g. Caspar, 1965). Because of their small size, the resolution of subunits has been difficult. However, it is probable that the arrangement is similar to that found for the structurally similar particles of poliovirus (Finch and Klug, 1959) and turnip yellow mosaic virus (Klug et al., 1966; Finch and Klug, 1966) - namely, that there are 180 chemical subunits assembled into 20 hexamers and 12 pentamers, making 32 morphological subunits. There is some controversy as to the particle weight of the encephalomyocarditis virion, Faulkner et al. (1961) having reported a value of  $10 \times 10^6$  daltons for EMC virus, whereas Hausen and Schäfer (1962) reported  $5.7 \times 10^6$  daltons for ME virus. Perhaps the true value lies somewhere in between.





That RNA is the genetic material in these viruses has been demonstrated by the isolation of infectious RNA from Mengo virus (Colter et al., 1957), from EMC virus (Huppert and Sanders, 1958), and from ME virus (Franklin et al., 1959). The infectious RNA obtained by phenol extraction is single-stranded (Hausen and Schäfer, 1962), and its sedimentation coefficient is in the range 28-37 svedbergs (Hausen and Schäfer, 1962; Burness et al., 1963). Most investigators have placed the percentage composition of the virion at 30% RNA and 70% protein. The possibility of some carbohydrate material being an integral part of the virion has been suggested by Rueckert (1965); however, there is no real proof that this is the case. Ether and chloroform stability of the virion argues against the presence of essential lipid. The viral protein itself appears to consist of several different polypeptides (Rueckert, 1965; Rueckert and Duesberg, 1966; Burness and Walter, 1967). These polypeptides, separated by polyacrylamide gel electrophoresis, have similar amino acid compositions and molecular weights (Burness and Walter, 1967), but are unlinked by disulfide bridges in the virion (Rueckert, 1965). Their molecular weights are of the order of 30,000 daltons.

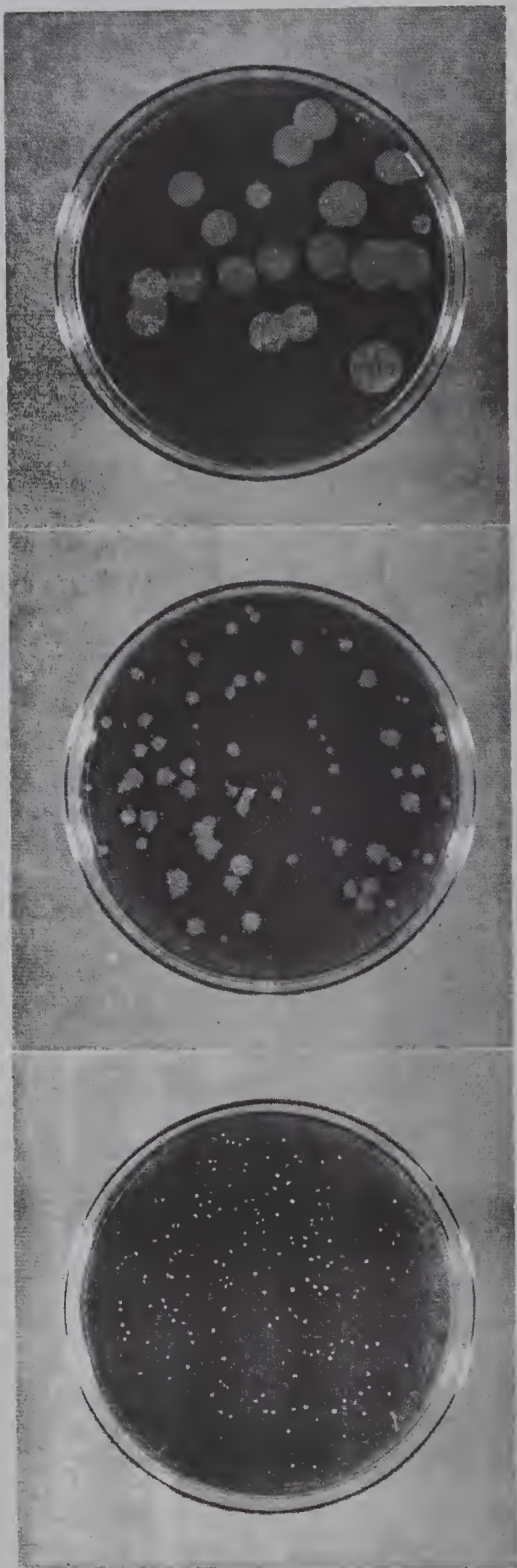
Encephalomyocarditis virus particles probably attach to cells by complementary interaction with specific receptors on the cell surface (Colter et al., 1964b). Attachment triggers a pinocytosis process, and the whole virion is taken into the cell. The genetic material, the viral RNA, is released (uncoated) intracellularly (see, e.g. Joklik, 1965). Cytopathologically, the first observed changes are seen in



the cell nucleus (Hinz et al., 1962) and involve condensation and margination of the chromatin and nuclear shrinkage. However, viral RNA and protein appear to be produced near the cell nucleus, rather than in it, and virions are assembled in cytoplasmic inclusions (Franklin, 1962; Dales and Franklin, 1962). A virus-induced RNA polymerase (Baltimore and Franklin, 1963; Horton et al., 1966; Roberts et al., 1966) converts the single-stranded viral genome to a double-stranded template form (Montagnier and Sanders, 1963). The synthesis of progeny viral RNA from this template is resistant to actinomycin-D (Homma and Graham, 1963); and the template itself seems to be stable because there is no transfer of parental viral RNA to progeny virus particles (Goodheart, 1967). A non-capsid viral protein is responsible for the initiation of cell disintegration, presumably by causing a leakage of hydrolases from the cell's lysosomes (Amako and Dales, 1967; Gauntt and Lockhart, 1968).

All strains of encephalomyocarditis virus are infectious for a variety of rodents, and it is likely that these animals serve as reservoirs for the virus in nature (Warren, 1965). Monkeys and swine (Murnane et al., 1960) can be fatally infected. In experimentally infected animals, lesions are found in the tissues of the central nervous system and in cardiac and striated muscles, although a strain has been isolated which produces necrosis of the pancreas, parotid, and lacrimal glands (Craighead, 1966a,b). Infection in man (Smadel and Warren, 1947; Dick et al., 1948b; Gajdusek, 1955; Casals, 1963) results in a febrile illness with central





S-MENGO

M-MENGO

L-MENGO

Figure A.1. Plaques produced by the three variants of Mengo encephalomyelitis virus in monolayers of L-929 mouse fibroblasts under nutrient agar overlay. The plaques were visualized by staining with neutral red after 72 hours' incubation at 37° in an atmosphere of 5% CO<sub>2</sub> in air.

nervous system involvement, but not myocarditis. Although Mengo virus has been isolated from mosquitos (Dick et al., 1948a), insects do not appear to be important as a vector for these viruses. It has been suggested that rodents become infected by nasal absorption (Vizoso and Hay, 1964).

Three variants of Mengo virus were isolated by Ellem and Colter (1961). On the basis of the types of plaques produced in monolayers of the L-929 strain of mouse fibroblasts under agar overlay, these variants were designated L-Mengo (for large, "fuzzy" plaques), M-Mengo (for sharply defined, medium-sized plaques), and S-Mengo (for minute plaques). Figure A.1 (from Campbell, 1965) shows the characteristic plaque morphologies. The basis for the differences in plaque morphology was sought out, and it was discovered that the Mengo variants differ in their sensitivities to an anionic component present in the Noble agar used to overlay infected cell monolayers (Colter et al., 1964b). The agar factor was shown to combine directly with the virus particle, thereby blocking virus-cell interaction. The S-Mengo variant is the most, and the L-Mengo variant the least sensitive to inhibition by this factor. The inhibitory effect may be reversed by adding protamine, which complexes with the agar factor. At a protamine concentration of 400-500  $\mu\text{g/ml}$  in overlay, the plaques produced by each of the three variants are of approximately the same diameter and appearance.

Subsequently, experiments were conducted to define a broad spectrum of the biological characteristics of the L-,





M-, and S-Mengo variants. The results of some of these experiments are summarized below.

Single cycle growth curves of the variants in suspended cell cultures are virtually identical for L- and S-Mengo; however, the length of the eclipse phase for M-Mengo is only 4 to 4.5 hours as compared to 5.5 to 6 hours for the other two variants. This suggests that intracellular uncoating of the viral genome may be more rapid for M- than for L- and S-Mengo virions (Campbell, 1965). The variants were also found to differ in their rates of attachment to stationary L-929 cells, M- and S-Mengo reaching maximum attachment (i.e. attaining attachment-elution equilibrium) after 10-15 min incubation at 37°, whereas L-Mengo did not reach maximum attachment before 60 min incubation had elapsed. In suspension cultures of L-929 cells, S-Mengo attaches most rapidly and L-Mengo least rapidly (Colter et al., 1964a).

An examination of the effect of pH on infectivity also revealed differences. An increase of pH from 6.8 to 7.8 was found to increase the infectivities of the L-, M-, and S-Mengo variants for monolayer cultures by factors of 2, 3000 and 10, respectively (Colter et al., 1964a). The loss of infectivity produced by lowering the pH of the attachment medium probably involves (i) alteration of the charged nature and/or conformation of attachment groups on the surfaces of the virions as the pH is lowered from 7.8 to 7.0; and (ii) instability of the M-Mengo virion at pH's less than 7.0. An hypothesis compatible with the available data is that at pH's less than 7.0,



the M-Mengo capsid "loosens", allowing the viral genome to be degraded by ribonucleases present in crude lysates. Infectious RNA cannot be extracted from M-Mengo that has been inactivated by incubation at pH's of 6.0-6.5 (Campbell, 1965), - and electron micrographs of M-Mengo virions incubated at low pH and stained with PTA revealed numerous empty capsids (unpublished).

Perhaps the most striking of the biological differences found for the Mengo virus variants is in their relative virulence for laboratory mice. The LD<sub>50</sub>'s for 14-16 g mice inoculated intraperitoneally were found to be 1 pfu for L-Mengo, 10,000-50,000 pfu for M-Mengo, and at least 10,000,000 pfu for S-Mengo (Colter et al., 1965). The reasons for the high virulence of L-Mengo virus have been difficult to ascertain. L-Mengo was found to have a lower affinity for mouse tissues, including brain and heart, than did either S- or M-Mengo (Campbell and Colter, 1967a). Furthermore, L-Mengo neither induces less interferon in mice than the other variants, nor is it less susceptible than S- or M-Mengo to the inhibitory action of exogenous interferon (Campbell and Colter, 1967b). The L-Mengo variant does, however, produce a marked viremia in mice, which reaches a peak some 24 hours after intraperitoneal injection. Not more than trace amounts of virus were ever recovered from the circulation of mice injected with up to 100,000,000 pfu of either M- or S-Mengo. The hypothesis has been advanced that the in vivo adsorption of L-Mengo may be inhibited by components of the circulation (such as heparin), and that this variant can therefore more easily reach the central





nervous system and cause death (Campbell and Colter, 1967a).

With this work as background, an attempt to relate the biological characteristics of the Mengo variants to the physical and chemical properties of the virus particles was begun. To date, relatively little progress in correlation has been made; however, a partial catalogue of the properties of the Mengo variant virions has been compiled. This thesis summarizes data concerning the production and purification of L-, M- and S-Mengo virions, the physicochemical properties of these virions and their RNA and protein components, and some differences which exist among them.





## ROUTINE MATERIALS AND METHODS

### Mengo encephalomyelitis virus

The virus was obtained originally from Dr. K. Smith-burn of the Division of Medicine and Health of the Rockefeller Foundation. It had been maintained for several years by intracerebral passage in 10-12 g Swiss mice. The pools from which the three variants were isolated were prepared by propagating the virus in Ehrlich ascites carcinoma cells in vivo (Ellem and Colter, 1961).

### Tissue Culture: Cells and Media

Cells. Earle's L-929 strain of mouse fibroblasts (Sanford et al., 1948) was used for the propagation and assay of L-, M-, and S-Mengo viruses. These cells were obtained from the American Type Culture Collection, Rockville, Md.

Growth medium. A medium containing Earle's salts (Earle, 1943) and Eagle's nutrients (Eagle, 1959) was obtained in powder form from the Grand Island Biological Co., Grand Island, N. Y. ("Basal medium, Eagle, Diploid"). The powder was dissolved in deionized water and sterilized by filtration. "Basal medium" was then supplemented by addition of the following materials at the final concentrations indicated:

1. Sodium bicarbonate, 0.26%.
2. Horse serum (Baltimore Biological Laboratory, Baltimore, Md.), 10%.
3. Aureomycin (Lederle Laboratories, Pearl River, N. Y.), 50 µg/ml.; pencillin G (Ayerst Laboratories, Montreal, Que.), 100 I.U./ml.; and streptomycin sulfate (Glaxo-Allenburys



Ltd., Weston, Ont.), 100 µg/ml.

Spinner medium. Identical to growth medium, except that the basic powdered medium used lacked calcium - "minimum essential medium (Eagle) with spinner salts" (Grand Island Biological Co.).

#### Maintenance of cells

L-cells in growth medium were added to 1-liter Blake bottles (Kimble Products, Owens-Illinois Co., Toledo, Ohio) and incubated at 37° for 3 to 4 days. The cell monolayers which had formed were detached by replacing the growth medium with 0.25% trypsin in Hanks' balanced salt solution (Hanks and Wallace, 1949) and incubating at room temperature for 10 min. Cells were then collected by centrifugation, resuspended in spinner medium, and transferred to 1-liter spinner flasks (Bellco Biological Glassware, Vineland, N. J.) at a concentration of 200,000 cells/ml. The cells were kept in suspension by means of a magnetic stirring device and incubated at 37° to allow further growth to take place.

#### Titration of viruses

Preparation of cell monolayers. Cells were collected from spinner culture by centrifugation and resuspended in growth medium to give a suspension containing  $2.5 \times 10^6$  cells/6 mls. Six ml aliquots of this suspension were introduced into 60 mm plastic petri dishes (Falcon Plastics, Los Angeles, Calif.). After incubation at 37° for 24 hours in a humidified atmosphere of 5% CO<sub>2</sub> in air, confluent monolayers containing about  $6 \times 10^6$  cells were formed.





Virus diluent. The phosphate-buffered saline solution (PBS) of Dulbecco and Vogt (1954) was supplemented by the addition of bovine plasma albumin, fraction 5 (Pentex Inc., Kankakee, Ill.) at a final concentration of 0.2%. Also added were phenol red, penicillin G, and streptomycin sulfate to final concentrations of 0.02%, 100 I.U./ml, and 100 µg/ml., respectively.

Overlay diluent. This solution contained three times the normal concentration of Hanks' salts, six times the normal concentration of Eagle's nutrients, 0.75% sodium bicarbonate, 0.02% phenol red, and 30% pre-heated (56° for 45 min) calf serum.

Regular agar overlay. Two volumes of 1.5% Noble agar (Difco Laboratories, Detroit, Mich.) were mixed at 45° with one volume of overlay diluent.

Special agar overlay. In order to increase the plaque size of S-Mengo plaques for easier counting, protamine sulfate (Calbiochem, Los Angeles, Calif.) was added to the regular agar overlay to give a final concentration of 0.025% (Colter et al., 1964b).

Plaque assay. Virus samples were diluted to appropriate concentrations in virus diluent. Growth medium was removed from the preformed L-cell monolayer and replaced with 0.1 ml of diluted virus. After a one-hour incubation period at 37° to allow for attachment of the virus particles to susceptible cells (Colter et al., 1964a), 4.5 ml of melted agar overlay were applied. Then, after an additional 48-hour incubation at 37° in an atmosphere of 5% CO<sub>2</sub> in humidified air, the dish was overlaid with 3 ml of agar overlay which





contained the vital stain, neutral red (Fisher Scientific Co., Fair Lawn, N. J.) at a concentration of 1:10,000 (w/v). Virus plaques could be visualized within a few hours, and the plaque counts reached maximum levels after an additional 24-hour incubation period.

#### Preparation of stock virus pools

Material from 2 or 3 plaques was removed with a Pasteur pipet and added to 2 ml of virus diluent. The virus suspension was then added to a pre-formed cell monolayer - approximately  $18 \times 10^6$  cells - in a 250 ml milk dilution bottle (Kimble Products). After 1 hour incubation at  $37^{\circ}$ , 10 ml of growth medium were added and incubation was continued until the cell monolayer was destroyed (about 48 hours). Virus was released from unlysed cells by freezing and thawing and the cell debris was removed by low-speed centrifugation. The supernatant fluid containing the virus was assayed for sterility and for the concentration of plaque-forming units (pfu), and stored at  $-60^{\circ}$ .

#### Sterilization Procedures

The basic media, neutral red solutions, and balanced salt solutions were sterilized by filtration through a Seitz filter, the first portion of each filtrate being discarded. Agar suspensions were sterilized by autoclaving at  $125^{\circ}$  for 15 min. All solutions were tested for sterility by incubating samples in sterile thioglycollate medium (Baltimore Biological Laboratory, Baltimore, Md.) and sterile brain heart infusion medium (Difco Laboratories, Detroit, Mich.).

Glassware which had been in contact with virus was soaked overnight in Wescodyne (West Chemical Products,



Montreal, Que.), rinsed, washed thoroughly with Wedac detergent (West Chemical Products), rinsed again, and sterilized by autoclaving at  $375^{\circ}$  for 2.5 hours. Pipets were immersed in Wescodyne for 24 hours, rinsed, immersed in concentrated  $H_2SO_4$  for an additional 24 hours, rinsed again, and sterilized by heating in an oven at  $375^{\circ}$  for 2-3 hours. The final rinsing of all glassware was done with deionized water.



## CHAPTER 1

### The Production and Purification of Viruses

#### Introduction

In order for physical and chemical studies of any virus to be a feasible proposition, three obvious prerequisites must be satisfied: (i) milligram quantities of the virus must be produced; (ii) the virions must be separated from cellular material with a high degree of efficiency; and (iii) the purification procedure must give intact virions in good yield. This chapter summarizes the methods used and the results obtained in attempts to produce large quantities of highly purified Mengo virus.

#### Procedures and Results

##### Growth of viruses in Povitsky bottles

Twenty ml of a virus suspension (in virus diluent) were added to a confluent monolayer of L-929 cells in a 2-liter Povitsky bottle (approximately  $50 \times 10^6$  cells). The multiplicity of infection was 5 to 10 pfu per cell. After a 1-hour incubation at  $37^{\circ}$ , 100 ml of growth medium (1% horse serum) were introduced. Incubation was continued for 24 hours, at which time the cell mass could be dislodged from the glass by gentle shaking. Lysates from 8 to 12 bottles were pooled and centrifuged at 850 g for 10 min. The pellet was resuspended in a few ml of the supernatant fluid, frozen and thawed several times to release attached virus, and centrifuged again. The two supernatants were combined, and



Table 1.1

Virus Yields in the Presence of "Enhancing" Agents

Variant	pfu/Povitsky bottle		
	Control	+ Semicarbazide	+Aminonucleoside
L	$3.0 \times 10^9$	$4.3 \times 10^9$	$2.0 \times 10^9$
M	$55.3 \times 10^9$	$57.8 \times 10^9$	$52.8 \times 10^9$
S	$55.5 \times 10^9$	$54.8 \times 10^9$	$37.6 \times 10^9$

cooled in an ice bath. Methanol was added to a final concentration of 35% (v/v), and the solution was allowed to stand for at least 4 hours at 4°. The precipitated material was collected by sedimentation at 8000 g and resuspended in 16 ml of TRIS-HCl buffer (pH 8.0). Virus thus partially freed of cellular material was frozen and stored at -20° prior to final purification.

Attempts were made to increase the yield of virus from Povitsky cultures by adding various drugs during the viral growth period. We were encouraged to try this approach by the reports of Farnham (1965) that the aminonucleoside of puromycin enhanced the production of EMC virus in L-cells, and of Grossberg et al. (1966) that semicarbazide enhanced the production of poliovirus in KB cells.

Aminonucleoside (6-dimethylamino-9-[3'-amino-3'-deoxy- $\beta$ -D-ribofuranosyl] purine; Nutritional Biochemicals Corp., Cleveland, Ohio) was added to cell monolayers at a concentration of  $1 \times 10^{-4}$  M in the growth medium during the viral growth period. Virus from test and control bottles was collected as outlined above, and samples from the TRIS-HCl suspensions were taken for titration. The same procedure was followed using semicarbazide ( $\text{NH}_2\text{-NH-CO-NH}_2$ ; Fisher Scientific Co., Fair Lawn, N. J.) at a concentration of  $2 \times 10^{-2}$  M. The results of these experiments are presented in Table 1.1. Clearly, in the system employed here, these drugs had no enhancing effect on virus yield.



### Growth of viruses in roller bottles

Since increasing the virus yield per cell did not appear to be readily accomplished, it was decided to increase the number of virus-producing cells per unit volume of culture medium by using roller flasks. Confluent L-cell monolayers were prepared in large cylindrical bottles (growth area =  $1410 \text{ cm}^2$ ; Bellco Biological Glassware, Vineland, N. J.) in the following manner. The bottles were first coated with fetal calf serum (Baltimore Biological Laboratory, Baltimore, Md.) to facilitate attachment of cells, after which 150 ml of growth medium (5% horse serum) were added. L-929 cells, harvested from suspension culture, were added to give a concentration of about  $10^6$  cells/ml and the bottles were rotated on a Bellco roller apparatus at 0.2 rpm. After 3 hours, the speed was increased to 1 rpm. The cells grew to confluency (approximately  $250 \times 10^6$  cells/bottle) after incubation at  $37^\circ$  for 24 to 48 hours.

The growth medium was removed from the cell monolayers and replaced with 50 ml of a suspension of Mengo virus at a concentration of 2 to  $4 \times 10^7$  pfu/ml. After rotation at 0.2 rpm for 2 hours to permit attachment of the virus, 100 ml of growth medium (1% horse serum) were added and the bottles were rotated at 1 rpm for 24 hours ( $37^\circ$ ). At the end of this time, the cell mass could be dislodged from the glass by shaking (except in the case of S-Mengo-infected cells, which sometimes required an additional 8 to 24 hours of incubation). The cell lysates were treated as described above to concentrate the virus and partially free the latter from cellular debris.





The yield of virus per roller bottle exceeded that per Povitsky bottle by a factor of approximately 5.

#### Partial purification

Suspensions of methanol-insoluble material from Povitsky or roller bottles were subjected to sonic oscillation for 60 sec at maximum output in a Raytheon Model DF 101 oscillator (Raytheon Company, Waltham, Mass.) in order to disrupt large aggregates. A solution of  $\alpha$ -chymotrypsin (3 times crystallized; Worthington Biochemicals, Freehold, N. J.) was added to give a final enzyme concentration of 0.8 mg/ml, and the mixture was incubated at 37° for 45 min. An equal volume of 0.2 M sodium pyrophosphate (pH 8.0) was then added, followed by ribonuclease (crystalline, salt-free; Worthington Biochemicals) to give a final concentration of 0.08 mg/ml, and incubation was continued for 30 min. The mixture was then chilled and clarified by centrifugation at 8000 g for 30 min. Virus was recovered from the supernatant by centrifugation at 100,000 g for 60 min, and was resuspended in a few ml of potassium phosphate buffer (pH 7.1 for the S- and M-variants, pH 6.2 for the L-variant). The partially purified virus was not stored in this state because degradation occurred, even at -60°.

#### Column chromatography

Final purification of the virus involved chromatography of the enzyme-treated suspension on a column of hydroxylapatite, equilibrated and run at 4°. The adsorbent was prepared by the method of Levin (1962), except that one-fourth or one-third the recommended quantities were used. A column of dimensions 1.6 x 22 cm (diameter x length) was packed under pressure and washed with about 300 ml of 0.13 M potassium

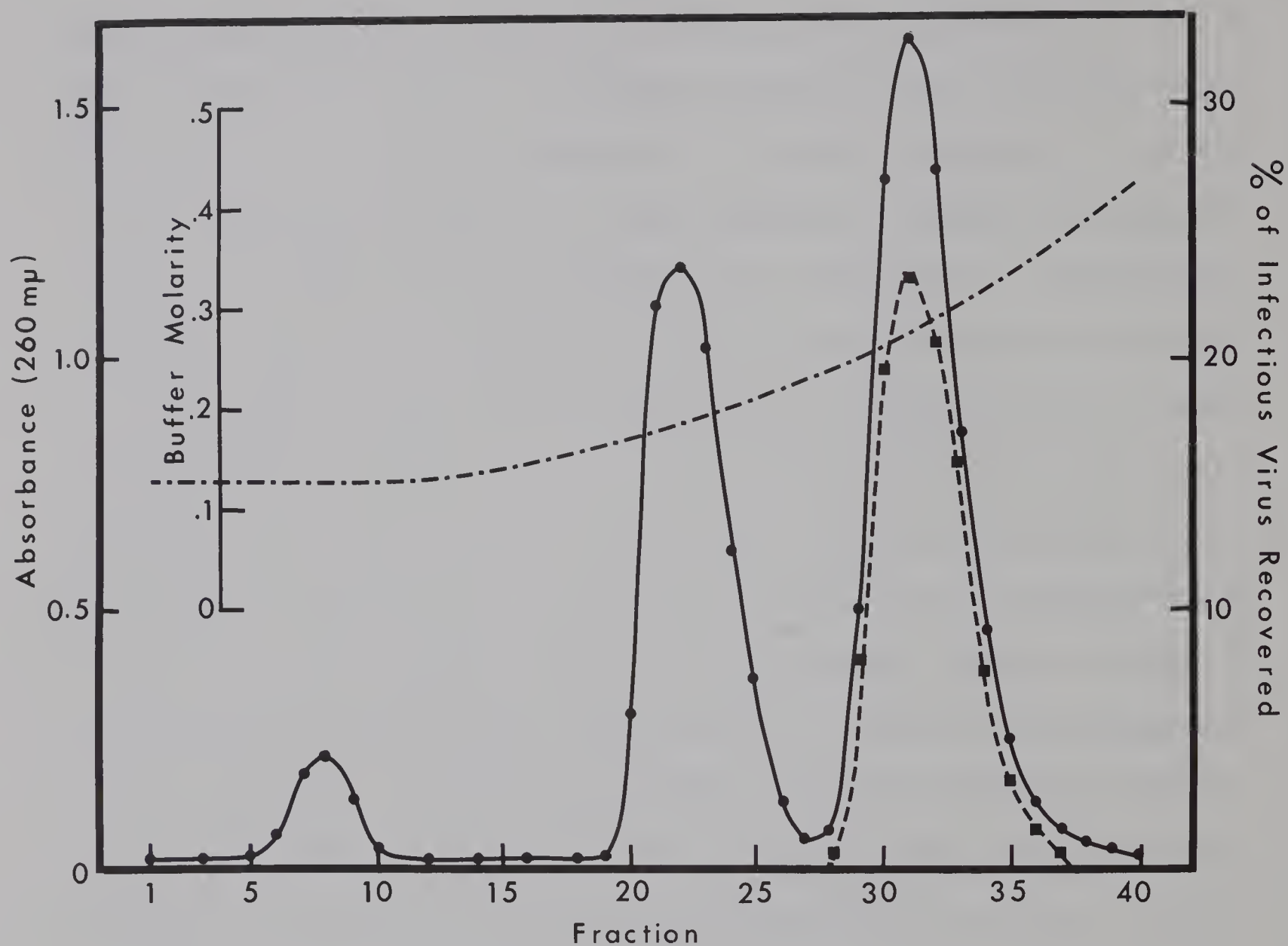


Figure 1.1 Chromatography of partially purified M-Mengo virus on hydroxylapatite at pH 7.1. The absorbance profile is represented by the circles, and the eluted virus by the squares. The total infectious virus recovered was  $2 \times 10^{12}$  pfu (67% of that added).

Absorbances were determined using a Beckman DU spectrophotometer. Conductivities of each fraction were measured on a Conductivity meter type CDM-2d (Radiometer, Copenhagen, Denmark), and these values were converted to phosphate molarities using a standard curve. Infectious virus was determined by plaque assay.



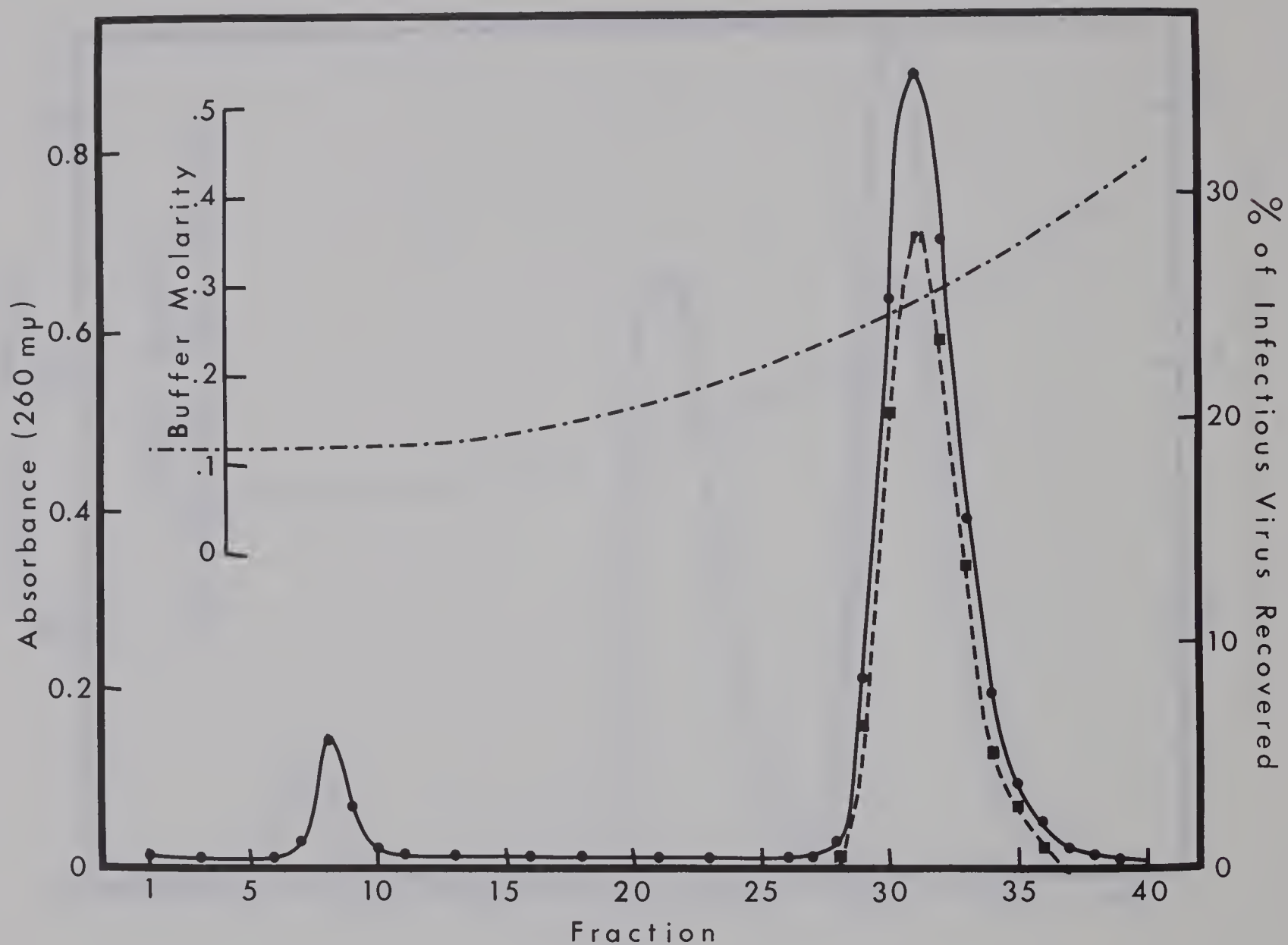


Figure 1.2. Re-chromatography of highly purified M-Mengo virus on hydroxylapatite at pH 7.1. The total infectious virus recovered was  $5 \times 10^{11}$  pfu (90% of that added).

phosphate buffer (pH 7.1 for chromatography of S- or M-Mengo, pH 6.2 for chromatography of L-Mengo). The virus suspension (in 0.02 M potassium phosphate) was added to the packed, equilibrated column, and allowed to soak in under gravity. Two small volumes of 0.13 M buffer were added to wash in the virus sample. Material was eluted from the column by means of a concave phosphate buffer gradient, produced by using 3 chambers in a Varigrad mixing device (Buchler Instruments Inc., Fort Lee, N. J.). The starting phosphate concentration was 0.13 M, and the limiting concentration was 0.8 M. A flow rate of 0.5 ml/min was maintained by a peristaltic pump, and 40 5-ml fractions were collected. The elution profile of one such column purification is shown in Figure 1.1.

To check the efficiency of the hydroxylapatite chromatography, a portion of the virus from the column that provided the data shown in Figure 1.1 was collected by high-speed centrifugation, the column itself was recycled by flushing with 0.8 M phosphate and equilibrated with 0.13 M phosphate, and the virus was rechromatographed. The elution pattern is shown in Figure 1.2. Comparing this pattern with the first one suggests that the initial absorbance peak contained some degraded virus, while the second peak was composed of cellular material. No second peak was discernible when column-purified virus was rechromatographed.

Additional evidence that the first two absorbance peaks consisted almost exclusively of cellular contaminants was obtained from chromatography of radioactive virus. <sup>3</sup>H-M-Mengo virus was prepared for experiments designed to study



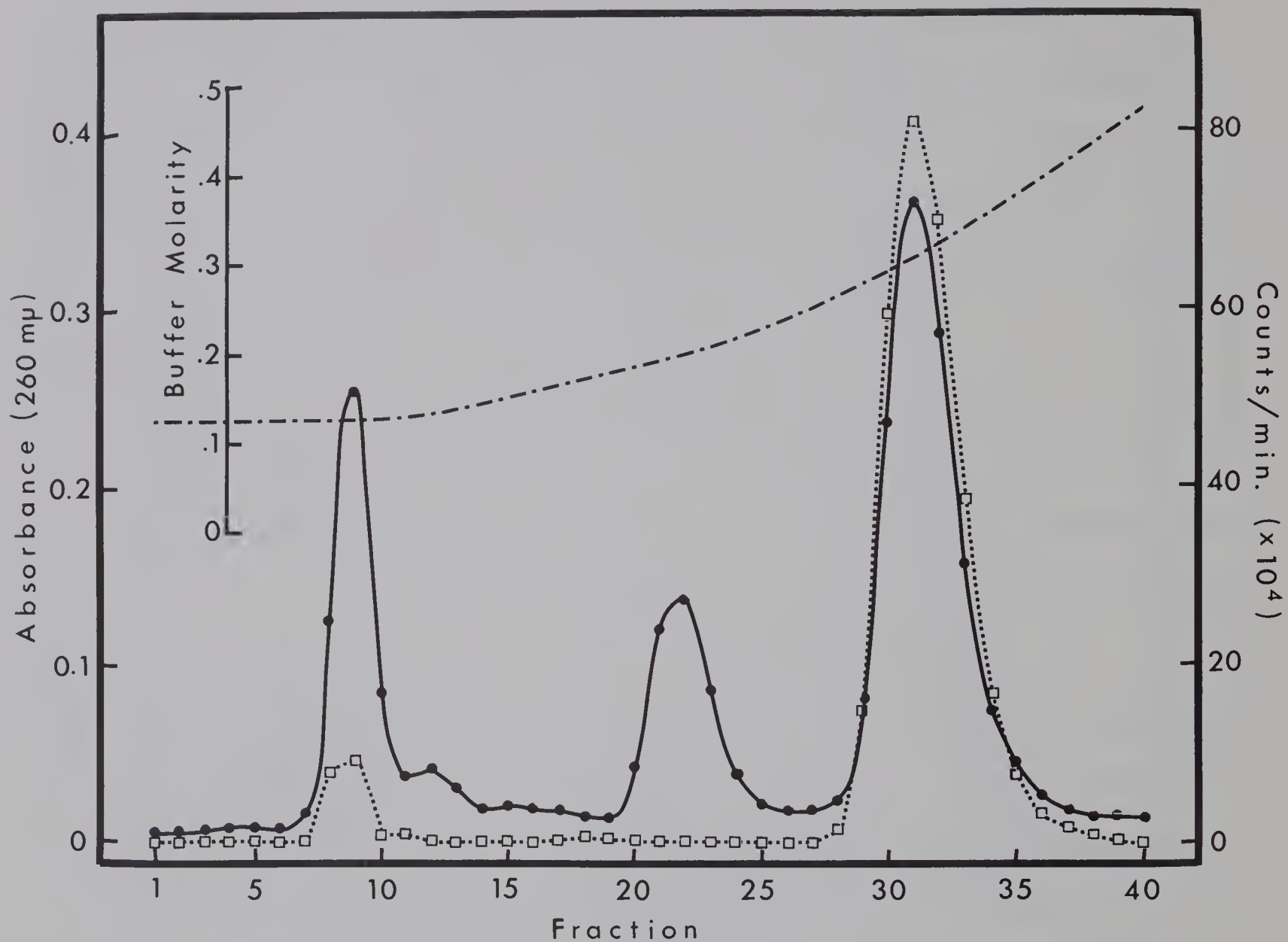


Figure 1.3. Chromatography of partially purified <sup>3</sup>H-M-Mengo virus on hydroxylapatite (pH 7.1). The absorbance profile is represented by the filled circles, and the radioactivity profile by the open squares.

the infectivity of the viral RNA (Tovell and Colter, 1968). Since actinomycin-D was present during the growth cycle, the added  $^3\text{H}$ -uridine was incorporated into viral RNA only.

Labelled virus was partially purified and chromatographed on hydroxylapatite in the usual manner. All column fractions were assayed for radioactivity, using a Beckman Model 100 liquid scintillation counter (Beckman Instruments, Inc., Palo Alto, Calif.). The results are shown in Figure 1.3. Some virus (probably degraded) is present in the initial absorbance peak, but cellular material is also present - as evidenced by the ratio of absorbance to radioactivity. The second absorbance peak appears to contain no virus, and the third peak only virus.

#### Efficiency of the purification procedure

A virus purification procedure designed to yield virions for physical and chemical studies must remove essentially all of the cellular material present in a crude lysate. Our procedure was tested in this regard as described below.

A modified growth medium, which contained no calcium chloride, one-tenth the normal amount of sodium phosphate, and in which lactalbumin hydrolysate (0.009 mg/ml) replaced Eagle's amino acids, was prepared. To 495 ml of this medium were added 2.0 millicuries (2 ml) of sodium phosphate- $^{32}\text{P}$  and 0.3 millicuries (3 ml) of algal protein- $^{14}\text{C}$  hydrolysate (New England Nuclear Corp., Boston, Mass.). The radioactive medium was poured into a spinner flask and  $1 \times 10^8$  mouse L-cells were added. After incubation for 65 hours at  $37^\circ$ , the number of cells had increased to  $2 \times 10^8$ . These  $^{32}\text{P}$ ,  $^{14}\text{C}$ -

Table 1.2

Partial Purification of M-Mengo Virus: Removal of Labelled Cellular Material

Stage of Purification	Volume (ml)	Total $^{14}\text{C}$ cpm	Total $^{32}\text{P}$ cpm	Total infectious virus (pfu)
Crude lysate	500	$160 \times 10^6$ (100%)	$75 \times 10^6$ (100%)	$6.9 \times 10^{12}$ (100%)
After methanol precipitation	96	$89 \times 10^6$ (55.6%)	$27 \times 10^6$ (36.0%)	$6.9 \times 10^{12}$ (100%)
After enzymic digestion and differential centrifugation	7.5	$3.11 \times 10^6$ (1.9%)	$2.3 \times 10^6$ (3.0%)	$6.7 \times 10^{12}$ (97.1%)

\*The figures in parentheses in this table and in Table 1.3 show the percentage recovery of radioactivity as  $^{14}\text{C}$  or  $^{32}\text{P}$ ) and of infectious virus at each stage of the purification procedure. They are based on the level of radioactivity in and infectious virus content of the crude lysate which are taken as 100%.

labelled cells were collected by centrifugation, washed free of radioactive medium, resuspended in 25 ml of 0.02 M potassium phosphate (pH 7.1), and were artificially lysed by repeated cycles of freeze-thawing and homogenization. The lysate was added to non-radioactive medium to give a final volume of 500 ml, and 0.2 ml samples were removed for radioisotope counting.<sup>1</sup> The solution was then chilled and methanol was added to a final concentration of 35% (v/v). After incubation for 18 hours at 4<sup>o</sup>, the methanol-insoluble material was collected by centrifugation at 8000 g for 30 min and added to a normal methanol-precipitated pool of M-Mengo virus. Samples were removed for radioisotope counting<sup>1</sup> and virus titration.

Partial virus purification (sonication, enzymic digestion, and differential centrifugation) was carried out as described previously. The final virus pellets were resuspended in 0.02 M potassium phosphate (pH 7.1) and samples were removed for radioisotope counting<sup>1</sup> and virus titration. The results summarized in Table 1.2 show that partial purification removes 97-98% of cellular proteins and nucleates, while retaining essentially all of the infectious virus.

Partially purified virus was split into two aliquots. One aliquot was added to a freshly prepared column of hydroxylapatite and eluted in the usual manner. Each fraction collected was subsequently assayed for infectious virus and

---

<sup>1</sup>The <sup>32</sup>P and <sup>14</sup>C radioactivity was assayed by adding 10 ml volumes of scintillation fluid (10% naphthalene, 0.5% 2,5-diphenyloxazole in 1,4-dioxane) to 0.2 ml samples and counting at two energy levels in a Beckman Liquid Scintillation System, Model LS-200B. All samples were counted on the same day to eliminate discrepancies due to <sup>32</sup>P decay.

Table 1.3

Final Purification of M-Mengo Virus by Chromatography on Hydroxylapatite:  
Removal of Labelled Cellular Material

	Total $^{14}\text{C}$ cpm	Total $^{32}\text{P}$ cpm	Total infectious virus (pfu)
Added to Column I	$1225 \times 10^3$ (1.9%)	$936 \times 10^3$ (3.0%)	$2.6 \times 10^{12}$ (97.1%)
Recovered from Column I in fractions 29-33	$36.8 \times 10^3$ (0.06%)	$28.5 \times 10^3$ (0.08%)	$1.7 \times 10^{12}$ (63.5%)
Added to Column II	$1183 \times 10^3$ (1.9%)	$874 \times 10^3$ (3.0%)	$2.5 \times 10^{12}$ (97.1%)
Recovered from Column II in fractions 28-32	$29.6 \times 10^3$ (0.05%)	$27.7 \times 10^3$ (0.08%)	$1.7 \times 10^{12}$ (66.1%)





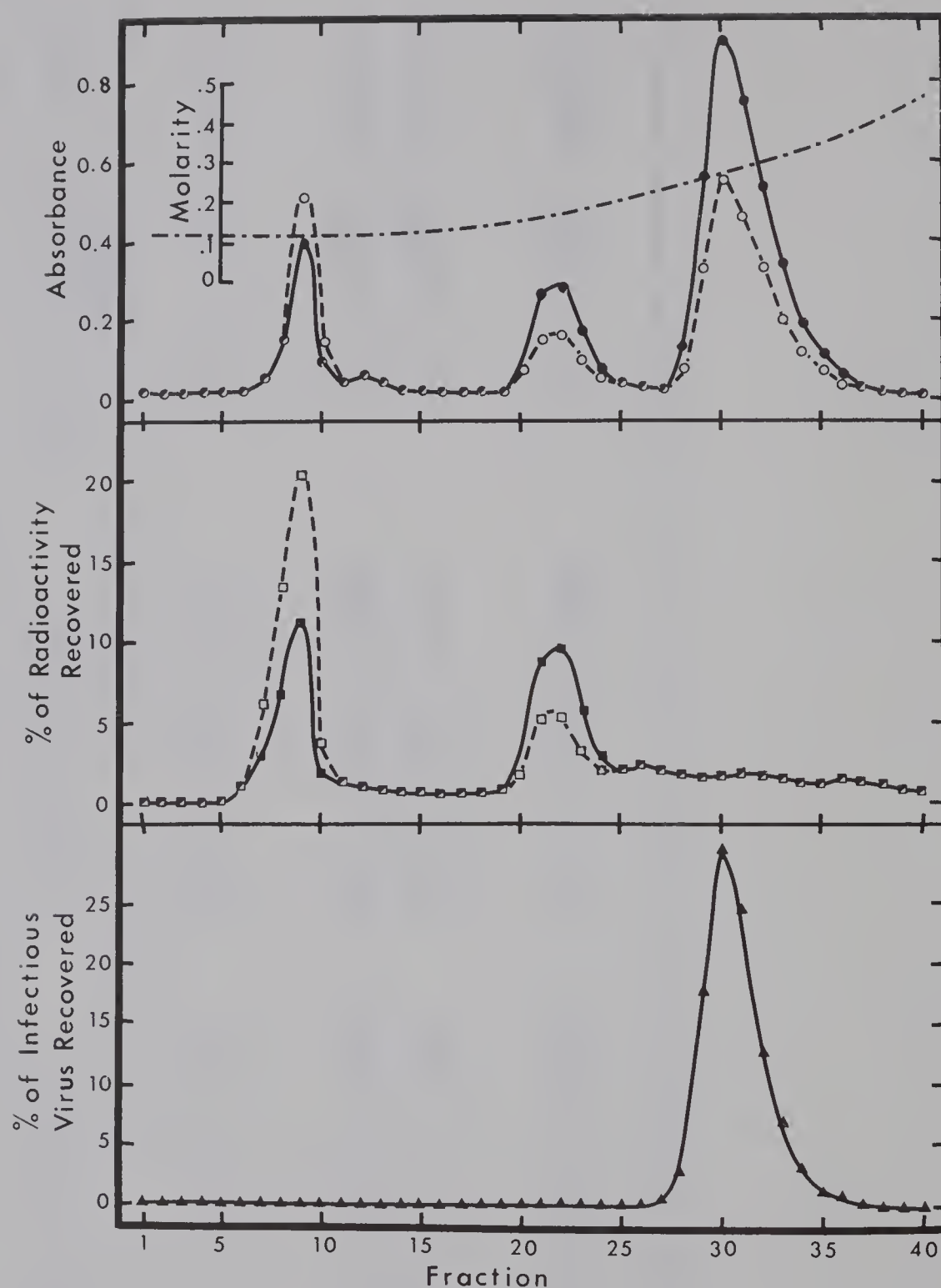


Figure 1.4. Chromatography of partially purified M-Mengo virus on hydroxylapatite (pH 7.1).  $^{32}\text{P}$ ,  $^{14}\text{C}$ -labelled cellular material was collected from a lysate of uninfected L-cells by methanol precipitation and added to a methanol precipitate of unlabelled virus. The mixture was partially purified by methods described in the text, and then chromatographed.

- = absorbance at 260 mμ,      ○ = absorbance at 280 mμ,
- =  $^{32}\text{P}$  radioactivity,      □ =  $^{14}\text{C}$  radioactivity,
- ▲ = infectious virus.



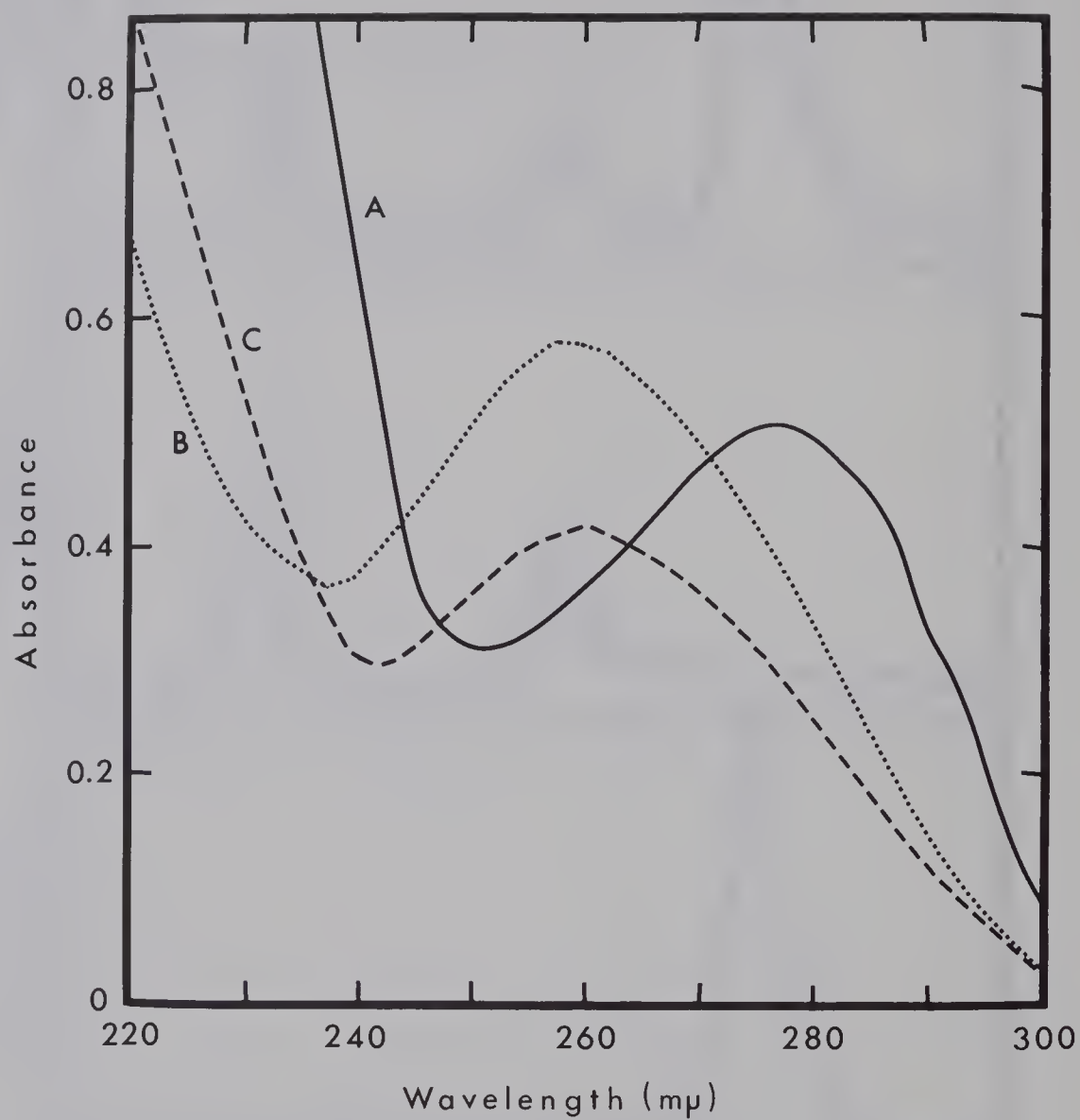


Figure 1.5. Chromatography of M-Mengo virus: ultraviolet absorption spectra of the peak fractions shown in Figure 1.4.

A = fraction 9, B = fraction 22, C = fraction 30.

radioisotope content.<sup>1</sup> The column was then recycled and the second aliquot of virus was added. Elution and analysis were performed as outlined above. The results of the column purifications are summarized in Table 1.3; and the absorbance, radioactivity, and infectivity profiles for the first column are depicted in Figure 1.4.

It is clear from these data that the procedure employed does indeed yield highly pure virus - at least 99.92% of contaminating cellular protein and nucleates is eliminated. The recovery of infectious virus in this particular experiment was about 65%. In a large number of purifications of each of the variants, recovery of infectious virus was always found to be in the range 60-90%. The loss of infectivity could be the result of some irreversible adsorption to the hydroxylapatite, or to surface damage to some virions during elution.

Figure 1.5 shows the spectra of the three ultraviolet-absorbing peaks from the hydroxylapatite column purification described in Figure 1.4. Considering these spectra, the  $A_{260}/A_{280}$  ratios, and the  $^{32}\text{P}/^{14}\text{C}$  ratios, it seems clear that the first peak (fraction 9) contains cellular protein, the second peak (fraction 22) contains cellular nucleoprotein (possibly degraded ribosomes), and the third peak (fraction 30) contains the virus.

#### Chromatography on large columns

Recently, with the improved production of virus using roller bottles, it became necessary to use larger capacity columns for the final purification step. Glass columns (Kontes Glass Co., Vineland, N. J.) of dimensions 23 x 2.0 cm (length x



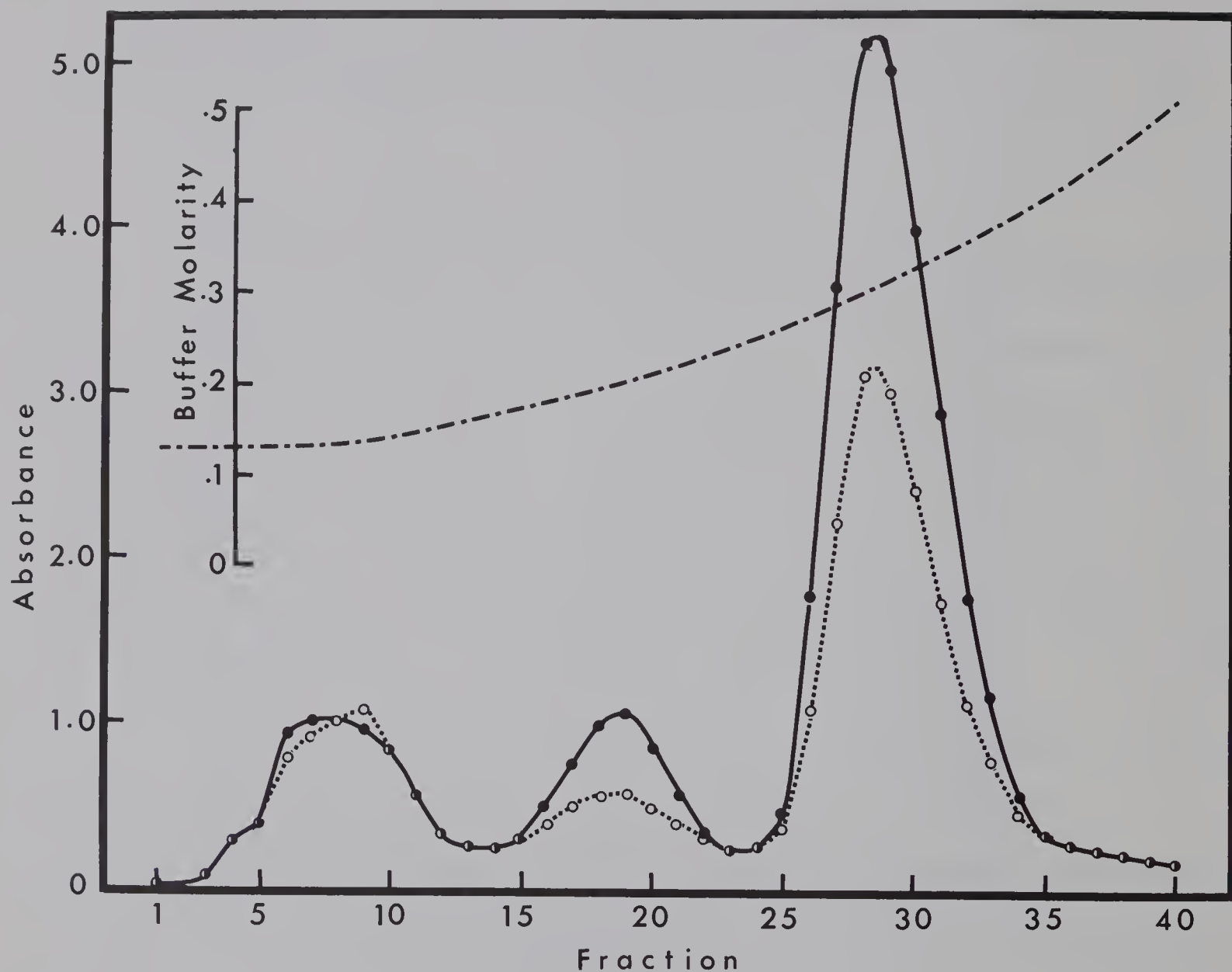


Figure 1.6. Chromatography of S-Mengo virus partially purified from 50 roller bottles. The filled circles represent the absorbance at 260 mμ, and the open circles represent the absorbance at 280 mμ. The pH of the eluting potassium phosphate buffer was 7.1. The amount of infectious virus contained in fractions 27-31 was approximately  $7.5 \times 10^{12}$  pfu.



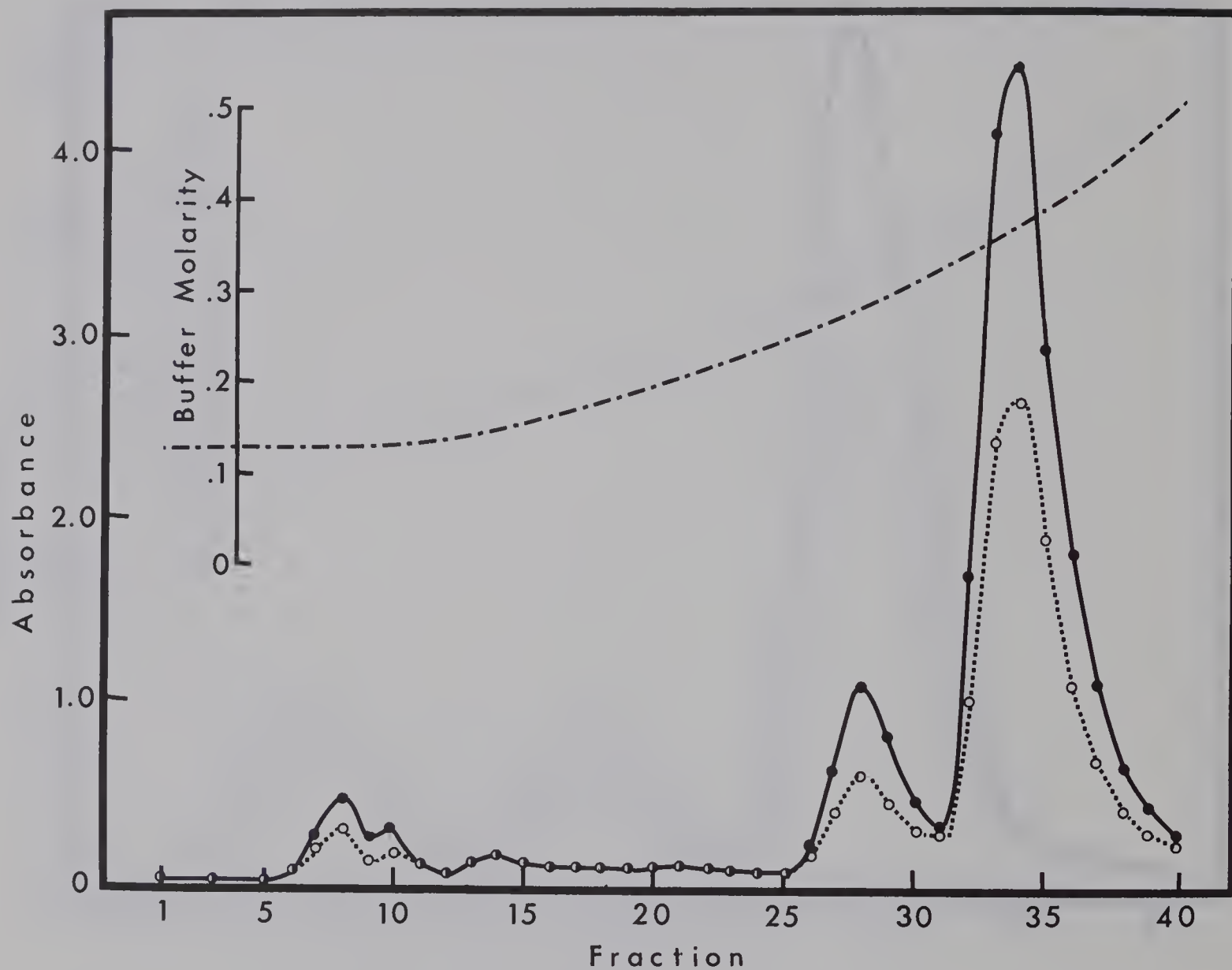


Figure 1.7. Chromatography of L-Mengo virus partially purified from 36 roller bottles. The filled circles represent the absorbance at 260 mμ, and the open circles represent the absorbance at 280 mμ. The pH of the eluting phosphate buffer was 6.2. There was a total of  $2.5 \times 10^{11}$  pfu contained in fractions 32-37.

inside diameter) were silicone coated ("Siliclad"; Clay-Adams Inc., New York, N. Y.) and packed with hydroxylapatite. The total volume of these columns was approximately 1.6 times that of the plexiglas columns used earlier, and their capacity was sufficient to chromatograph virus prepared from 50 to 60 roller bottles. The same loading and elution procedures as outlined previously were used except that the limiting phosphate buffer concentration was 1.0 M, and the first 40 ml eluted were discarded. Elution profiles of partially purified S-Mengo and L-Mengo viruses from these large columns are depicted in Figures 1.6 and 1.7, respectively. Comparing these profiles with those shown in preceding figures indicates that production of virus in roller bottles yields a better proportion of virions to cellular material than does production in Povitsky bottles.

Based on the value of 76.3 for the extinction coefficient ( $E_{260\text{m}\mu}^{1\%}$ ) of Mengo virus (see Chapter 3), the amount of S-Mengo virus recovered from the column that provided the data shown in Figure 1.6 was about 13 mg, and the amount of L-Mengo virus recovered from the column corresponding to Figure 1.7 was about 10 mg.

### Discussion

Procedures have been developed which yield milligram quantities of the Mengo virus variants in a state of purity sufficient to permit meaningful physical and chemical analyses to be made.

The most efficient method for producing large quantities of virus appears to be growth in roller bottle cultures





of cells. Growth in stationary cultures (i.e. in Povitsky bottles) requires more medium and more labor to produce equivalent amounts of virus. Neither the aminonucleoside of puromycin nor semicarbazide were found to enhance virus production in the Mengo virus-L-cell system.

The procedure for partially removing cellular debris from crude lysates takes advantage of the fact that the Mengo virus variants are remarkably resistant to the enzymes  $\alpha$ -chymotrypsin and ribonuclease, while these enzymes degrade cellular proteins and nucleates. Viruses of the encephalomyocarditis group seem to be stable in the presence of proteolytic enzymes (Weil et al., 1952; Faulkner et al., 1961; Kaighn et al., 1964), but other picornaviruses are not (Brown et al., 1963). Stability in the presence of proteolytic enzymes suggests a highly compact and inflexible conformation of the capsid protein. Ribonuclease is unable to penetrate the capsid and degrade the viral RNA at the pH employed (8.0).

Hydroxylapatite chromatography has been used as a final purification step for EMC virus (Kaighn et al., 1964) and also for tick-borne encephalitis virus (Mayer et al., 1967). Brushite, an intermediate in the preparation of hydroxylapatite, has also been used successfully in the purification of polio (Ozaki et al., 1965) and EMC (Burness, 1967; Faulkner et al., 1961) viruses. It is perhaps worth noting here that commercially available preparations of hydroxylapatite ("Biogel-HT", BioRad Laboratories, Richmond,



Calif., "Hypatite-C", Clarkson Chemical Co., Williamsport, Pa.) did not effectively resolve virus from cellular material.



## Chapter 2

### Physicochemical Studies of Whole Virions

#### Introduction

With adequate amounts of highly purified virus available, experiments were undertaken to establish the size, shape, buoyant density, and particle weight for each of the L-, M-, and S-Mengo virions, and to see if any differences in these parameters could be detected. This chapter summarizes the results of these experiments.

#### Materials and Methods

##### Viruses

Column-purified virus was either used directly as obtained, or was concentrated in a collodion bag apparatus (Carl Schleicher and Schuell Co., Keene, N. H.). When a change of buffer was required, virus from appropriate column fractions was collected by sedimentation at 100,000 g for 60 min and resuspended in the new buffer.

##### Electron Microscopy

Specimen grids were prepared by the lowered-drop method of Pinteric and Taylor (1962). Virus particles were visualized either by staining with 2% PTA or by shadowing with palladium. The actual microscopy was kindly performed by Dr. T. Yamamoto of the Microbiology Department, University of Alberta, using either a Siemens Elmiskop I or a Phillips EM-200 electron microscope.



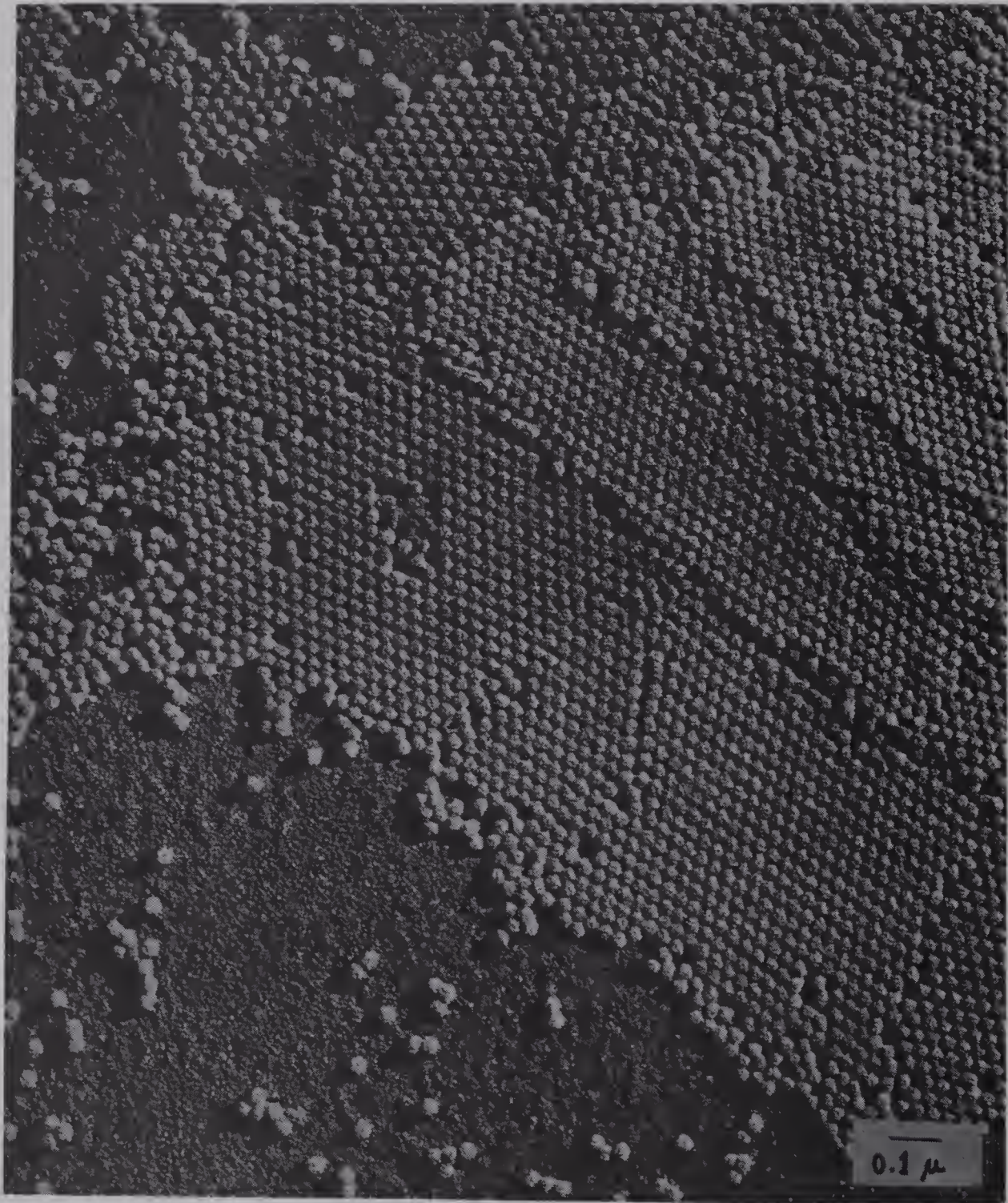


Figure 2.1. L-Mengo virus. Shadowed with palladium.





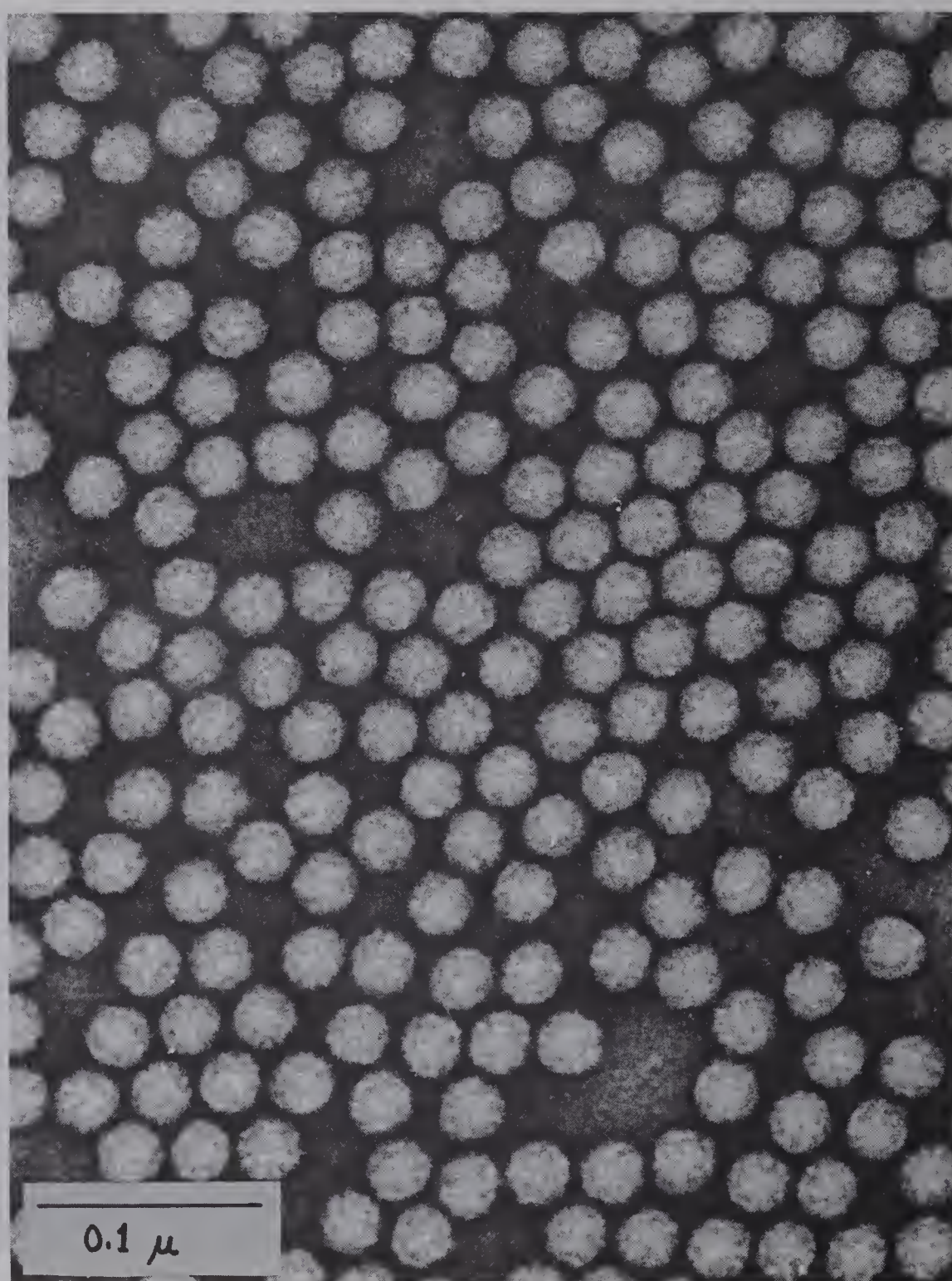


Figure 2.2. L-Mengo virus. Negatively stained with 2% phosphotungstic acid (pH 7.3).

### Analytical Ultracentrifugation

Sedimentation velocity and diffusion runs were carried out in a Spinco model E ultracentrifuge (Spinco Division, Beckman Instruments, Palo Alto, Calif.) equipped with an electronic speed control system and utilizing ultraviolet absorption optics. The sedimentation/diffusion boundaries were recorded photographically on Kodak blue-sensitive M film. Graphical representation of virus concentration as a function of cell position was obtained from the films using a Spinco Analytrol densitometer. Sedimentation/diffusion runs were carried out at temperatures near 5° and were corrected for solvent density and viscosity at 20°.

Sedimentation coefficients were determined by the procedure described by Schachman (1957), using data obtained from centrifugation at 30,000 rpm.

Diffusion coefficients were determined by the procedure of Möller (1964). The experiment was performed in two phases of the same operation: a 4-min run at 30,000 rpm followed by a 1200-min run at 2000 rpm. Diffusion coefficients were estimated from an analysis of boundary spreading during the low-speed phase (see Appendix, section 1, for details).

### Results

#### Electron Microscopy - shape and size of the virions

Figures 2.1 and 2.2 show electron microscope photographs of purified L-Mengo virus. It is clear from these photographs that the anhydrous virions are essentially spherical in shape. These particles were considered to be

Table 2.1

Diameters of Mengo Virus Particles

Variant	Photograph No.	Latex part- icles measured	Virus part- icles measured	Virus diam. (m $\mu$ )	Average diameter (m $\mu$ )
L-Mengo	1	6	10	27.2	26.6
	2	5	10	26.3	
	3	6	9	26.8	
	4	8	10	26.0	
M-Mengo	1	4	6	27.0	26.7
	2	4	10	26.3	
	3	5	10	26.7	
S-Mengo	1	6	10	26.6	26.7
	2	4	10	26.9	
	3	4	10	26.6	



anhydrous because photographs were taken under conditions of high vacuum, which would remove the water of hydration. The high magnification photograph of negatively stained virions (Figure 2.2) reveals some capsid subunit structure; however, the subunits are too small and ill-defined to permit an analysis of their arrangement. No differences in general appearance were discernible between preparations of L-, M-, and S-Mengo virions.

The diameters of the virus particles were estimated from photographs of purified virus which had been mixed with latex particles of known diameter (No. LS-040-A, 88 m $\mu$ ; Dow Chemical Co., Midland, Mich.). Virus and latex were made visible in the electron microscope by staining with 2% PTA (pH 7.3). Diameters were measured from photographic negatives in perpendicular directions using a Nikon microcomparator (obtained from Anglophoto Inc., Toronto, Ont.). Several preparations of each variant were examined, and different microscope magnifications were used. The results are summarized in Table 2.1. The anhydrous L-, M-, and S-Mengo virions all have the same diameter, namely  $26.7 \pm 0.5$  m $\mu$ . This value is in close agreement with other estimates of the particle diameter of Mengo virus. Dales and Franklin (1962) reported a value of 27-28 m $\mu$  based on micrographs of thin sections of virus-infected cells, and Homma and Graham (1965) reported a value of 27 m $\mu$  based on micrographs of purified virus.

The calculated diameter of anhydrous Mengo virus particles is 26.4 m $\mu$ , using data obtained from hydrodynamic experiments (see Appendix, section 6). This indicates good

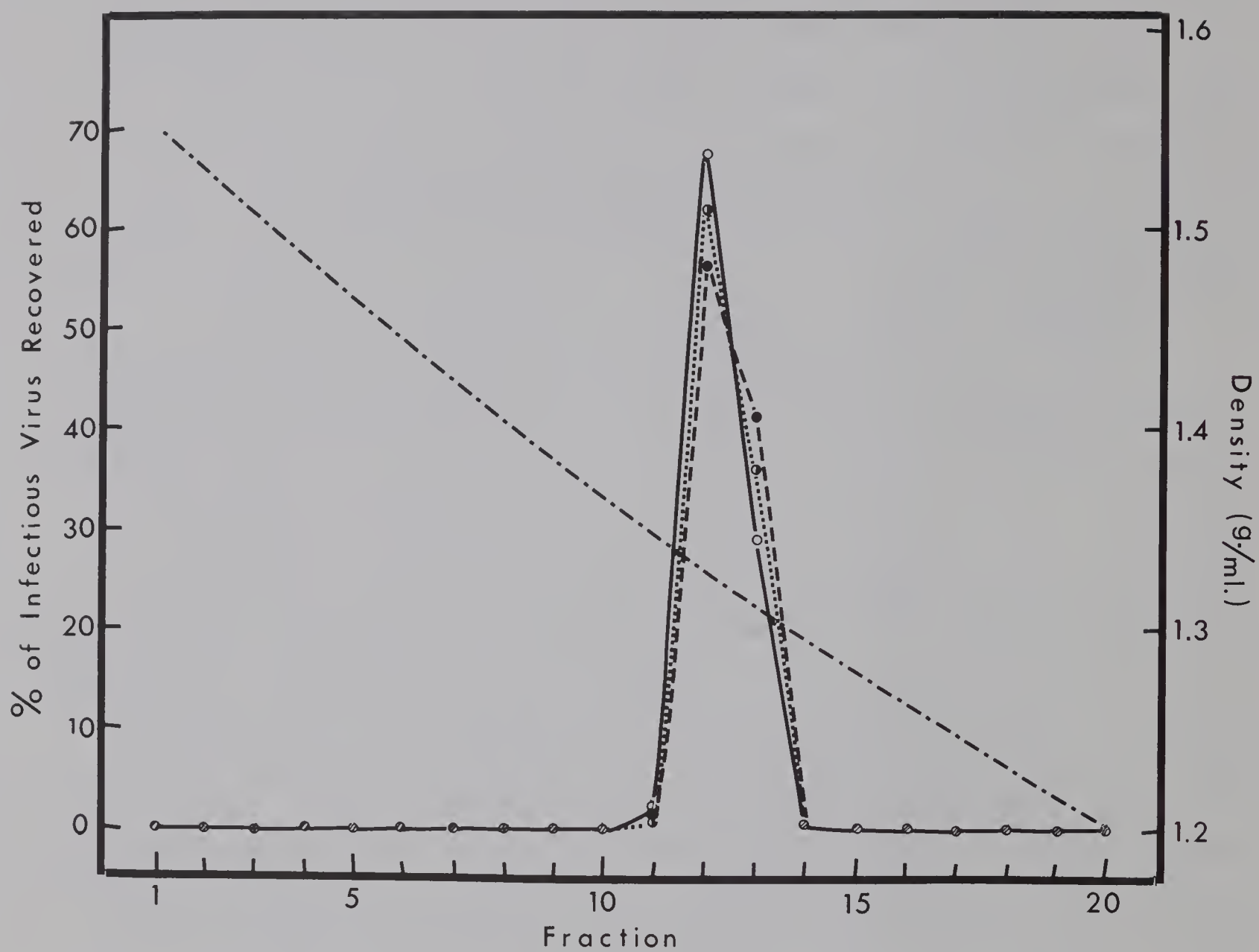


Figure 2.3. Equilibrium sedimentation of Mengo virus variants in  $\text{Cs}_2\text{SO}_4$  density gradients.

○ = L-Mengo, ◐ = M-Mengo, ● = S-Mengo.

agreement between data obtained from electron microscopy and from analytical ultracentrifugation.

#### Equilibrium centrifugation in cesium sulfate density gradients

The equilibrium buoyant densities for protein and for single-stranded RNA as determined by centrifugation in  $\text{Cs}_2\text{SO}_4$  gradients are approximately  $1.3 \text{ g/cm}^3$  and  $1.63 \text{ g/cm}^3$ , respectively (Kaiser, 1966; Billeter and Weissmann, 1966). If there were any real differences in the percentage of RNA in L-, M-, S-Mengo virions, these would be reflected in their buoyant densities - virions containing more RNA would have higher buoyant densities.

Four-ml samples of each of the three variants (in 0.02 M potassium phosphate, pH 7.1) were added to 1.800 g  $\text{Cs}_2\text{SO}_4$  (Gallard-Schlesinger Chemical Mfg. Corp., Carle Place, N. Y.) in 5-ml cellulose nitrate centrifuge tubes. The mixtures were centrifuged at 35,000 rpm for 50 hours (SW-39 rotor, Spinco preparative ultracentrifuge - model L). Under the influence of the centrifugal field, a density gradient of the salt was produced and the virus banded at an equilibrium position corresponding to its own density in the solution. After centrifugation, 0.2 ml fractions were collected dropwise from the bottom of each tube. All fractions were assayed for infectivity (by virus titration) and for density. Densities were estimated from measurements of refractive index (at  $25^\circ$ ) made with a temperature-regulated Abbé-3L refractometer (Bausch and Lomb, Rochester, N. Y.), and employing a previously constructed standard curve.

The results are depicted in Figure 2.3, and indicate





that the buoyant densities of L-, M-, and S-Mengo are identical. This in turn suggests that the three types of Mengo virus particles have identical percentage compositions of RNA and protein. The experimental buoyant density of the Mengo virions was estimated to be  $1.320 \text{ g/cm}^3$ . However, the densities of fractions were determined at  $25^\circ$ , whereas centrifugation was carried out at approximately  $5^\circ$ . The true buoyant density, namely  $1.331 \text{ g/cm}^3$ , was obtained by multiplying the experimental value by a correction factor of 1.009. This factor was estimated from data on the densities of  $\text{Cs}_2\text{SO}_4$  solutions at various temperatures listed in International Critical Tables.

The infectious virus recovered was only 30-50% of that added, indicating that banding in  $\text{Cs}_2\text{SO}_4$  would not be a satisfactory method of purifying Mengo virus.

#### Velocity sedimentation in sucrose density gradients

The relative rates of sedimentation of L-, M-, and S-Mengo viruses in pre-formed sucrose density gradients were ascertained in order to obtain an indication of whether the particles differed in intrinsic sedimentation coefficients (see Martin and Ames, 1961) and hence in molecular (i.e. particle) weights.

Three linear density gradients (4.5 ml) of 5-40% sucrose in phosphate-buffered saline (Dulbecco and Vogt, 1954) containing 0.2% bovine plasma albumin were prepared using a two-chamber mixing device (Buchler Instruments, Fort Lee, N. J.). A small volume (0.1 ml) of virus suspended in 0.02 M potassium phosphate (pH 7.1) was carefully layered on



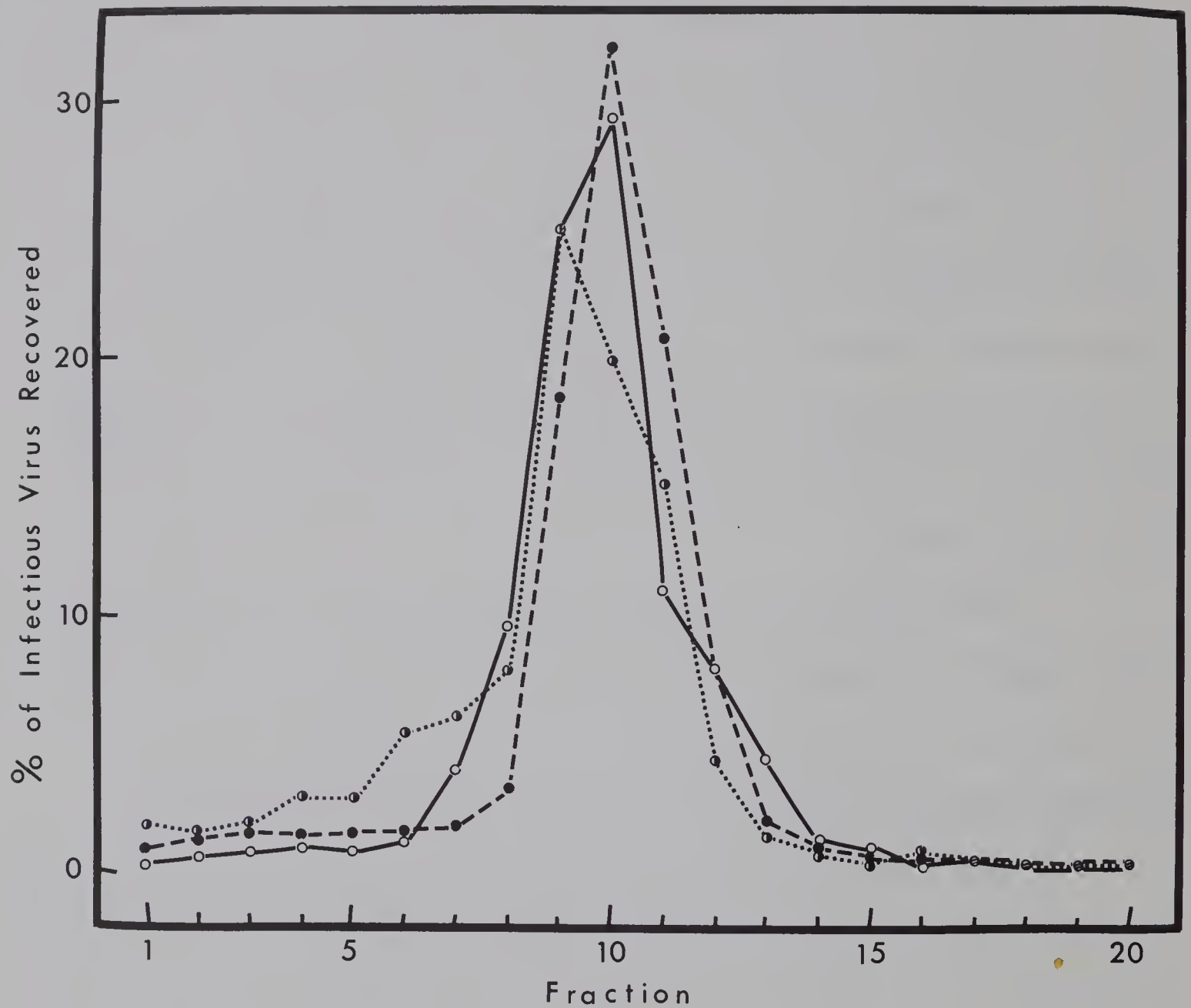


Figure 2.4. Velocity sedimentation of Mengo virus variants in 5-40% sucrose density gradients.

○ = L-Mengo, ◐ = M-Mengo, ● = S-Mengo.



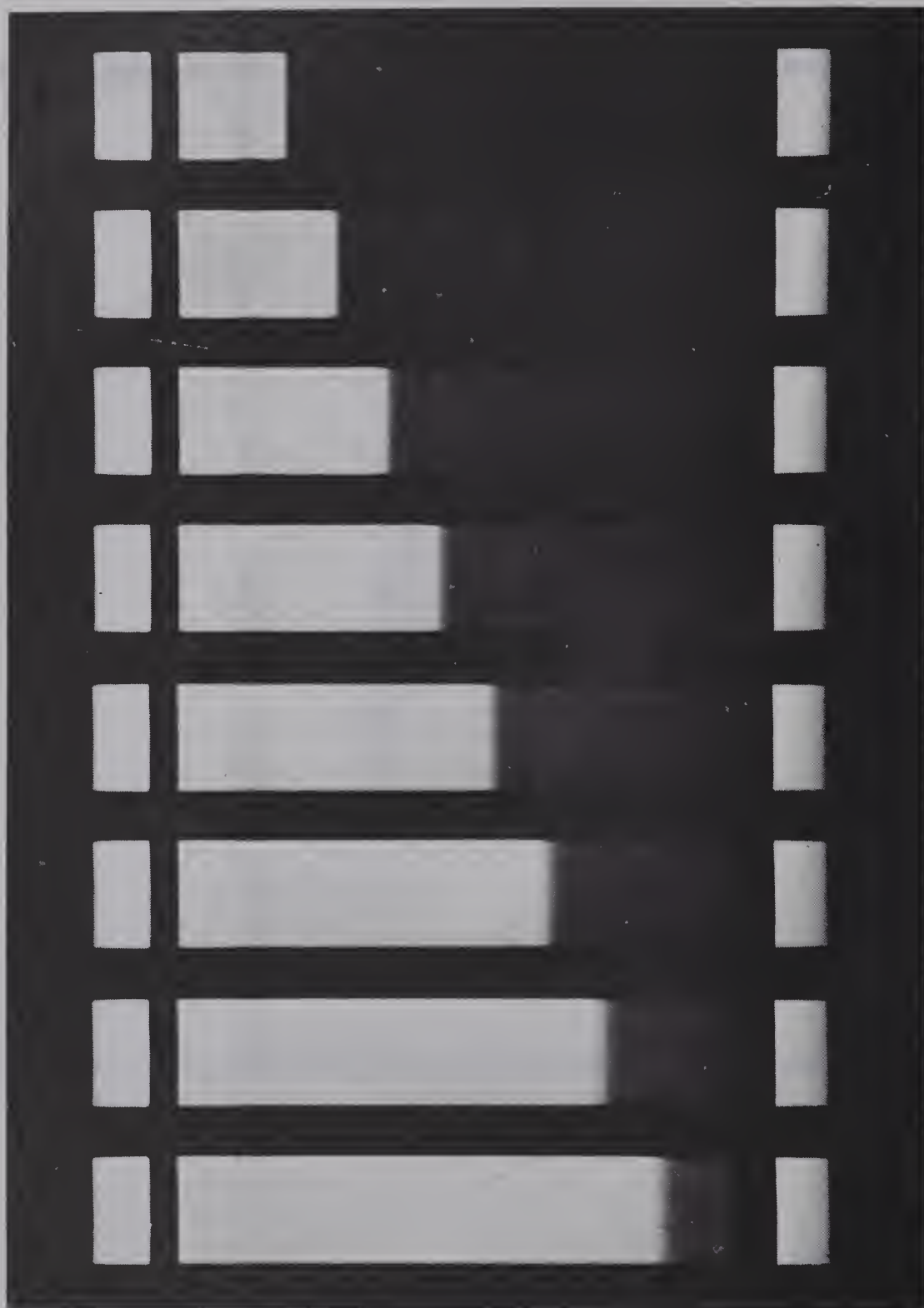


Figure 2.5. Ultraviolet photographs taken at 4-min intervals during the sedimentation of M-Mengo virus in the analytical ultracentrifuge, 30,000 rpm, 7°, 0.3 M potassium phosphate (pH 7.1).



Table 2.2  
Hydrodynamic Properties of Purified Variants  
of Mengo Virus

Variant	$S_{20,w}^0$ ( $\times 10^{13}$ sec)	$D_{20,w}^0$ ( $\times 10^7$ cm <sup>2</sup> /sec)	$\bar{v}$ (ml/g)	M ( $\times 10^{-6}$ )
L-Mengo	152	1.46	0.70	
M-Mengo	151	1.45	0.70	
S-Mengo	150	1.49	0.70	
Best average value (8-10 determinations) *				
	151 $\pm$ 2.6	1.47 $\pm$ 0.08		8.32 $\pm$ 0.7

\*Average value  $\pm$  1 standard deviation.



top of each of the gradients, which were then centrifuged for 80 min at 35,000 rpm in the SW-39 swinging-bucket rotor of the Spinco model L ultracentrifuge. Fractions of 0.1 ml were collected dropwise from the bottom of each gradient, and were titrated for infectious virus.

The results are depicted in Figure 2.4. No real differences in sedimentation rates among the three variants were found, indicating that they have similar (if not identical) molecular (particle) weights. The infectious virus recovered from the respective gradients was as follows: L-Mengo,  $1.2 \times 10^8$  pfu (48% of that added); M-Mengo,  $4.5 \times 10^8$  pfu (55%); and S-Mengo,  $2.0 \times 10^8$  pfu (46%).

#### Hydrodynamic parameters of the virions

##### Sedimentation coefficients

Typical ultraviolet absorption photographs obtained during a sedimentation velocity run on Mengo virus in the analytical ultracentrifuge are illustrated in Figure 2.5. The symmetrical boundary with minimum spreading under the conditions of high-speed centrifugation is evidence for the homogeneity of the preparation. The sedimentation coefficients observed for the three variants are listed in Table 2.2. For all practical purposes, these are infinite dilution values ( $S_{20,w}^0$ ) in view of the low concentrations of virus used. The data indicate that within the limits of experimental error, sedimentation coefficients are identical for L-, M-, and S-virions, and have an average value of  $151 \pm 2.6$  svedbergs.

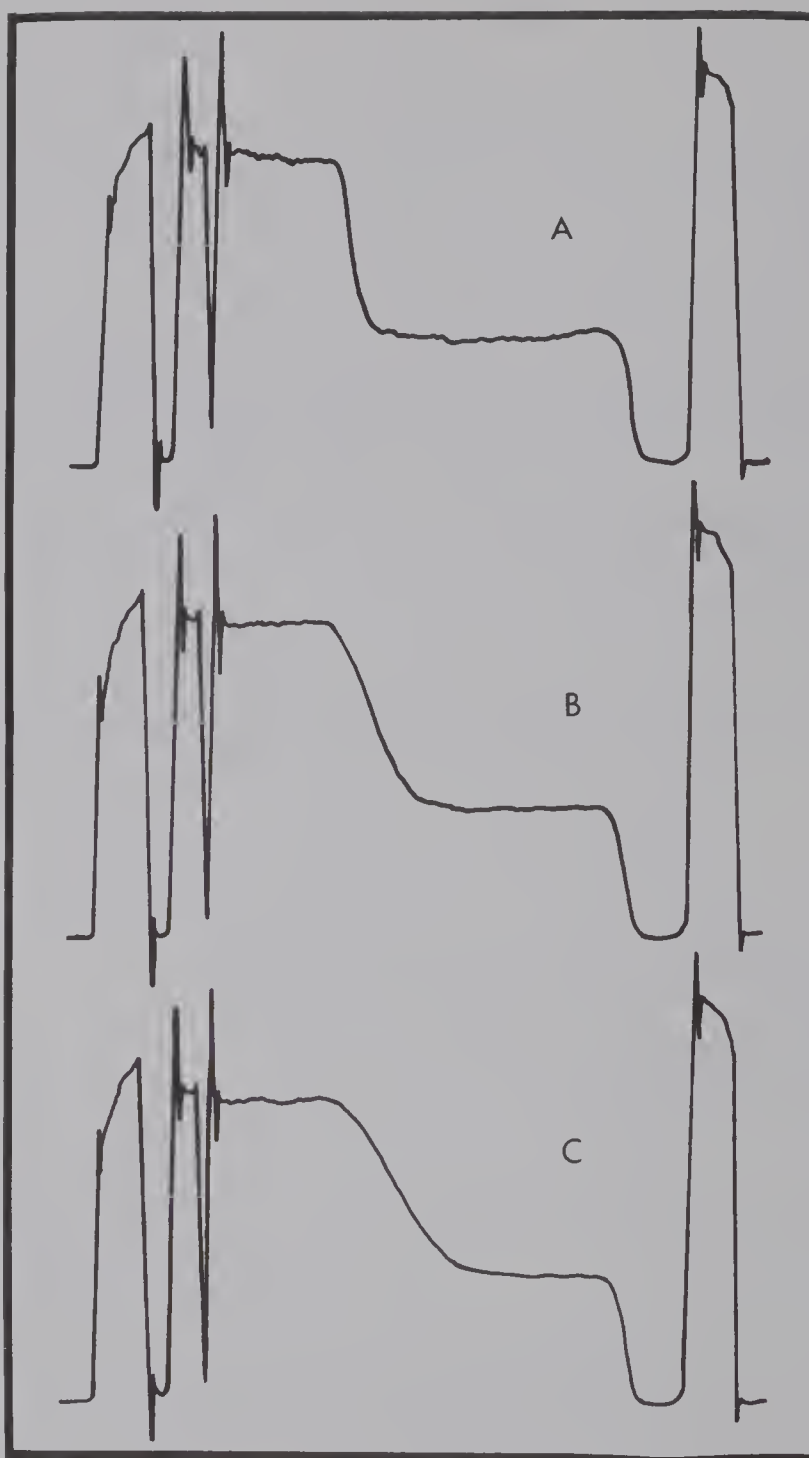


Figure 2.6. Selected densitometer tracings illustrating the diffusion of M-Mengo virus during the low-speed phase of a Möller run in the analytical ultracentrifuge. 2000 rpm, 4.5°, 0.25 M potassium phosphate (pH 7.1). The tracings A, B, and C correspond, respectively, to times of 0 min, 488 min, and 1088 min after deceleration to the low speed.



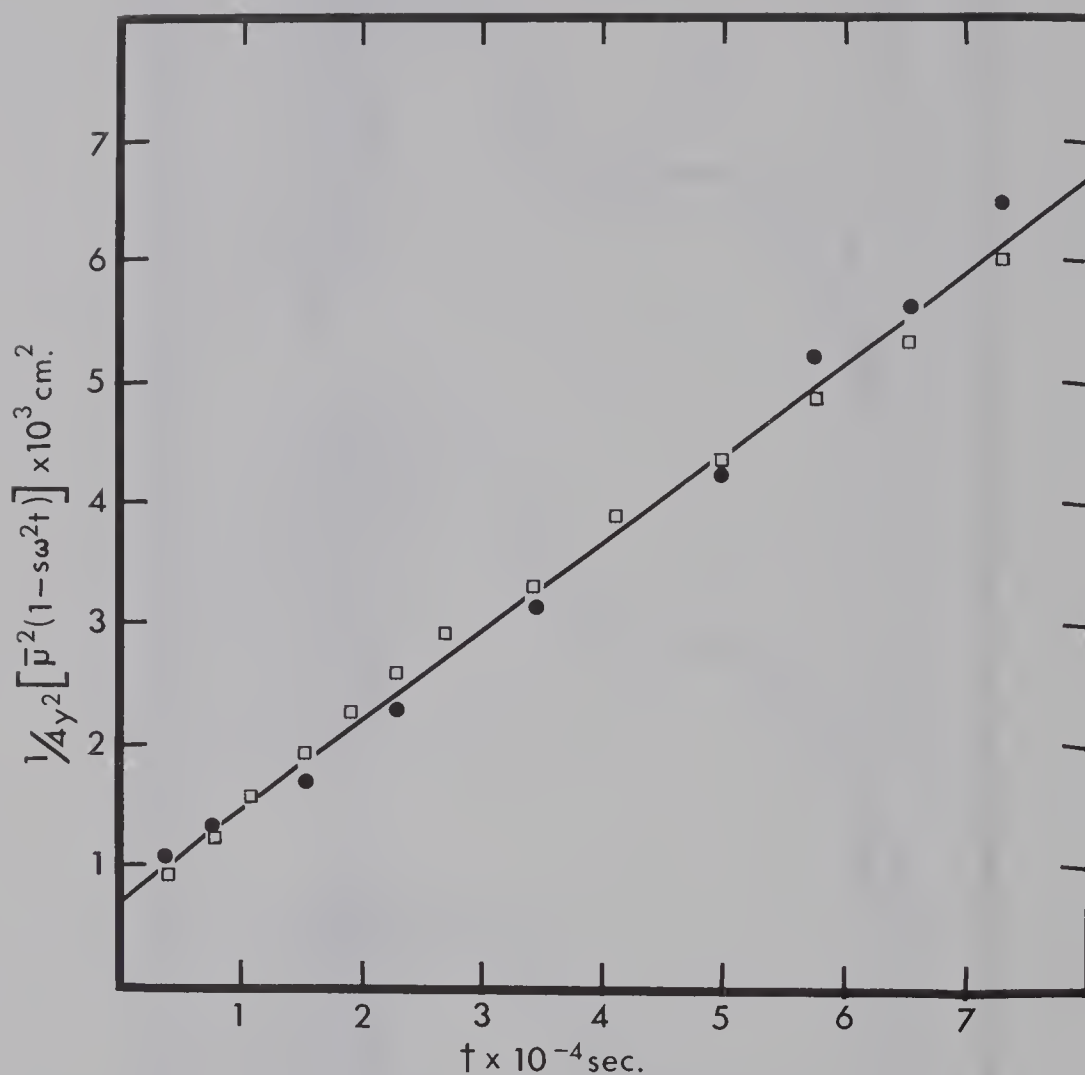


Figure 2.7. Plot of  $\frac{1}{4} y^2 [\bar{u}^2 (1 - s_w^2 t)]$  versus  $t$  for M-Mengo virus. The open squares represent measurements made at a  $c/c_0$  ratio of 0.2(0.8), while the filled circles represent measurements at a ratio of 0.3(0.7). 2000 rpm,  $2^\circ$ , 0.3 M potassium phosphate (pH 7.1).

### Diffusion coefficients

Figure 2.6 depicts densitometer traces of boundary patterns corresponding to selected photographs taken during the low-speed phase of a representative Möller diffusion run on Mengo virus. Diffusion coefficients were calculated from analyses of the boundary spreading, as described in the Appendix, section 1. Figure 2.7 shows a plot of the data obtained from one such analysis. In this case, two different  $c/c_0$  ratios were used to obtain values for  $\bar{u}$ . That the points derived from the two sets of measurements fit the same straight line is indicative of both boundary stability and homogeneity. From the slope of this plot, a  $D_{20}^0$  value of  $0.748 \times 10^{-7} \text{ cm}^2/\text{sec}$  was computed. Corrections for solvent density and viscosity resulted in a  $D_{20,w}^0$  value of  $1.44 \times 10^{-7} \text{ cm}^2/\text{sec}$ . A summary of the intrinsic diffusion coefficients for the three Mengo variants also appears in Table 2.2. Within the limits of error of the technique (variation in  $c_0$  and accuracy of measurement of  $\bar{u}$ , estimated to be  $\sim 10\%$ ), the diffusion coefficients of L-, M-, and S-Mengo variants are the same.

### Partial specific volumes

Since the amounts of highly purified virus available were not sufficient for pycnometry, an experimental estimate of the partial specific volume,  $\bar{v}$ , was obtained by an ultracentrifugal method (Schaffer and Schwerdt, 1955; described in Schachman, 1957). Sedimentation coefficients for L- and S-Mengo virions were determined in aqueous solutions of 0.1 M potassium phosphate containing varying percentages of



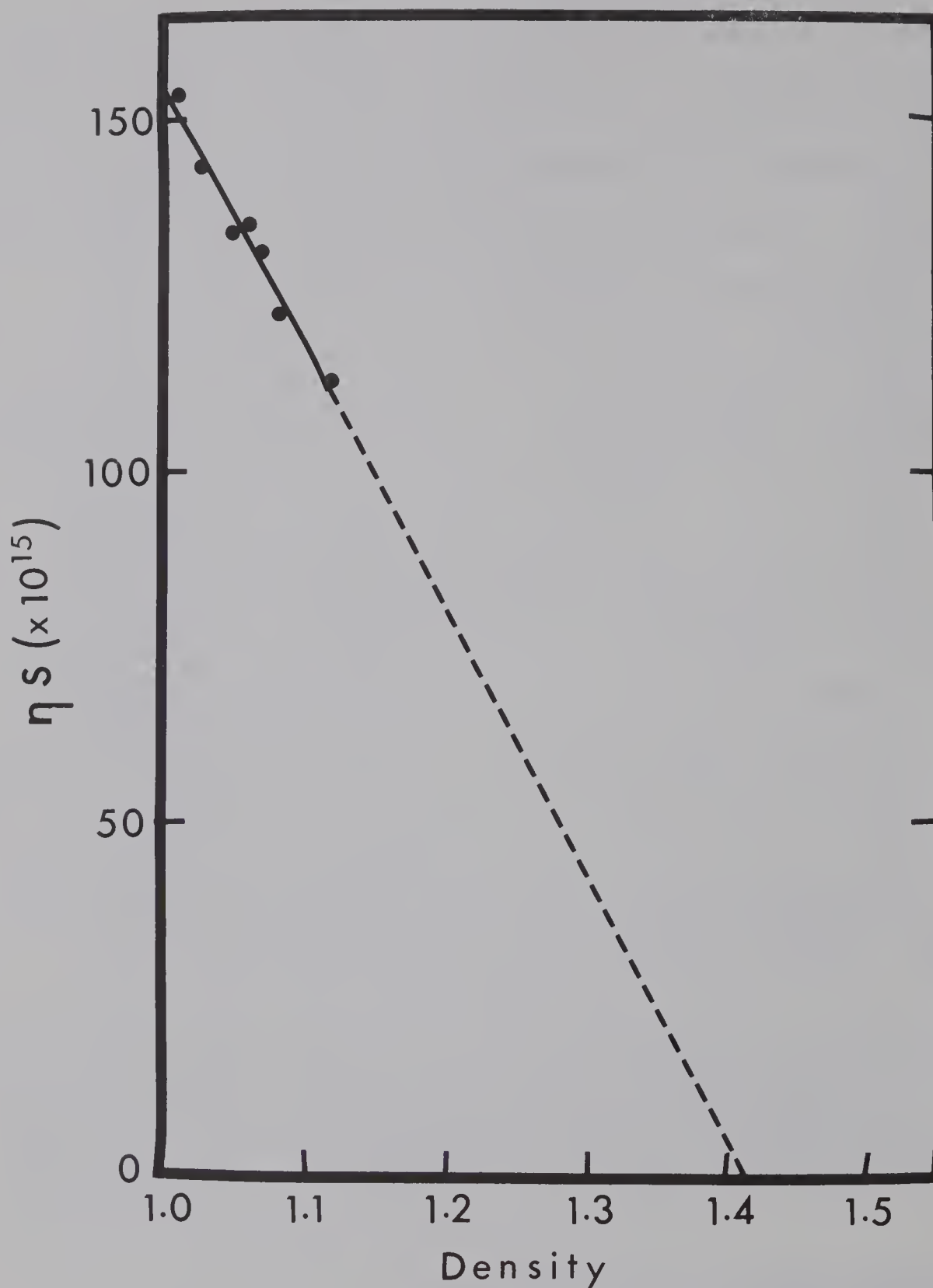


Figure 2.8. Sedimentation of L- and S-Mengo viruses in  $H_2O$ - $D_2O$  solutions. Viscosities ( $\eta$ ) were determined experimentally using Ostwald-type viscometers. Densities of  $H_2O$ - $D_2O$  solutions were taken from Longworth (1937), and corrected for the presence of 0.1 M potassium phosphate. The best-fitting straight line was obtained by the least squares method.

deuterium oxide, the function of the  $D_2O$  being to retard sedimentation by increasing the density and viscosity of the medium. The products of viscosity and sedimentation coefficient for the various mixtures were plotted as a function of solvent density, and extrapolation to zero sedimentation was made. The plot of the data obtained is shown in Figure 2.8. Since  $H_2O-D_2O$  acts as a one-component solvent (Svedberg and Eriksson-Quensel, 1936), the reciprocal of the solvent density at zero sedimentation is equivalent to the partial specific volume of the virus. Thus, for the Mengo virion,  $\bar{v}$  was calculated to be 0.709 ml/g.

It is noteworthy that sucrose, cesium salts, or bovine serum albumin cannot be used to compute  $\bar{v}$  values in the manner outlined, because these materials interact with the sedimenting macromolecule - giving rise to density differences between the hydration mantle of the macromolecule and the solvent itself (see Lauffer and Bendet, 1954). For example, the value of the reciprocal density of Mengo virus particles in  $Cs_2SO_4$  is 0.752 ml/g, which is a value higher than that calculated for the viral protein (Chapter 3). The long extrapolation necessary for  $H_2O-D_2O$  solutions has recently been obviated by the introduction of  $D_2O^{18}$  as a density- and viscosity-increasing substance (Edelstein and Schachman, 1967). As a result of this modification, the sedimentation method for determining  $\bar{v}$  for small quantities of material is likely to find increasing use in the future.

The partial specific volume for Mengo virions was also estimated from percentage composition data (see Appendix,



section 2), and the value so obtained was 0.684 ml/g. The best average value for purposes of calculation was taken to be  $\frac{0.709 + 0.684}{2}$ , or 0.70 ml/g.

#### Molecular (particle) weights

The particle weight for the Mengo virion was calculated by substituting the best average values for  $S_{20,w}^O$ ,  $D_{20,w}^O$ , and  $\bar{v}$  in the Svedberg equation (see Appendix, section 3), the result being  $8.32 \pm 0.7 \times 10^6$  daltons.

#### Discussion

No differences among the Mengo variant virions were detectable by electron microscopy or ultracentrifugal analysis. L-, M-, and S-virions are all spherical particles with dry diameters of  $26.7 \pm 0.5 \text{ m}\mu$  and "molecular" weights of  $8.32 \pm 0.7 \times 10^6$  daltons. Based upon the best average experimentally determined parameters for a typical Mengo virus virion, some additional molecular-kinetic properties have been calculated (see Appendix, sections 4-8). The hydrated diameter of the virion, calculated from the diffusion coefficient, is  $29.0 \text{ m}\mu$ , which is consistent with a spheroid having 0.228 g of water of hydration per g of dry weight (Faulkner et al. [1961] reported a value of  $30 \text{ m}\mu$  for the diameter of hydrated EMC virus particles based on x-ray analysis). The ratio of the frictional resistance of the hydrated molecule to that of the anhydrous equivalent sphere,  $f/f_0$ , was calculated from the hydrodynamic parameters to be 1.10. This suggests that the virus particle in solution is essentially spherical. From the frictional ratio

Table 2.3

Physical Properties of Mengo Virus

Property	Average value
Shape	Spherical
Dry diameter (m $\mu$ )	26.2-27.2
Hydrated diameter (m $\mu$ )	28.5-29.5
Hydration (g H <sub>2</sub> O/g virus)	0.23
Frictional ratio, $f/f_0$	1.10
Buoyant density in Cs <sub>2</sub> SO <sub>4</sub> (g/ml)	1.331
Particle weight ( $\times 10^{-6}$ )	8.32 $\pm$ 0.7
Percentage RNA	23



and the electron microscopic evidence that the anhydrous particle is spherical, the water of hydration was calculated to be 0.231 g per g of dry virus. The virtual equivalence in values for the frictional ratio and water of hydration by different methods of calculation, suggests that the physico-chemical data are all internally consistent, and that the preparations of virus examined were in fact homogeneous. The salient molecular-kinetic properties of Mengo virus are summarized in Table 2.3.

The use of the ultraviolet absorption optical system in the analytical ultracentrifuge has facilitated the determination of the hydrodynamic parameters of several species of RNA and RNA-containing particles (Möller, 1964; Kay and Oikawa, 1966; Wolfe and Kay, 1967). The advantages of this approach are its simplicity, the absence of particle-salt interactions (Meselson et al., 1957), and the small amounts of material required. The measurements made were additionally facilitated by the incorporation of the electronic speed control system into the Spinco model E ultracentrifuge, making it possible to maintain the uniform low speeds (2000 rpm) required for the estimation of  $D_{20,w}^O$ . The procedures used were checked by using highly purified bacteriophage R17 (kindly supplied by Dr. W. Paranchych) as an external standard. The values obtained for  $S_{20,w}^O$  and  $D_{20,w}^O$  of R17 were 81S and  $1.70 \times 10^{-7} \text{ cm}^2/\text{sec}$ , respectively. Assuming that  $\bar{v} = 0.67 \text{ ml/g}$  (Enger et al., 1963), the particle weight of R17 bacteriophage was computed to be  $3.6 \times 10^6$  daltons - in excellent agreement with the value of  $3.6 \pm 0.3 \times 10^6$  daltons

Table 2.4

Comparison of the Physical Properties of Some  
Picornaviruses

	Poliovirus	<u>Encephalomyocarditis viruses</u>		
		EMC	ME	Mengo
$S_{20,w}^O$ ( $\times 10^{13}$ sec)	157-160 <sup>b</sup>	151 <sup>g</sup> , 158 <sup>c</sup>	152 <sup>d</sup>	151
$D_{20,w}^O$ ( $\times 10^7$ cm <sup>2</sup> /sec)	-	-	1.8 <sup>d</sup>	1.47
$\bar{v}$ (ml/g)	0.69 <sup>a</sup>	-	-	0.70
M ( $\times 10^{-6}$ )	6.8 <sup>b</sup>	10 <sup>c</sup>	5.7 <sup>d</sup>	8.3
Dry diameter (m $\mu$ )	27 <sup>a</sup>	27-28 <sup>c, g, k</sup>	24 <sup>d</sup>	26.7, 27-28 <sup>h, k</sup>
Buoyant density (g/ml) *	1.34 <sup>i</sup>	1.33 <sup>f</sup>	1.35 <sup>d</sup>	1.33, 1.33 <sup>h</sup>
% RNA	22-24 <sup>a</sup>	30 <sup>c</sup>	30-35 <sup>d</sup>	23
Frictional ratio	-	-	1.04 <sup>d</sup>	1.10
Hydration (gH <sub>2</sub> O/g dry virus)	0.28-0.37 <sup>b</sup>	-	-	0.23

\*Buoyant densities were calculated from centrifugation in CsCl, except that the value for EMC virus was in RbCl and the value of 1.33 g/ml for Mengo virus was in Cs<sub>2</sub>SO<sub>4</sub>.

<sup>a</sup>Schwerdt and Schaffer (1955)

<sup>b</sup>Schwerdt (1957)

<sup>c</sup>Faulkner et al. (1961)

<sup>d</sup>Hausen and Schäfer (1962)

<sup>e</sup>Burness et al. (1963)

<sup>f</sup>Montaigner and Sanders (1963)

<sup>g</sup>Weil et al. (1952)

<sup>h</sup>Homma and Graham (1965)

<sup>i</sup>Schäfer and Frommhagen (1965)

<sup>j</sup>Rueckert and Schäfer (1965)

<sup>k</sup>Dales and Franklin (1962)

established by light scattering (Gesteland and Boedtker, 1964).

Data presented in Table 2.4 show the close physico-chemical relationships which exist among the encephalomyocarditis viruses; and also the similarities between these viruses and the virus of human poliomyelitis. The low "molecular" weight reported for ME virus by Hausen and Schäfer (1962) is a reflection of the rather high value which these investigators determined for its diffusion coefficient. Their estimation of  $D_{20,w}$  involved an ultracentrifugal method using the Schlieren optical system (Pickels, 1942). The actual values reported show a wide variation from experiment to experiment (e.g. for 5 experiments,  $1.6 \times 10^{-7} \text{ cm}^2/\text{sec} \leq D_{20,w} \leq 2.1 \times 10^{-7} \text{ cm}^2/\text{sec}$ ), indicating that the Pickels method may not be as reliable as the Möller method - especially for determining diffusion coefficients smaller than about  $2 \times 10^{-7} \text{ cm}^2/\text{sec}$ . Also, if one substitutes in the expression  $D = RT/6\pi r \eta_N$  (see Appendix, section 4), the value of  $1.8 \times 10^{-7} \text{ cm}^2/\text{sec}$  for  $D$ , one obtains a diameter of 23.7  $\mu$  for the hydrated ME virion. Hausen and Schäfer (1962) found by electron microscopic observation that the diameter of the anhydrous ME virion was 24  $\mu$ . The "molecular" weight of  $10 \times 10^6$  daltons for EMC virus (Faulkner et al., 1961) was calculated using a density of  $1.37 \text{ g/cm}^3$  for the virion. The  $\text{H}_2\text{O}$ - $\text{D}_2\text{O}$  sedimentation experiments discussed earlier gave a value of  $1.41 \text{ g/cm}^3$  for the Mengo virion.

It seems probable that all encephalomyocarditis viruses



are spherical particles with dry diameters of about 27 m $\mu$ , hydrated diameters of 30 m $\mu$ , and "molecular" weights of approximately  $8 \times 10^6$  daltons.





## Chapter 3

### The RNA and Protein Components of Mengo Virions

#### Introduction

The differences among the Mengo variants with respect to sensitivity to the agar inhibitor (Colter et al., 1964b), rate of attachment to L-cells (Colter et al., 1964a), and affinity for mouse tissues (Campbell and Colter, 1967) must reflect differences in the protein capsids of these variants, and therefore, differences in the sequences of bases in their ribonucleates. This chapter summarizes the results of some preliminary physical and chemical studies on the RNA and protein components of highly purified L-, M-, and S-Mengo virus particles.

#### Materials and Methods

##### Isolation of Viral RNA

RNA was isolated from freshly purified virus by a modified sodium dodecyl sulfate-phenol procedure. Macaloid (Stanley and Bock, 1965) and dextran sulfate (Dickman, 1958) were added to inhibit any ribonuclease which may have been present. All glassware coming into contact with the RNA solution was sterilized beforehand; and all manipulations were carried out between 0 and 5° unless otherwise indicated.

Virus from column chromatography was sedimented by centrifugation at 100,000 g for 1 hour and resuspended in a buffer containing 0.1 M KCl, 0.001 M EDTA, 0.001 M MgCl<sub>2</sub>, and 0.01 M TRIS (pH 7.2). This suspension was then made 1% (w/v)



in sodium dodecyl sulfate and 0.005% in dextran sulfate (molecular weight 60,000 to 90,000; Sigma Chemical Co., St. Louis, Mo.). After incubation at 37° for 10 min and subsequent chilling in ice, a Macaloid suspension was added to give a final Macaloid concentration of 0.2%. Protein was removed by shaking for 1 min with an equal volume of buffer-saturated phenol. The resulting emulsion was centrifuged at 2000 g for 10 min, and the upper aqueous layer was removed without disturbing the interface. Macaloid and phenol were added to this aqueous solution and the extraction procedure repeated twice. Residual phenol was removed by extracting the final aqueous solution 6 times with equal portions of ether; and the ether remaining after this step was removed by bubbling nitrogen through the solution for 30 min.

#### Isolation of protein

Several methods for isolating protein from purified Mengo virus have been tried, including acetic acid precipitation (Harris and Hindley, 1965), dialysis at pH 10-11 (Fraenkel-Conrat and Williams, 1955), and disruption with phenol (Rueckert, 1965). The best recoveries were obtained from the phenol method as outlined below.

Column-purified virus (8-12 mg) was collected by centrifugation at 100,000 g and resuspended in 5 ml of 0.1 M potassium phosphate (pH 7.1). The suspension was then made 1% in sodium dodecyl sulfate, and incubated at 37° for 10 min. After chilling in ice, 3 ml of water-saturated phenol were added, the mixture was shaken vigorously for 3-5





min, and then centrifuged at 2000 g. The protein-containing phenol layer was removed, and the aqueous layer extracted with another portion of water-saturated phenol. To the combined phenol extracts were added 5 volumes of 95% ethanol-0.1 M ammonium acetate. This mixture was warmed briefly ( $45^{\circ}$ ) and then allowed to stand for 2 hours at  $-20^{\circ}$ . The precipitated protein was removed by low-speed centrifugation, washed with 95% ethanol, dissolved in 0.05 M sodium hydroxide and re-precipitated by overnight dialysis ( $4^{\circ}$ ) against 0.05 M sodium phosphate (pH 7.6).

In order to avoid the formation of aggregates by inter-chain disulfide bond formation, the protein was reduced and carboxymethylated in the following manner. The precipitated protein from the dialysate (above) was collected by low-speed centrifugation and washed with 0.05 M sodium phosphate (pH 7.6). It was reduced by being dissolved in 1.8 ml of 0.05 M sodium phosphate (pH 7.6) containing 0.1 M dithiothreitol ("Cleland's reagent"; Calbiochem, Los Angeles, Calif.), 0.005 M EDTA, and 8 M urea (ultra-pure; Mann Research Laboratories, New York, N. Y.), and incubated under nitrogen for 60 min at room temperature. Carboxymethylation was carried out by adding 0.2 ml of freshly prepared 1.0 M sodium iodoacetate (Calbiochem) in 8 M urea and continuing the incubation for 30 min. The reaction was stopped by adding 2 ml of 0.1 M dithiothreitol in 0.05 M sodium phosphate (pH 7.6). The reduced, carboxymethylated (RCM-) protein was precipitated by overnight dialysis against 0.1 M sodium acetate (pH 5), collected by centrifugation, washed twice with water, and stored at  $-20^{\circ}$ .

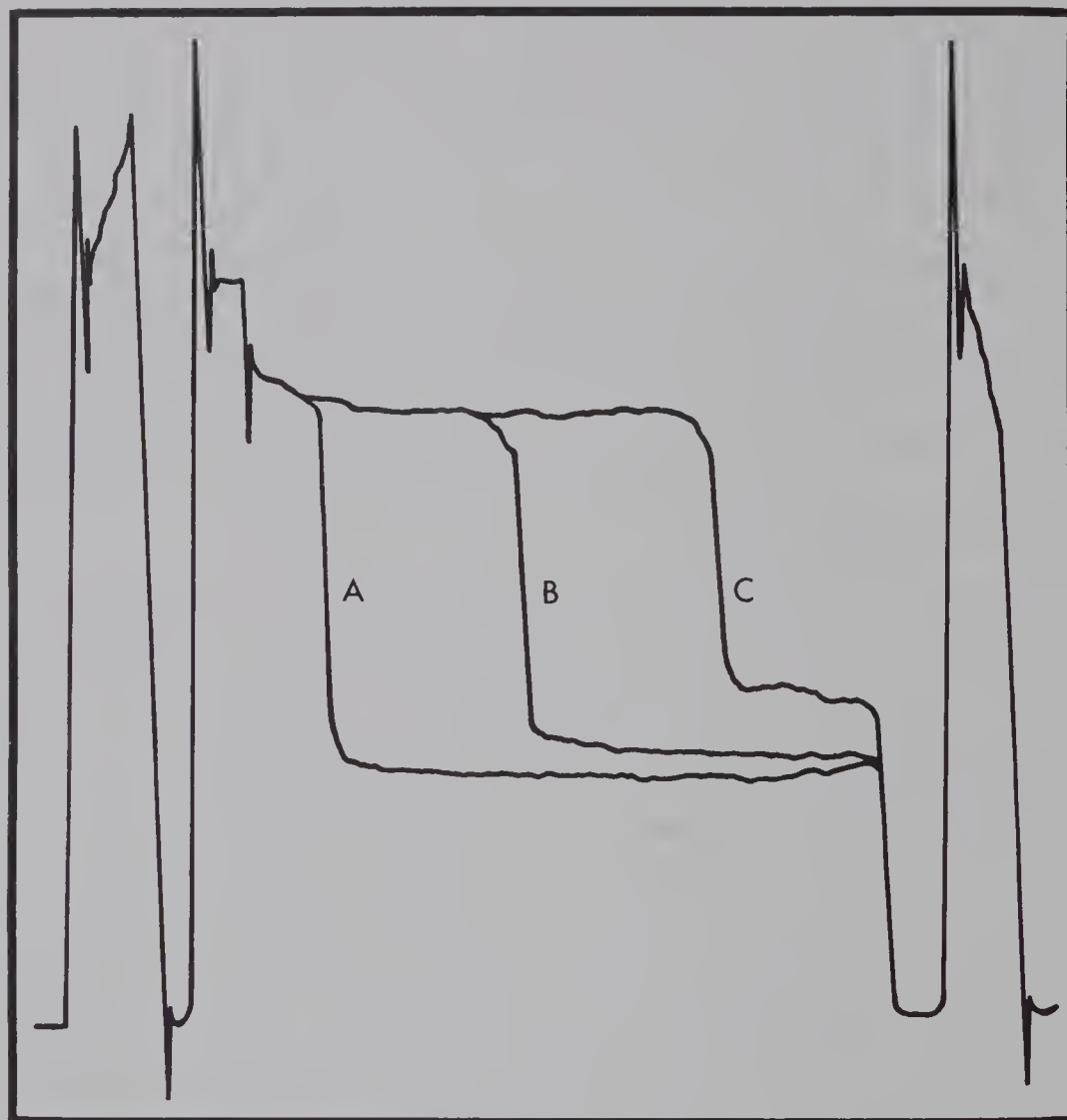


Figure 3.1. Densitometer tracings of photographs taken during the sedimentation of S-Mengo RNA at 60,000 rpm. The solvent was 0.1 M KCl, 0.001 M EDTA, 0.001 M  $\text{MgCl}_2$ , 0.01 M TRIS (pH 7.2). A, B, and C correspond to the boundary at 0, 8, and 16 min, respectively, after reaching top speed.



Table 3.1

Hydrodynamic Properties of the Mengo Virus  
Ribonucleates

Species	$S_{20,w}^0$ ( $\times 10^{13}$ sec)	$D_{20,w}^0$ ( $\times 10^7$ cm <sup>2</sup> /sec)	$\bar{v}$ (ml/g) M ( $\times 10^{-6}$ )
L-Mengo RNA	35.2	1.00	0.53
M-Mengo RNA	35.1	1.14	0.53
S-Mengo RNA	34.8	1.00	0.53
Best average value (4 to 6 determin- ations)	35.0 $\pm$ 0.6	1.04 $\pm$ 0.06	1.74 $\pm$ 0.2

Protein samples for amino acid analysis were prepared from purified virus by the phenol procedure outlined above, except that treatment with SDS was omitted. Some of this protein was oxidized with performic acid according to the procedure of Moore (1963) in order to assay the cystine-cysteine content. Alkylated protein for amino acid analyses was prepared by carboxymethylating the whole virus before isolating the protein (Rueckert, 1965).

### Results and Discussion

#### Hydrodynamic properties of the Mengo virus RNA's

As was done for suspensions of the intact virions, sedimentation and diffusion coefficients for L-, M-, and S-Mengo ribonucleates were determined by analytical ultracentrifugation using ultraviolet-absorption methods. Sedimentation velocity runs were carried out at rotor speeds of 60,000 rpm, while the two-phase diffusion runs on the RNA's involved an initial run for 4 min at 60,000 rpm followed by deceleration to 12,600 rpm and maintenance of that speed for 500 min. The densitometer tracings from a sedimentation velocity run on S-Mengo RNA are shown in Figure 3.1. Essentially all of the material (~90%) sedimented as a sharp boundary which maintained its normal distribution with time, indicating a homogeneous sample with little degradation. Again, sedimentation and diffusion coefficients were found to be the same, within experimental error, for ribonucleates isolated from the three variants. The hydrodynamic parameters for the Mengo virus RNA's are listed in Table 3.1.





Figure 3.2. Products of the hydrolysis of M-Mengo RNA by venom phosphodiesterase: ultraviolet photographs illustrating the separation of nucleotides by two-dimensional paper chromatography. The RNA digest was applied to ammonium sulfate-impregnated paper A alongside a control mixture of 5'-mononucleotides. Chromatographic development was achieved by the descending technique using 80% ethanol as solvent. The paper was then trimmed and sewn onto a second sheet. For development in the second dimension, B, a solvent system of 20 volumes saturated ammonium sulfate: 1 volume isopropanol was used.

The partial specific volume,  $\bar{v}$ , for viral RNA's was assumed to be the same as that for other RNA species (Kay and Oikawa, 1966).

#### Base compositions of the Mengo virus RNA's

Isolated viral RNA was precipitated from aqueous solution by the addition of 2.5 volumes of cold 95% ethanol, re-dissolved in a small amount of water, and lyophilized. For base composition analysis, approximately 20  $\mu\text{g}$  of this RNA was dissolved in 250  $\mu\text{l}$  of water. Fifty  $\mu\text{l}$  of 1.0 M ammonium formate (pH 9.2) and 100  $\mu\text{l}$  of a snake venom phosphodiesterase solution (Hudson et al., 1965) were added, and the mixture was incubated at 37° for 24 hours. During this period, the enzyme (which was kindly supplied by Dr. M. W. Gray), effected the hydrolysis of the ribonucleate to 5'-mononucleotides. Alternatively, RNA was hydrolyzed to 2'-, and 3'-mononucleotides by incubation in 1 N sodium hydroxide at 37° for 18 hours.

Ribonucleotide components of the hydrolysate were resolved by a two-dimensional paper chromatography system described by Gray and Lane (1967). Ultraviolet-absorbing areas were excised from the finished chromatogram, and the nucleotides extracted therefrom with 0.1 N hydrochloric acid. Absorbance spectra of the resulting solutions were recorded against appropriate blanks using a Bausch and Lomb Spectronic 505 spectrophotometer, and the amount of each nucleotide present was calculated from its extinction coefficient in acid (Beavan et al., 1955).

Figure 3.2 illustrates the separation of 5'-mononucleotides obtained by the digestion of M-Mengo RNA with snake

Table 3.2

Base Compositions of Ribonucleates Isolated from  
the Mengo Virus Variants

Variant RNA	Moles %				
	A	U	G	C	G + C
L-Mengo	26.1	26.0	23.0	24.9	47.9
M-Mengo	26.0	25.9	22.8	25.2	48.0
S-Mengo	25.4	26.6	23.7	24.3	48.0



Table 3.3  
Base Compositions of Ribonucleates Isolated  
from Some Picornaviruses

Source of RNA	Moles %				
	A	U	G	C	G + C
Encephalomyocarditis viruses:					
EMC <sup>a</sup>	27.4	25.6	23.7	23.5	47.2
ME <sup>b</sup>	25.1	26.9	23.7	24.2	47.9
Mengo	25.8	26.2	23.2	24.8	48.0
Poliovirus <sup>c</sup>	28.5	25.6	24.0	22.0	46.0

<sup>a</sup>Faulkner et al. (1961)

<sup>b</sup>Rueckert and Schäfer (1965)

<sup>c</sup>Schaffer et al. (1960)





Table 3.4

Amino Acid Compositions of Proteins Isolated from the  
Mengo Virus Variants\*

Amino Acid	L-Mengo Protein	M-Mengo Protein	S-Mengo Protein
Lys	4.1	4.2	4.0
His	1.8	2.2	1.8
Arg	4.0	3.7	3.6
Asp <sup>†</sup>	10.4	10.4	10.2
Thr	8.7	9.5	9.1
Ser	7.5	7.2	7.5
Glu <sup>†</sup>	8.3	8.5	8.5
Pro	7.7	8.0	8.0
Gly	7.3	7.2	7.3
Ala	7.7	6.9	7.2
Val	8.4	8.4	8.6
Met	1.0	1.0	1.2
Ile	3.5	3.4	3.6
Leu	7.5	7.5	7.3
Tyr	3.8	3.9	3.8
Phe	5.4	5.3	5.5
Cys-SH <sup>‡</sup>	1.4	1.7	1.3
Try <sup>§</sup>	1.4	1.6	1.6

\*Results are expressed as moles per 100 moles of amino acids recovered. The values reported are the averages of 24, 48, and 72 hour hydrolyses, except for threonine and serine. The values for these two amino acids were obtained by extrapolation to zero hydrolysis time. There was close agreement between the results of analyses of separate samples of S- and M-Mengo proteins, and agreement between analyses of samples which had been treated in different ways (unmodified, oxidized or carboxymethylated) prior to hydrolysis.

<sup>†</sup>No attempt was made to establish the percentage of acidic residues present in the amide form.

<sup>‡</sup>Cysteine was determined either as cysteic acid following oxidation of the protein, or as S-carboxymethyl cysteine after alkylation.

<sup>§</sup>Tryptophan was estimated by the ultraviolet absorption method of Goodwin and Morton (1946) as described by Beavan and Holliday (1952).

venom phosphodiesterase. No nucleotides other than the four principal ones were detected in any Mengo virus RNA hydrolysate. The two sets of data obtained from analyses of phosphodiesterase and alkaline hydrolysates of S-Mengo RNA were in very close agreement. The base composition data for the Mengo variant ribonucleates are presented in Table 3.2, and show that there are no significant differences among the three types.

Table 3.3, incorporating the average values for L-, M-, and S-Mengo RNA's, illustrates the close similarities in composition among the encephalomyocarditis virus ribonucleates. Poliovirus RNA is slightly different, having more adenine and less cytosine.

#### Amino acid compositions of the viral proteins

Weighed samples of phenol isolated protein (unmodified, carboxymethylated, or oxidized) were dissolved in 6 N hydrochloric acid at a concentration of 0.1 mg/ml in pyrex test tubes (150 x 18 mm, l.x.o.d.). The tubes were then evacuated and sealed, and hydrolysis was effected by heating the samples in an oven at 110°. At appropriate intervals, the tubes were removed, opened, and the acid evaporated at 40° on a rotary evaporator (Buchler Instruments, Fort Lee, N. J.). Analysis of the hydrolysates was carried out according to the procedure of Moore and Stein (1963) using a Beckman/Spinco model 120B automatic amino acid analyzer.

Table 3.4 summarizes the results of amino acid composition analyses of protein isolated from each of the Mengo variants. Tryptophan was determined from the absorption

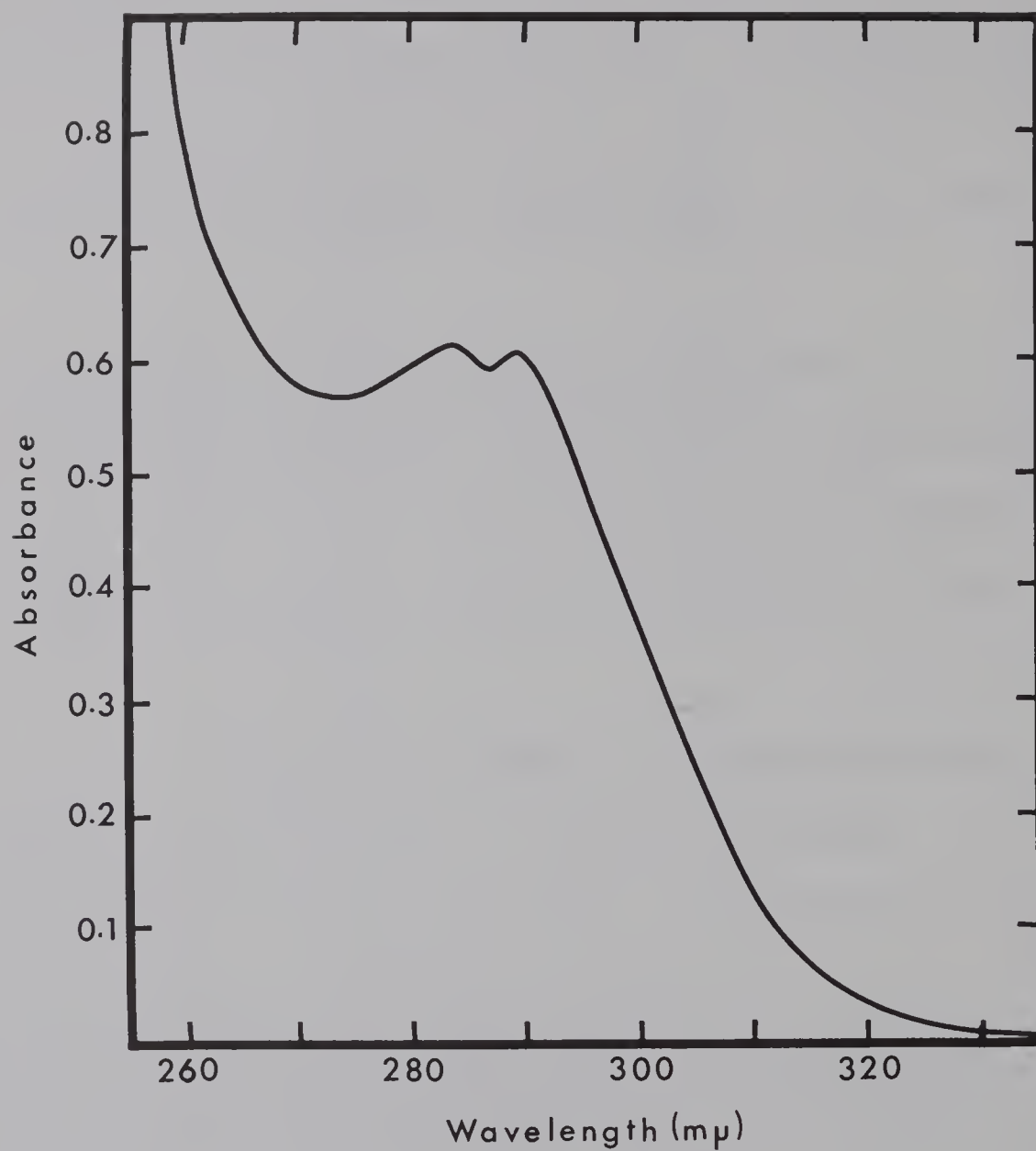


Figure 3.3. Ultraviolet absorption spectrum of M-Mengo virus protein in 0.1 N sodium hydroxide. The concentration was 350  $\mu$ g protein/ml.



spectra of viral proteins in 0.1 N sodium hydroxide (see Figure 3.3). The extinction coefficients ( $E_{280\text{m}\mu}^{1\%}$ ) in alkali were found to be 17.1, 16.8, and 17.0 for L-, M-, and S-Mengo viral proteins, respectively.

Only minor differences in overall amino acid composition exist among the Mengo variant proteins. This finding is not unexpected in view of the fact that the variants are antigenically indistinguishable (Ellem and Colter, 1961). Considering average values, some of the characteristics of Mengo virus protein may be summarized:

1. There is an excess of acidic residues (asp, glu) compared to basic residues (lys, his, arg). The magnitude of this excess is not known because the assay of amide content has not been done.

2. There is a high content of proline (8 mole %), which is known to be a disrupter of the  $\alpha$ -helix. In addition, there is a high percentage (45 mole %) of amino acid residues (val, ile, ser, cys, thr, gly, pro) which are "non- $\alpha$ -helix formers" (Fasman, 1963). These data are consistent with the conclusion, based on ORD measurements, that the viral protein in situ has a low  $\alpha$ -helical content.

3. There are very few sulfur-containing amino acid residues (met, cys-SH, cys) in Mengo virus proteins. Moscarrello and Kaighn (1964) have suggested that "a low amount of sulfur-containing amino acids may be a general property of virus proteins".

4. The high proportion (55 mole %) of non-polar amino acid residues in Mengo virus protein may account for its insolubility in aqueous solvents at pH's below 9. Whole virus, on the other hand, is easily suspended



Table 3.5

Amino Acid Compositions of Some  
Picornavirus Proteins\*

Amino Acid	Poliovirus <sup>a</sup>	<u>Encephalomyocarditis Viruses</u>		
		EMC <sup>b</sup>	ME <sup>c</sup>	Mengo
Lys	4.7	4.9	3.8	4.1
His	2.4	1.2	1.8	1.9
Arg	4.7	3.0	3.5	3.8
Asp <sup>†</sup>	11.9	11.1	10.0	10.3
Thr	9.1	8.7	9.7	9.1
Ser	7.0	8.3	8.0	7.4
Glu <sup>†</sup>	7.7	9.2	7.8	8.4
Pro	7.2	7.0	8.3	7.9
Gly	6.8	8.1	7.0	7.3
Ala	7.8	7.5	7.5	7.3
Val	7.2	6.9	7.0	8.5
Met	1.5	1.4	1.8	1.1
Ile	4.8	4.1	3.8	3.5
Leu	8.5	8.9	7.6	7.4
Tyr	3.9	3.3	4.1	3.8
Phe	4.4	5.4	5.4	5.4
Cys-SH	0.8	1.6	1.2	1.5
Try	-	-	2.3	1.5

\*Results expressed as moles per 100 moles of amino acids recovered.

<sup>†</sup>Includes both acid and amide forms.

<sup>a</sup>Levintow and Darnell (1960).

<sup>b</sup>Faulkner et al. (1961).

<sup>c</sup>Rueckert (1965).



Table 3.6

Calculation of the Partial Specific Volume  
of the Protein from S-Mengo Virus

Amino acid residue	micromoles/mg protein	W% <sup>*</sup>	Vi <sup>†</sup>	W% $\times$ Vi
Lys	0.284	4.15	0.82	3.40
His	.128	1.98	.67	1.33
Arg	.264	4.59	.70	3.21
Asp	.708	9.42	.595 <sup>‡</sup>	5.60
Thr	.644	7.66	.70	5.36
Ser	.504	5.29	.63	3.33
Glu	.588	8.65	.665 <sup>‡</sup>	5.75
Pro	.564	6.49	.76	4.93
Gly	.516	3.87	.64	2.48
Ala	.528	4.70	.74	3.48
Val	.592	6.93	.86	5.96
Met	.096	1.43	.75	1.07
Ile	.256	3.35	.90	3.02
Leu	.504	6.60	.90	5.94
Tyr	.284	5.14	.71	3.65
Phe	.392	6.47	.77	4.98
Cys-SH	.076	0.91	.63	0.57
Try	.116	2.37	.74	1.75
		90.00		65.81

$$\bar{v} = \frac{65.81}{90.00} = 0.731$$

\* Values are expressed as grams of amino acid residue per 100 g protein analyzed.

† Values for the partial specific volumes of amino acid residues, Vi, were taken from Cohn and Edsall (1943).

‡ Values for the acid and amide forms were averaged.

("dissolved") in aqueous buffers at neutral pH values. This suggests that the conformations of polypeptides in the intact virus are such that non-polar residues are directed towards the interior, and polar residues are exposed on the surface.

Table 3.5 presents a comparison of the amino acid compositions of proteins isolated from the encephalomyocarditis viruses and poliovirus. There are a few apparent differences in composition among EMC, ME, and Mengo viral proteins, but the overall patterns are closely similar - and not unlike that for the protein component of poliovirus. The poliovirus protein does appear to have slightly more basic character than the encephalomyocarditis virus proteins: 11.8% lys + his + arg as compared to about 9.3%.

Amino acid composition data may be used to compute the partial specific volumes of proteins (see Schachman, 1957). Table 3.6 illustrates such a calculation done for the protein isolated from a sample of purified S-Mengo virus. The values of  $\bar{v}$  obtained from composition analyses of two samples of M-Mengo protein, two of S-Mengo protein, and one of L-Mengo protein were, respectively, 0.733 ml/g, 0.729 ml/g, 0.731 ml/g, 0.733 ml/g, and 0.729 ml/g. Therefore, an average value of  $\bar{v}$  for Mengo viral protein is 0.731 ml/g.

The total for the W% column in Table 3.6 should be 100.0 if the material isolated from the virus was all peptide in nature. Rueckert (1965), finding that amino acids accounted for only 85% of the weight of "protein" isolated from ME virus, suggested that the virus capsid may contain some carbohydrate material. In the  $\bar{v}$ -determinations for Mengo viral





proteins, it was found that  $\Sigma W\%$  varied considerably - from 72% to 109% - suggesting that in our case, at least, the discrepancies in  $\Sigma W\%$  were the result of errors in determining the exact dry weight of very small quantities of viral protein.

#### Acrylamide gel electrophoresis of disrupted virions

In order to determine whether or not the Mengo virus proteins were composed of more than one type of polypeptide chain, purified virions were disrupted by chemical means and the resulting mixtures were subjected to electrophoresis on polyacrylamide gels. Two methods were used:

1. Polyacrylamide gels were prepared in silicone-coated 5 mm (inside diameter) glass tubes according to the procedure of Davis (1964), except that urea (ultrapure; Mann Research Laboratories, New York, N. Y.) at a final concentration of 8 M was incorporated into all solutions. The "stacking" gel (pH  $\sim 7$ ) consisted of 2.5% acrylamide (Electrophoresis grade; Eastman Organic Chemicals, Rochester, N. Y.), 0.6% BIS (N,N'-methylenebisacrylamide; Eastman), 0.06% TEMED (N,N,N',N'-tetramethylethylenediamine; Eastman); 20% sucrose,  $5 \times 10^{-4}\%$  riboflavin (Mann Research Laboratories, New York, N. Y.), and 0.06 M TRIS (ultrapure; Mann). Polymerization was achieved by exposure to fluorescent light. The "separating" gel (pH  $\sim 9$ ) consisted of 7% acrylamide, 0.18% BIS, 0.03% TEMED, and 0.375 M TRIS. Polymerization was catalyzed by ammonium persulfate (Matheson, Coleman, and Bell, East Rutherford, N. J.) at a final concentration of 0.07%. The electrophoresis runs were carried out in a Canalco model 12 disc electrophoresis apparatus (Canal Industrial Corp.,



Rockville, Md.), equipped with a Harrison model 890A d.c. power supply (Harrison Laboratories, Berkeley Heights, N. J.) which had been modified for constant current output. The time of the runs was 80 min at a current of 3 mA per gel. The upper and lower tray buffer (pH 8.5) was 0.0025 M TRIS, - 0.05 M glycine (ammonia-free; Matheson, Coleman, and Bell). Following electrophoresis, the gel columns were removed from the tubes and stained for 1-2 hours with 1% Aniline Blue Black (Matheson, Coleman, and Bell) in 7% acetic acid. Destaining was done electrophoretically and the gels were stored in 7% acetic acid.

2. The second method used was that of Maizel (Maizel, 1963; Summers et al., 1965), developed for the study of poliovirus capsid proteins. Samples of virus (0.1 ml of a suspension containing 1 mg virus/ml in 0.13 M potassium phosphate) were acidified by the addition of 0.01 ml of glacial acetic acid. Urea and sodium dodecyl sulfate (recrystallized from ethanol) were then added to final concentrations of 0.5 M and 1.0%, respectively. After incubation at 37° for 1 hour, the mixtures were dialyzed for 16 hours against 2500 volumes of 0.01 M sodium phosphate buffer (pH 7.1), containing 0.5 M urea, 0.1% sodium dodecyl sulfate, and 0.1%  $\beta$ -mercaptoethanol. After dialysis, the samples were mixed with one-sixth volume of 60% sucrose and 0.2 ml were layered, under buffer, onto the prepared acrylamide gel columns. Each 5 x 55 mm column was made up of 10% acrylamide, 0.25% BIS, 0.1% sodium dodecyl sulfate, and 0.5 M urea. Polymerization had been catalyzed by final concentrations of 0.05% TEMED and

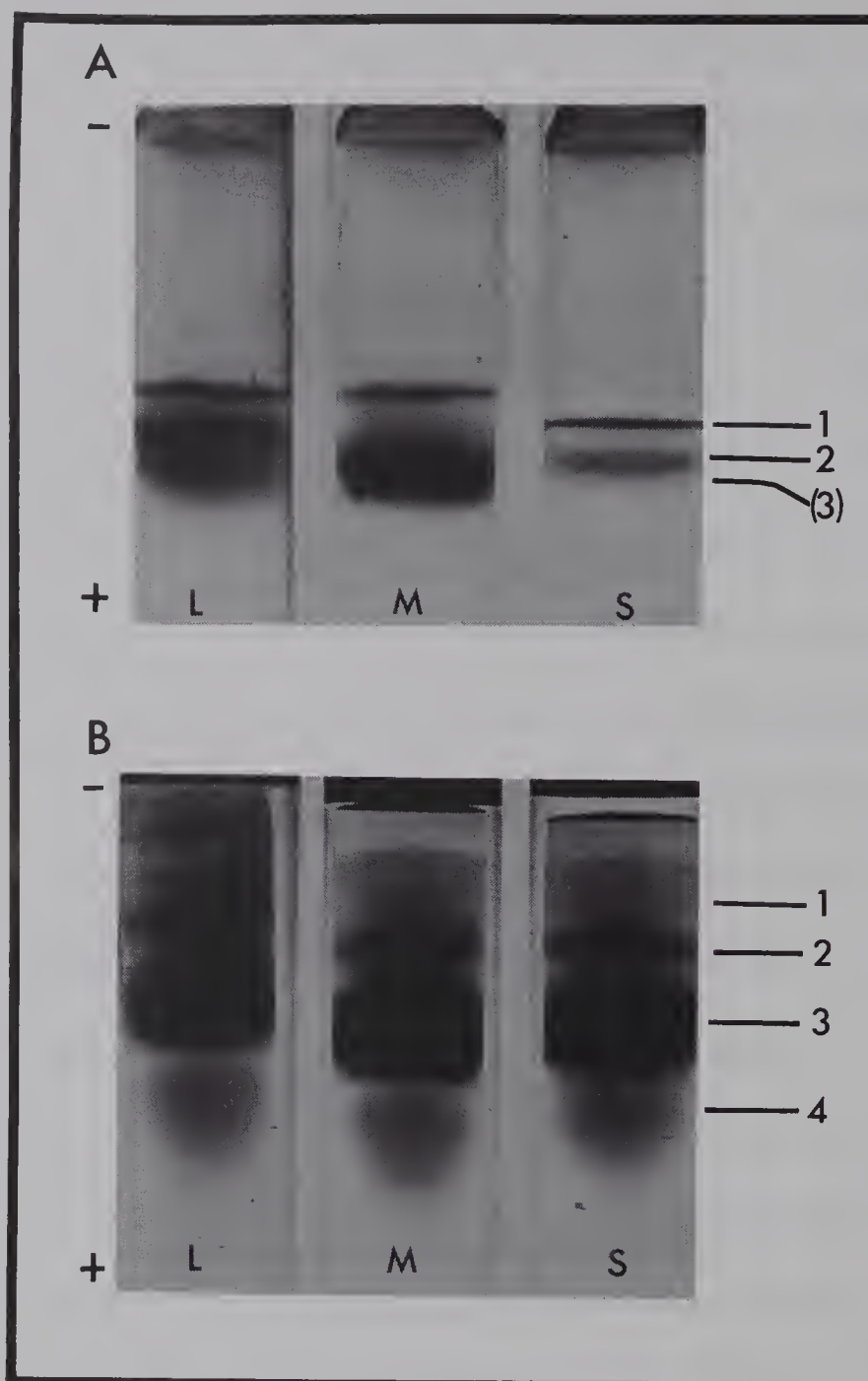


Figure 3.4. Polyacrylamide gel electrophoresis of disrupted L-, M-, and S-Mengo virions. Photograph A is of gels prepared and runs made according to the first method described in the text. Photograph B is of gels prepared and runs made according to the second (Maizel) method. There is no correspondence intended between the protein band numbers in A and those in B.





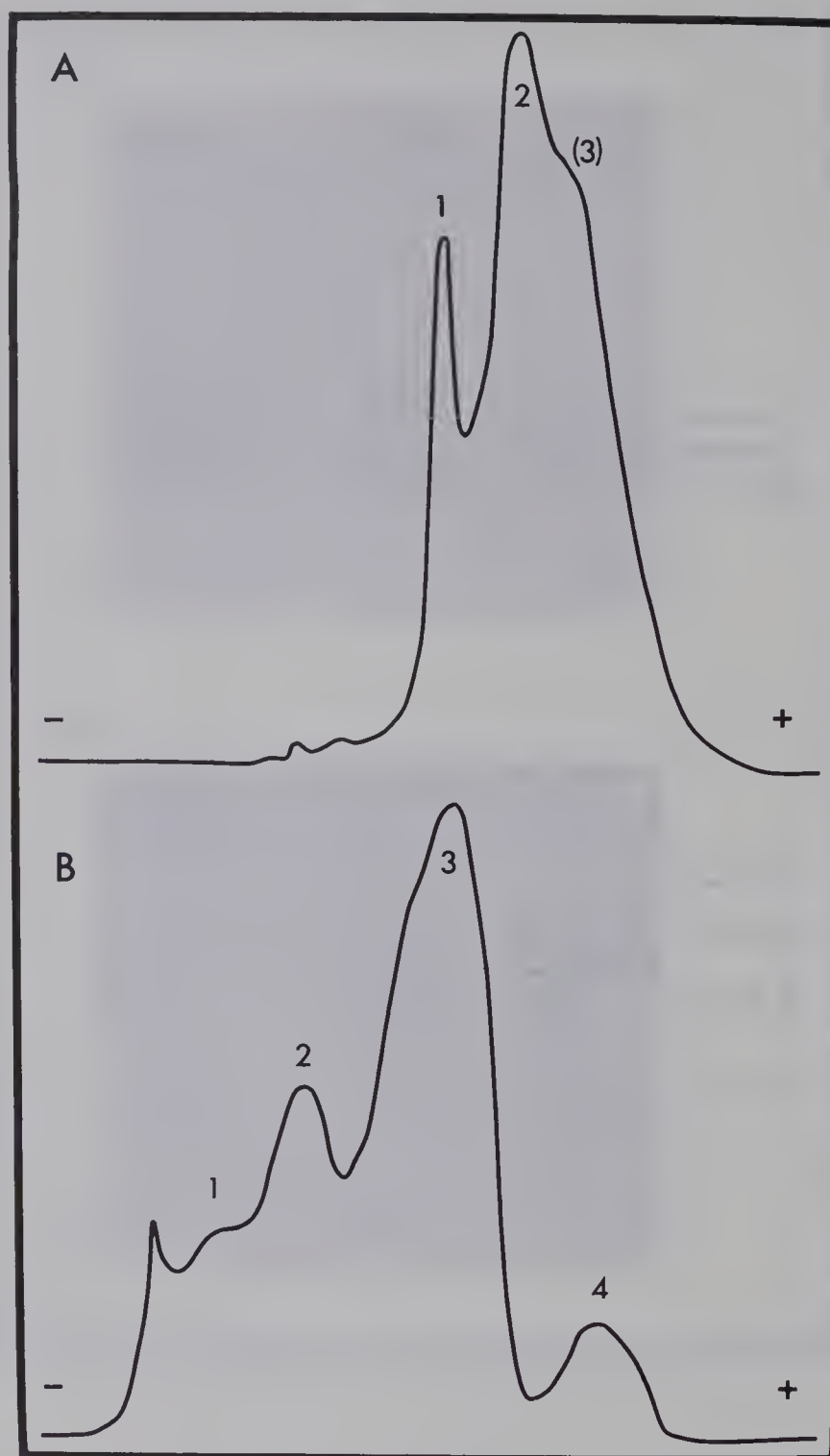


Figure 3.5. Densitometer tracings of the polyacrylamide gels shown in Figure 3.4 for the L-Mengo variant. The tracings were made by using a Gilford model 240 spectrophotometer (Gilford Instruments, Oberlin, Ohio) equipped with a gel scanning device and a recorder. The numbers of the peaks correspond to the bands shown in the photographs of Figure 3.4. Direction of movement was from left to right.



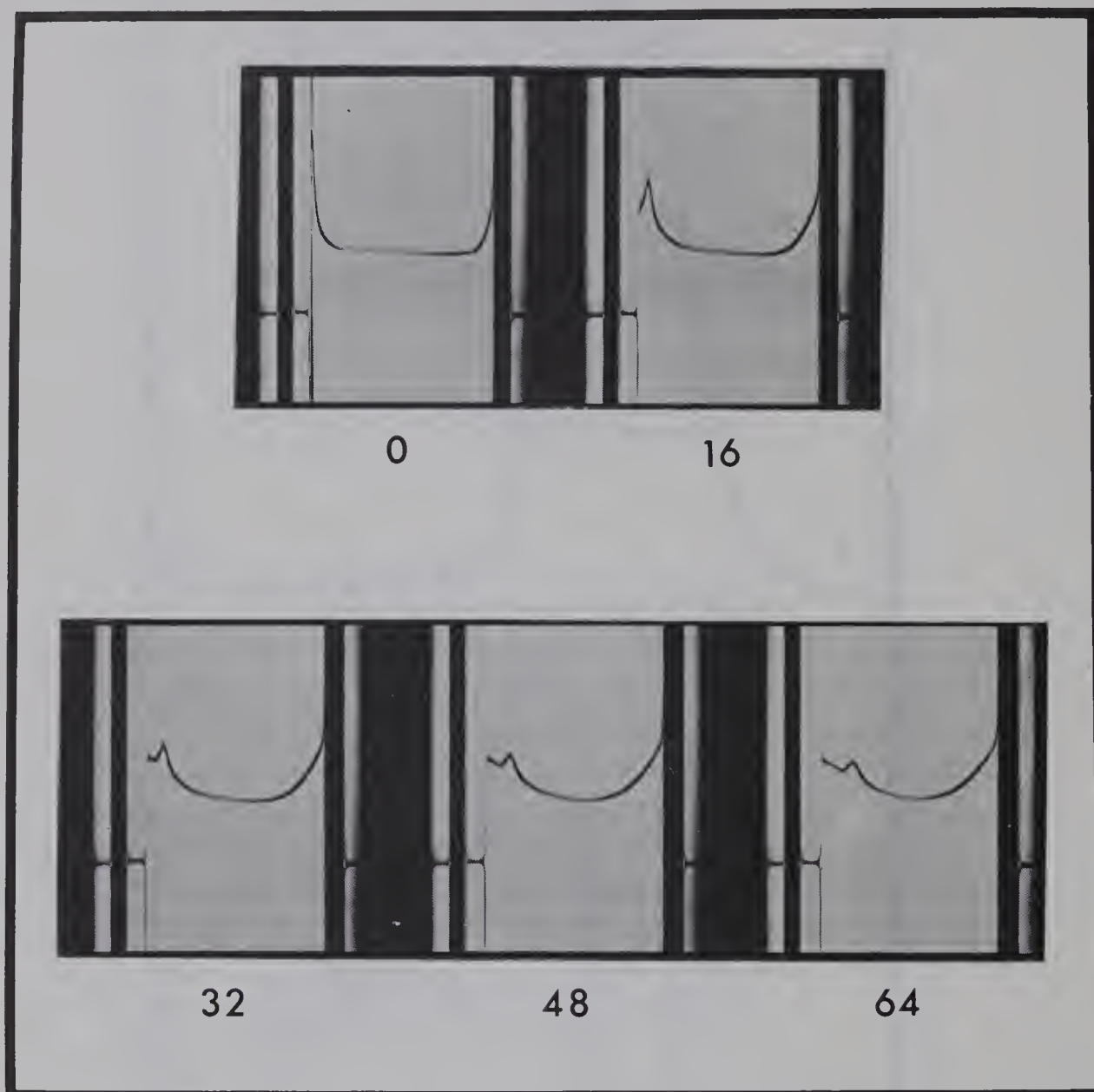


Figure 3.6. Schlieren photographs taken during the sedimentation of carboxymethylated L-Mengo protein in the analytical ultracentrifuge. 20°, 68,000 rpm, 8 M urea. The numbers indicate times after reaching top speed.

0.075% ammonium persulfate. The electrophoresis buffer was 0.1 M sodium phosphate (pH 7.1), containing 0.1% sodium dodecyl sulfate. Separation of components was accomplished by maintaining a current of 4 ma per gel for 3 hours. Following electrophoresis, the gel plugs were removed and stained with Coomassie Brilliant Blue (Consolidated Laboratories, Weston, Ont.), following the procedure of Chrambach et al. (1967).

Photographs of the finished, stained gels appear in Figure 3.4, and densitometer tracings of the two types of gels containing disrupted L-Mengo virus are shown in Figure 3.5. From these preliminary results, it would appear that Mengo virions have two major capsid proteins, and one or two minor ones. Some variations in the electrophoretic mobilities of the proteins isolated from different variants can be seen in Figure 3.4,A.

Rueckert and Duesberg (1966) have reported the existence of three polypeptides in the capsid of ME virus, and Burness and Walter (1967) have found four distinct polypeptides in the capsid of EMC virus.

Some physical properties of carboxymethylated L-Mengo protein

Protein from the L-variant of Mengo virus was isolated, reduced, and carboxymethylated as described under Materials and Methods, the purpose of carboxymethylation being to prevent aggregation by disulfide bond formation (see Rueckert, 1965). This preparation was dissolved in 8 M urea and subjected to analytical ultracentrifugation. Photographs taken during centrifugation are presented in Figure 3.6. The





carboxymethylated protein sedimented as an apparently homogeneous species with an  $S_{20, \text{urea}}$  value of  $1.87 \times 10^{-13}$  sec.

The molecular weight of carboxymethylated L-Mengo protein was estimated by employing the sucrose density gradient centrifugation method of Martin and Ames (1961) as modified by Burness and Walter (1967). Linear gradients of 5-20% sucrose in 8 M urea were prepared in 5-ml centrifuge tubes. The total volume of each gradient was 4.7 ml, and the distance from the meniscus to the bottom of the tube was 4.1 cm. Protein samples of 0.1 ml (in 8 M urea) were layered on top of the gradients, and they were then centrifuged at 38,000 rpm for 72 hours (SW-39 rotor, Beckman-Spinco model L ultracentrifuge). The temperature was maintained at  $13^{\circ}$  during the run to prevent crystallization of the urea. Following centrifugation, fractions of 0.23 ml (10 drops) were collected from the bottom of each gradient, and were assayed for absorbance at 280 m $\mu$ . The sedimentation coefficient of L-Mengo protein was estimated by comparison with that of  $\alpha$ -chymotrypsinogen (kindly supplied by Dr. L. B. Smillie) which was used as an experimental standard. For  $\alpha$ -chymotrypsinogen,  $S_{20, w} = 2.54 \times 10^{-13}$  sec,  $\bar{v} = 0.73$  ml/g, and  $M = 25,000$  (Schwert, 1951). Since the value of  $\bar{v}$  for L-Mengo protein is also 0.73 ml/g, 
$$\frac{\text{distance moved by L-Mengo protein}}{\text{distance moved by } \alpha\text{-chymotrypsinogen}} = \frac{S_{20, w} \text{ of L-Mengo protein}}{2.54 \times 10^{-13} \text{ sec}}$$
 (Martin and Ames, 1961). From this relationship,  $S_{20, w}$  for L-Mengo protein was estimated to be  $2.92 \times 10^{-13}$  sec. This corresponds to a molecular weight of approximately 31,000 (see Schachman, 1959). This value is similar to those found for EMC virus protein (30,000). ME virus

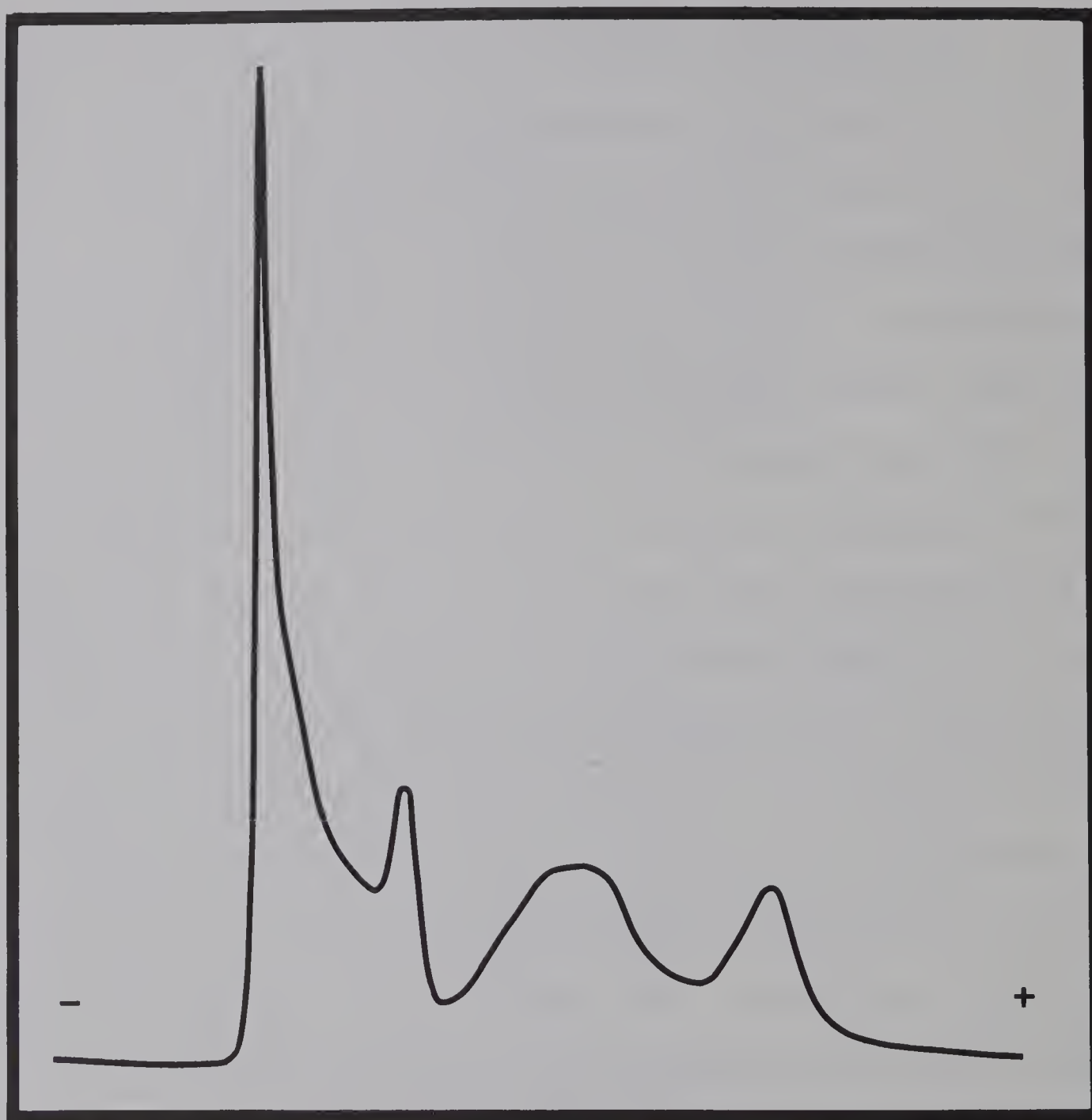


Figure 3.7. Densitometer tracings of stained polyacrylamide gels following the electrophoresis of carboxymethylated L-Mengo protein according to the method of Vande Woude and Bachrach (1968). Direction of movement was from left to right.

protein (26,000) and poliovirus protein (27,000) by Burness and Walter (1967), Rueckert (1965), and Maizel (1963), respectively.

The ultracentrifuge experiments suggested that the capsid of the Mengo virion may, in fact, be composed of a single type of polypeptide. Vande Woude and Bachrach (1968) have reported this to be the case for foot-and-mouth disease virus. These authors found that phenol-extracted FMDV protein gave rise to 5 distinct bands during electrophoresis on polyacrylamide gels containing 8 M urea, but that only one band was observed when the protein was dissolved in 8 M urea, 1% sodium dodecyl sulfate, 0.14 M  $\beta$ -mercaptoethanol and subjected to electrophoresis on 6% polyacrylamide gels containing no urea. They concluded that the presence of urea in the polyacrylamide gels promoted aggregation of the viral protein, which in turn produced multiple bands. Accordingly, carboxymethylated L-Mengo protein was subjected to electrophoresis under the conditions which were reported to give a single band with FMDV protein. The results are shown in Figure 3.7. The appearance of four distinguishable bands argues for the presence of four different polypeptides in the protein capsid of Mengo virus. These may have similar molecular weights, which would rationalize the results of the ultracentrifuge experiments. Burness and Walter (1967) actually separated three proteins from EMC virus and found by sucrose gradient centrifugation that their molecular weights were 32,500, 29,300, and 30,300, respectively.

Further studies are necessary to establish the exact

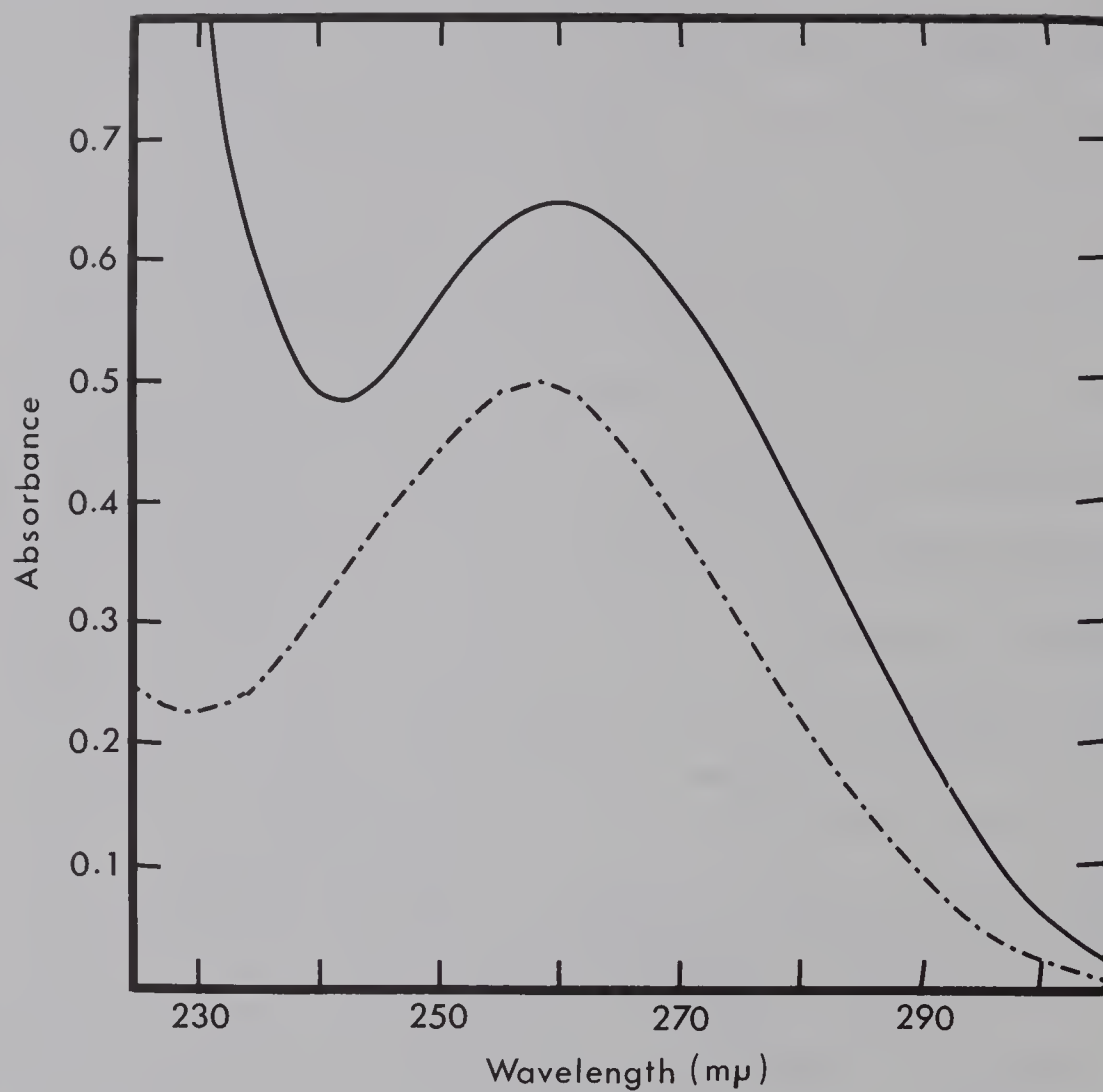


Figure 3.8. Ultraviolet absorption spectra of highly purified Mengo virus (solid line) and Mengo RNA (broken line). The virus concentration was about 85  $\mu\text{g/ml}$ , and the RNA concentration was about 22  $\mu\text{g/ml}$ .



number of polypeptides which compose the Mengo virus protein and the manner in which they are assembled to form the viral capsid. One would also wish to investigate the physical and chemical characteristics of each of the separate polypeptides from each of the three Mengo variants to see what differences might exist among them. Such studies, however, will require somewhat more material than is presently available, and must await the development of methods for isolating or for modifying the viral protein to render it soluble in common buffers. The protein preparations obtained thus far have been found to be soluble only in 8 M urea or in 0.1 N NaOH.

#### Optical properties of the Mengo virions and their RNA's

##### Ultraviolet absorption spectra

The ultraviolet absorption spectra of typical whole virus and viral RNA preparations are depicted in Figure 3.8. The virus is characterized by an absorption trough centered at 242 m $\mu$  and a peak at 260 m $\mu$ , while the RNA exhibits the absorption minimum (at 230 m $\mu$ ) and maximum (at 258 m $\mu$ ) typical of other viral RNA's (Mitra et al., 1963). The  $A_{260 \text{ m}\mu} / A_{280 \text{ m}\mu}$  were 1.65 for whole virus and 2.16 for the extracted RNA. No differences among the three variants were observed.

##### Virus extinction coefficients

Column-purified virus was collected by high-speed centrifugation and resuspended in 0.13 M potassium phosphate (pH 7.1). Samples of 0.010 ml were diluted in 1.000 ml buffer, and their absorbances at 260 m $\mu$  were determined using a Beckman DU spectrophotometer and cuvettes of 1 cm path length. The average absorbance of four samples was used in





the calculation. One-ml aliquots of the original virus suspension and the phosphate buffer were dried to constant weight in a vacuum oven at 60°. From the weight of virus in 0.010 ml, and its absorbance at 260 mμ, the extinction coefficient,  $E_{260\text{m}\mu}^{1\%}$ , was calculated. The values obtained for L-, M-, and S-Mengo viruses were 79.4, 74.0, and 75.6, respectively. It was concluded that the differences were not significant in view of the experimental procedure used, and that for the Mengo variants, the best average value for the extinction coefficient at 260 mμ is 76.3. Rueckert and Schäfer (1965) have reported that ME virus has an  $E_{260\text{m}\mu}^{1\%}$  value of 78 in 0.1 M NaCl (pH 7.2).

#### Optical rotatory dispersion

Optical rotatory dispersion measurements on both virus and RNA preparations were carried out using a Cary model 60 recording spectropolarimeter over a wavelength range of 300 to 210 mμ. The slit width of the instrument was programmed to yield maximum and constant light intensity at all wavelengths. The polarimeter tubes had a light path length of 1 cm, and for measurements in the region of absorption, the absorbance was not allowed to exceed 1.5. The ORD was not measured at wavelengths longer than 300 mμ, since much higher concentrations of virus and RNA would have been required; consequently no data are available for the calculation of Drude or Moffitt constants (see Fasman, 1963). The rotations were expressed in terms of specific rotation,  $[\alpha] = 100 \alpha / cd$  where  $\alpha$  is the measured rotation in degrees,  $c$  the concentration in g/100 ml, and  $d$  the path length in decimeters. The virus concentration was estimated from its extinction

Table 3.7

Optical Rotatory Dispersion Parameters of Mengo  
Viruses and their RNA Components

Species	Cotton effect (m $\mu$ )	$[\alpha]_{\text{max}}^{\circ}$ (284-285m $\mu$ )	$[\alpha]_{\text{min}}^{\circ}$ (251-253m $\mu$ )	$[\alpha]_{234}^{\circ}$
M-Mengo	270	+466	-1689	-1311
L-Mengo	270	+420	-1560	-1160
S-Mengo	270	+490	-1510	-1110
M-Mengo RNA	265	+4100	-4000	-325
L-Mengo RNA	265	+3975	-3875	-400
S-Mengo RNA	265	+4238	-3938	-398



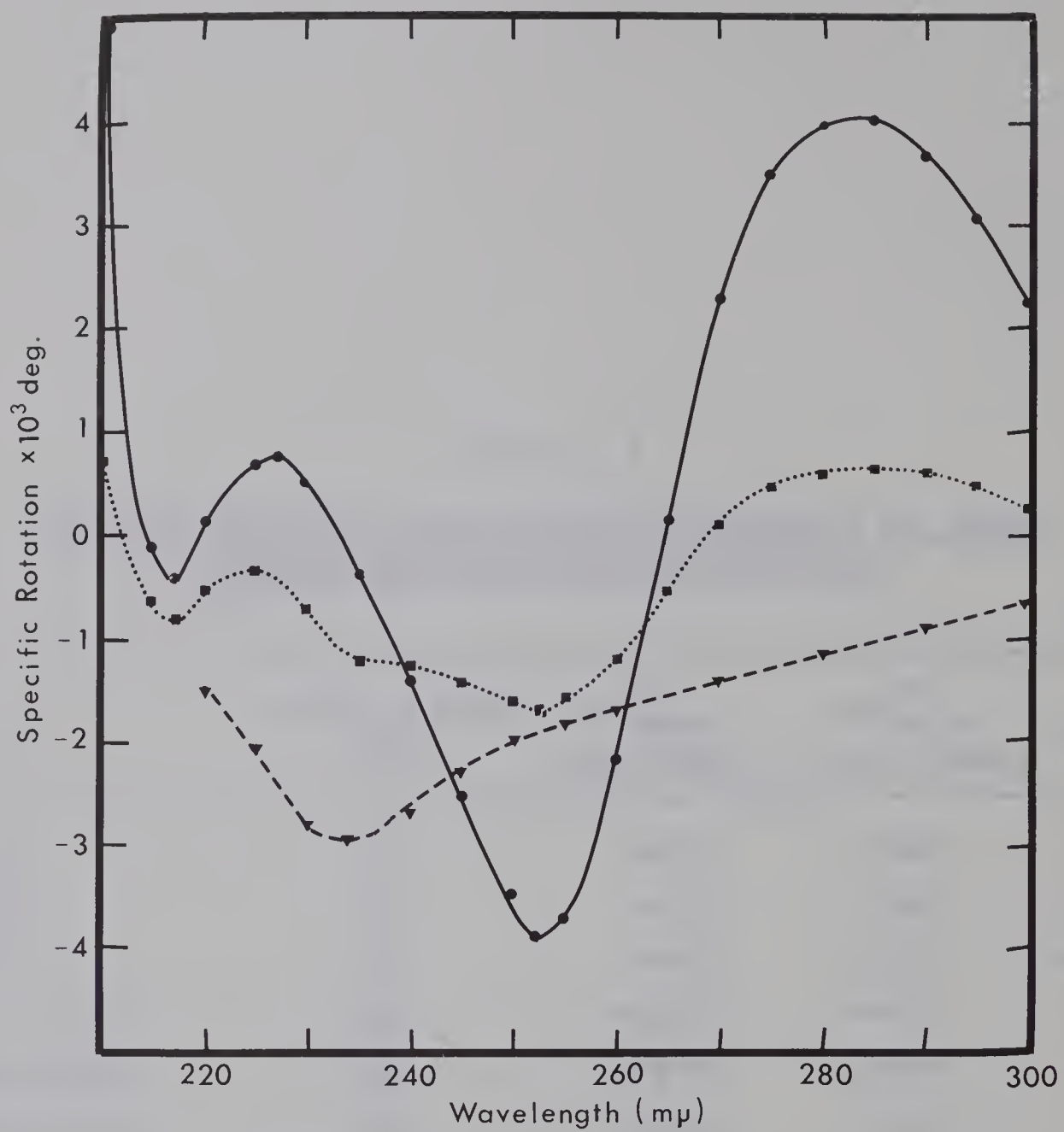


Figure 3.9. Optical rotatory dispersion spectra of M-Mengo virus (■), viral RNA (●), and viral protein (▼). The solvent was 0.1 M KCl, 0.001 M MgCl<sub>2</sub>, 0.001 M EDTA, 0.01 M TRIS (pH 7.2).



coefficient,  $E_{260\text{m}\mu}^{1\%} = 76.3$ ; and the RNA concentration was estimated from an assumed extinction coefficient of  $E_{260\text{m}\mu}^{1\%} = 225$  (Cohen and Stanley, 1942).

In order to examine the ORD of the viral protein in situ, virus was placed in one of the 1-cm cells of a differential cell holder (Applied Physics Corp., Palo Alto, Calif.) and RNA at the same concentration as that in the virus was placed in the matched cell. The difference spectrum, corresponding to the ORD of the viral protein, was scanned over the wavelength range of 300 to 210  $\text{m}\mu$ .

The optical rotatory dispersion of the Mengo virus variants was found to be highly reproducible, and a representative illustration of the data obtained with a preparation of M-Mengo is depicted in Figure 3.9. The prominent Cotton effect is centered at about 270  $\text{m}\mu$ , the position characteristic of the viral RNA, but the existence of an additional feature due to the presence of  $\alpha$ -helical protein is evident in the negative limb. A comparison of the ORD for the three variants and their constituent ribonucleates shows that the curves are essentially identical to one another, with similar cross-over points, positions of troughs and peaks, and amplitudes. The pertinent features of the ORD of the Mengo viruses and RNA's are summarized in Table 3.7.

Figure 3.9 also shows the ORD of the protein in the M-Mengo virus (triangles), deduced by experimentally subtracting the ORD of the RNA component from that of the virus. The protein curve exhibits a negative Cotton trough with the minimum at about 234  $\text{m}\mu$ , the position characteristic of an



$\alpha$ -helical polypeptide chain. The validity of the protein ORD curve rests upon the assumptions that the rotations due to the protein and RNA components within the virus are additive, and that the rotations of the isolated RNA are the same as those of the RNA in the virus. These assumptions have some experimental support. Studies on wheat embryo ribosomes (Wolfe and Kay, 1967) have shown that the protein-by-difference ORD curve, obtained as described above, corresponded remarkably well with the ORD curve for isolated ribosomal protein, and that a calculated curve for a hypothetical mixture of 55% ribosomal RNA and 45% ribosomal protein was virtually identical to the measured ORD curve for intact ribosomes.

Accepting these assumptions, one can estimate a value for the helical content of the Mengo virus protein based upon the depth of the Cotton trough at 233-234 m $\mu$  (Yang, 1967). The helical content was estimated to be about 4% (see Appendix, section 9).

In view of the essentially identical ORD characteristics of the three variants of Mengo virus as well as of their constituent ribonucleates, it may be concluded that the manner in which the protein subunits are arranged around the RNA chains in the virus is precise and similar in all three cases. It is interesting that the protein in its native environment possesses little  $\alpha$ -helix, based upon measurements of the amplitude of the Cotton trough minimum at 234 m $\mu$ . The trough is shallow in this region, a feature also indicative of low helical content (Jirgensons, 1966). It would appear that the



viral protein possesses little  $\beta$ -structure, since this form is characterized by a trough at 230  $m\mu$  (Sarkar and Doty, 1966). The finding of low helical content is in contrast to the high degree of helicity ( $>90\%$ ) observed for the protein of the rod-shaped bacteriophage, fd (Day, 1966), and the 30% helicity of the protein of rod-shaped tobacco mosaic virus (Simmons and Blout, 1960). Perhaps asymmetry of the protein and helicity are closely related in the case of viral proteins, as they apparently are for fibrous proteins (Cohen and Szent-Györgyi, 1957).





## Chapter 4

### Differences Among L-, M-, and S-Mengo Virions

#### Introduction

The results of the investigations outlined in Chapters 2 and 3 did not reveal any significant differences among the L-, M-, and S-Mengo virions or among their isolated protein and ribonucleate components. Indeed, at this stage, one can only state that "Mengo is Mengo is Mengo ..." in terms of gross physical and chemical parameters. It must be concluded, therefore, that subtle differences in the sequences of bases in the polynucleotides, and consequently in the primary structures and, possibly, conformations of the polypeptide components are responsible for the diverse biological properties of the Mengo virions.

That there are subtle molecular differences among L-, M-, and S-Mengo virions has been demonstrated by the results of experiments to be discussed in this chapter.

#### Procedures and Results

##### The resolution of L-Mengo virus from M- or S-Mengo

Hydroxylapatite chromatography. Column chromatography of partially purified S- or M-Mengo at pH 7.1 was shown to result in a clean separation of virus from contaminating cellular material; but separation of L-Mengo virus from contaminants is not achieved unless the pH of the eluting phosphate buffer is lowered to 6.2. This phenomenon probably reflects differences in the nature, number, and/or distribution of charged

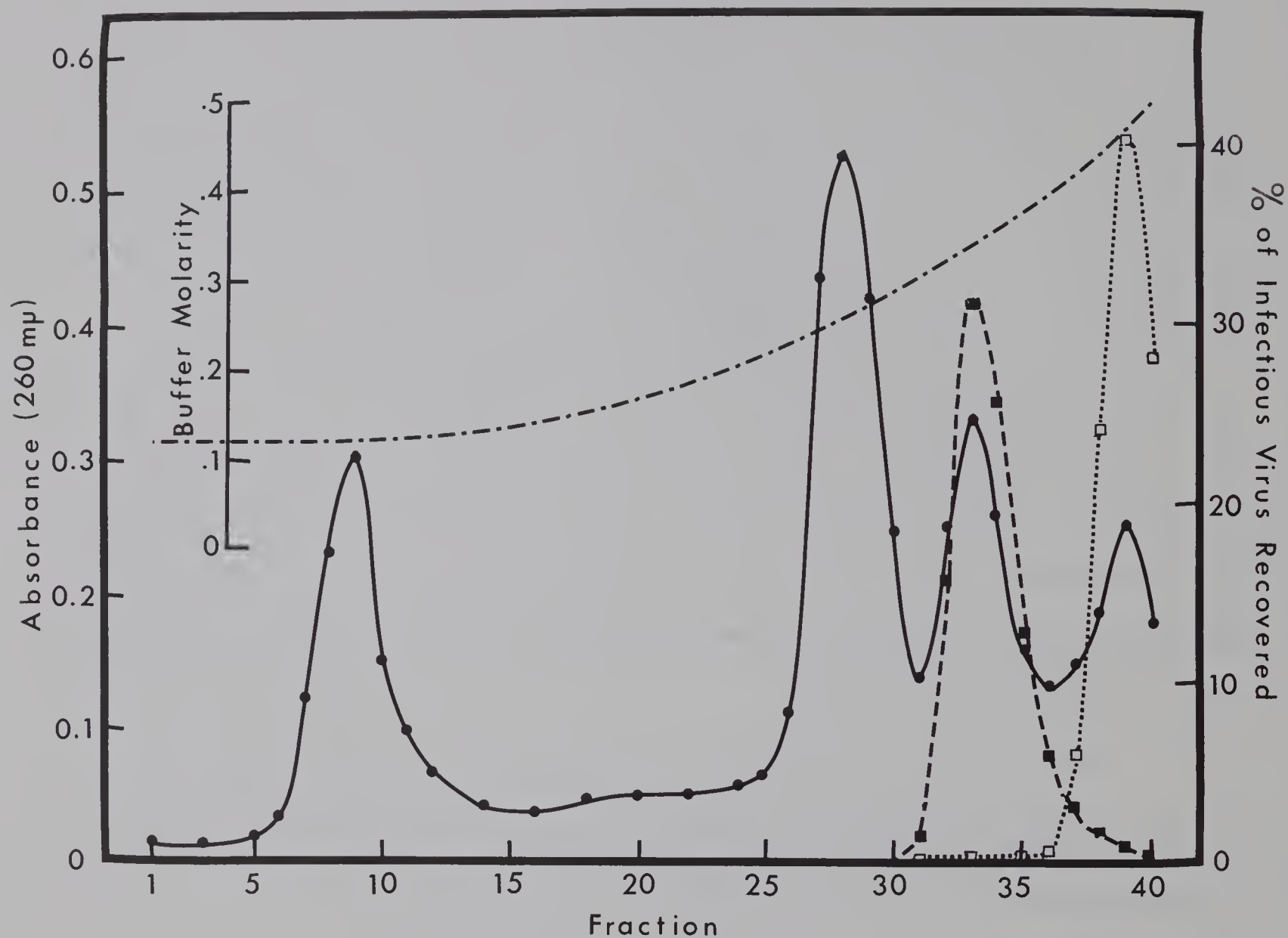


Figure 4.1. Chromatography of a mixture of L-Mengo and M-Mengo viruses (partially purified) on hydroxylapatite. Elution was at pH 6.2, and 5-ml fractions were collected.

● = absorbance, ■ = L-Mengo virus, □ = M-Mengo virus.



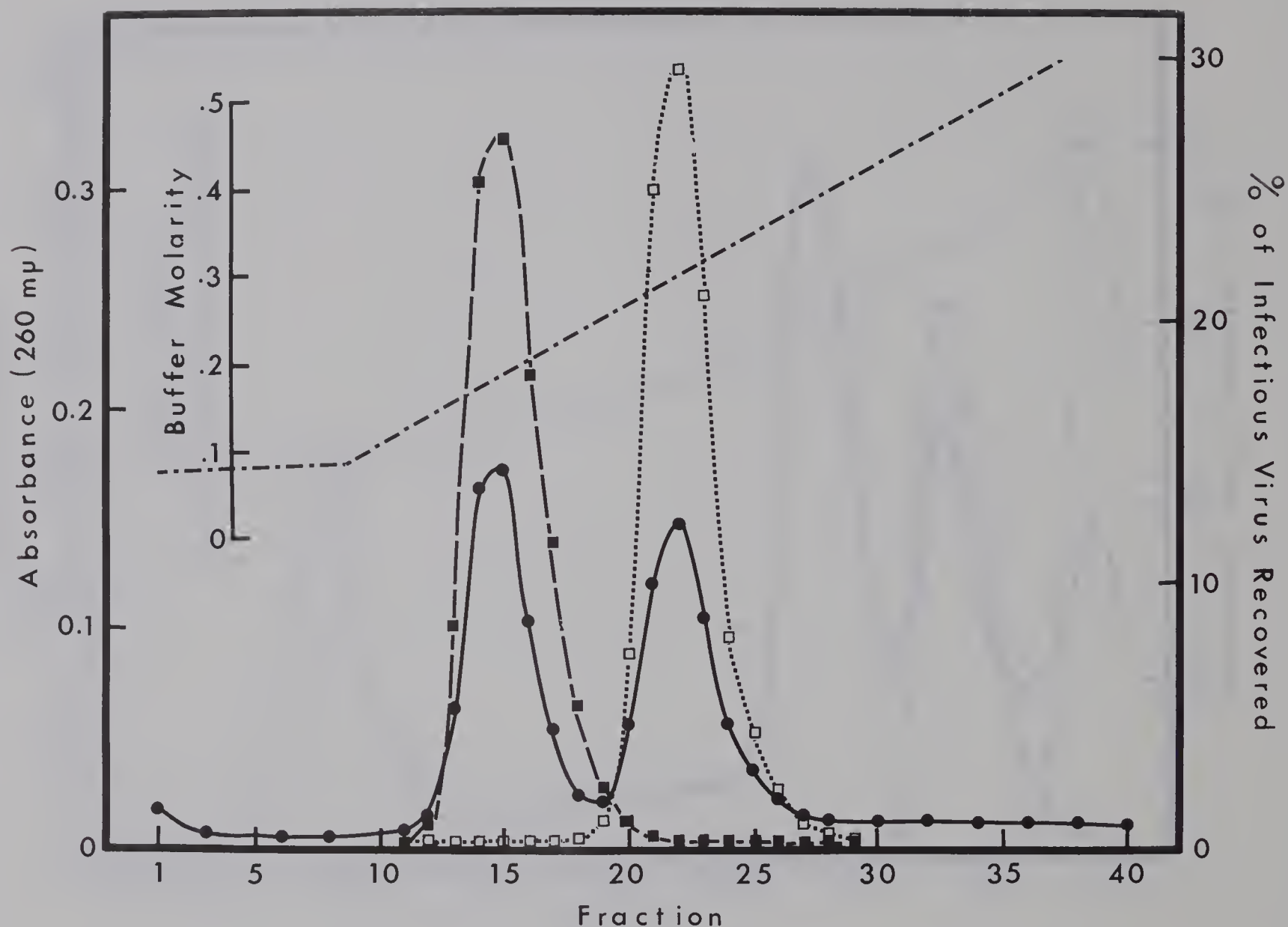


Figure 4.2. Chromatography of a mixture of L-Mengo and S-Mengo viruses (highly purified) on hydroxylapatite. Elution was achieved by a linear gradient of potassium phosphate at pH 7.1. 5-ml fractions were collected.

● = absorbance, ■ = L-Mengo virus, □ = S-Mengo virus.



groups on the surfaces of the three types of virions, and makes it possible to resolve L-Mengo from either M- or S-Mengo by hydroxylapatite column chromatography. Figure 4.1 illustrates the elution pattern obtained when a partially purified mixture of L- and M-Mengo was chromatographed at pH 6.2. The virus peaks were characterized as L-Mengo and M-Mengo on the basis of plaque morphology. When highly purified L- and S-Mengo samples were mixed and chromatographed on hydroxylapatite at pH 7.1 using a linear buffer gradient, the elution pattern shown in Figure 4.2 was obtained. Chromatographic separation of M- and S-Mengo was not achieved by any of the experimental conditions examined.

Dextran sulfate density gradient centrifugation.

Bengtsson et al. (1964) demonstrated that strains of poliovirus that differ in plating efficiency in the presence of polyanions may be separated by centrifugation in pre-formed gradients of dextran sulfate. Since the Mengo variants differ in sensitivity to the anionic "agar inhibitor" (Colter et al., 1964b), it was considered possible that they too might sediment at different rates in dextran sulfate gradients.

Dextran sulfate-2000 (prepared from dextran with an average molecular weight of  $2 \times 10^6$ ) was obtained from Pharmacia (Uppsala, Sweden), and was fractionated by alcohol precipitation according to the procedure of Bengtsson et al. (1964) before use. Linear gradients of 1.0 to 4.5% dextran sulfate, stabilized with sodium iodide (0 to 1.8%), were prepared in 5-ml centrifuge tubes by using a two-chamber

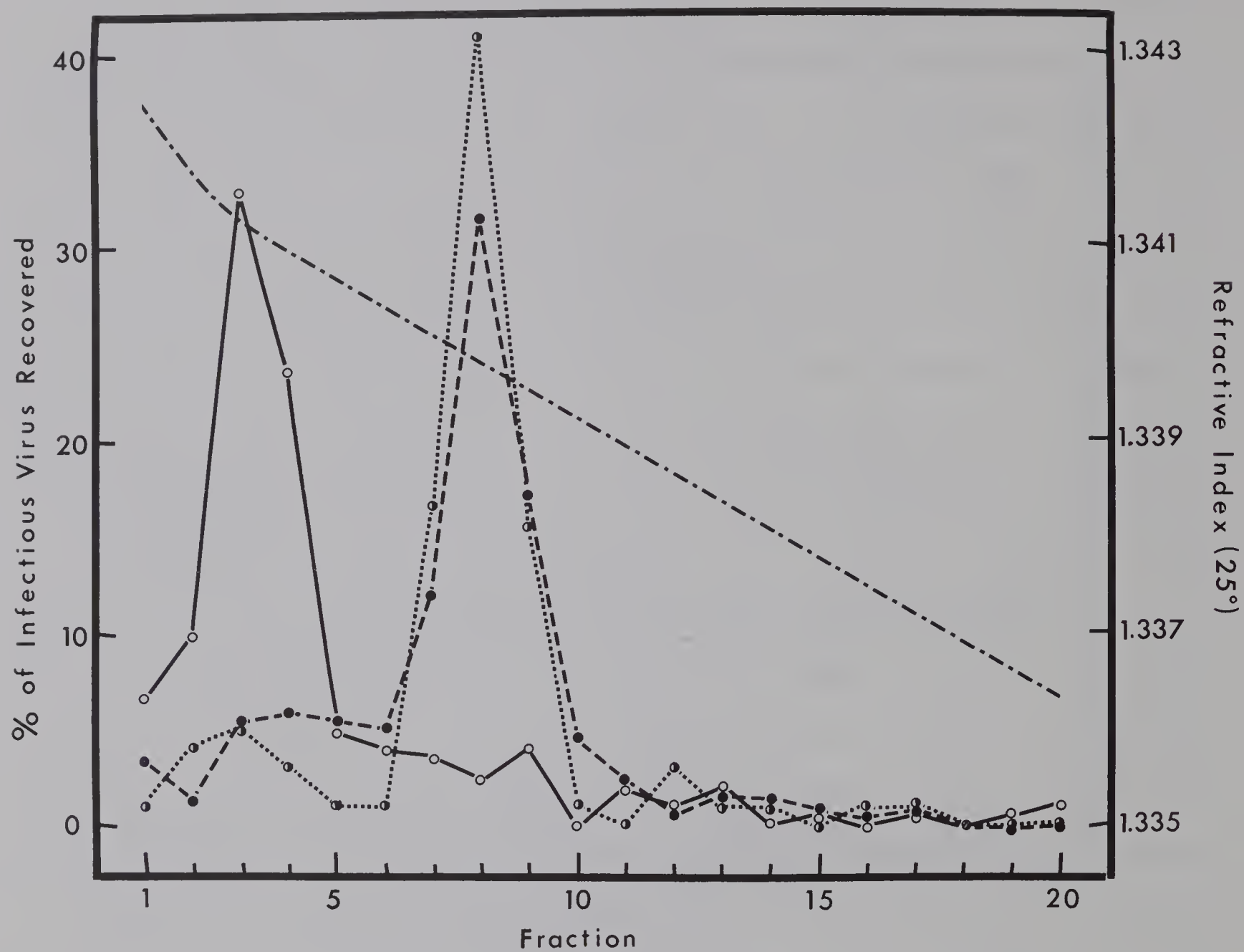


Figure 4.3. Sedimentation of Mengo virus variants in density gradients of dextran sulfate.

○ = L-Mengo, ◐ = M-Mengo, ● = S-Mengo

mixing device (Buchler Instruments, Fort Lee, N. J.). The buffer used was 0.05 M potassium phosphate (pH 7.0) containing 0.1% bovine plasma albumin (Mann Research Laboratories, New York, N. Y.). An aliquot of highly purified virus (0.1 ml) in 0.05 M potassium phosphate (pH 7.1) was carefully layered on top of each gradient, which was then centrifuged at 35,000 rpm for 70 min in the SW-39 swinging-bucket rotor of the Spinco model L ultracentrifuge. After centrifugation, 0.2 ml fractions were collected dropwise from the bottom of each gradient, and were assayed for infectious virus. The refractive index of each fraction was also measured using an Abbé-type refractometer (Bausch and Lomb, Rochester, N. Y.) in order to establish that the gradients were linear and directly comparable.

The results, depicted in Figure 4.3, show that M- and S-Mengo sediment at the same rate in such gradients, but that L-Mengo sediments significantly faster. Since binding of dextran sulfate by polioviruses tends to decrease their sedimentation rates in these gradients (Bengtsson et al., 1964), it would seem likely that at pH 7, L-Mengo binds less dextran sulfate than does M- or S-Mengo.

This interpretation fits reasonably well with the relative sensitivities of the variants to the "agar inhibitor" (Colter et al., 1964b). On the basis of relative sensitivities to this sulfated polysaccharide (Campbell, 1965), the expectation was that the Mengo virus variants would bind increasing amounts of dextran sulfate in the order  $S > M > L$ ; i.e., L-Mengo was expected to sediment most rapidly in dextran sulfate





gradients, and S-Mengo, least rapidly.

The binding of dextran sulfate by the Mengo variants is likely electrostatic in nature, because other experiments have shown that it is weak and readily reversible. For example, pre-incubation of purified L-, M-, or S-Mengo virions with 1% dextran sulfate was found to have no effect on either their melting profiles or their rates of sedimentation in sucrose gradients.

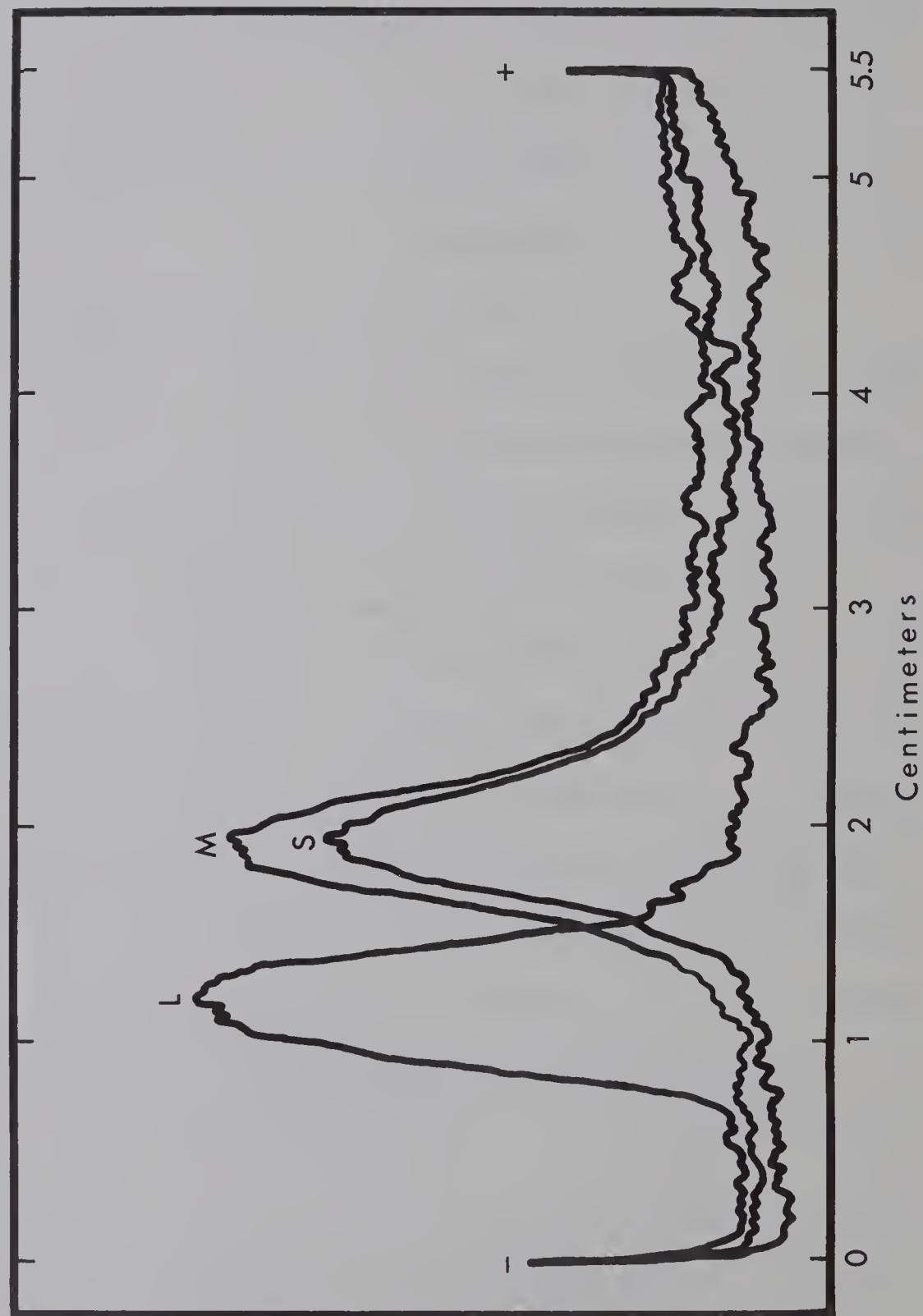
Also, since each of the variant virions carries a net negative charge at pH 7 (see below), the binding of dextran sulfate probably occurs at discrete sites on the surfaces of the virions which carry a positive charge.

The clear separation of L-Mengo from the other two variants by centrifugation in dextran sulfate density gradients is closely reminiscent of the separation of mutants of poliovirus differing in plating efficiency in the presence of polyanions. Perhaps there is a correlation among sensitivity to polyanions, sedimentation rate in dextran sulfate gradients, and virulence for several of the picornaviruses.

Agarose gel electrophoresis. Several attempts were made to determine if there were differences in net surface charge among the three types of Mengo virions at physiological pH's. Electrophoresis of whole virus in agarose gels indicated that each of the three Mengo virions carries a net negative charge at pH 7.1, and that the magnitude of this



Figure 4.4. Densitometer tracings of stained agarose gels following electrophoresis of the L-, M-, and S-variants of Mengo virus. Direction of movement was from left to right.



negative charge is smaller for L- than for M- or S-Mengo virions.

Electrophoresis was performed using a Canalco model 6 apparatus (Canal Industrial Corp., Bethesda, Md.), fitted with silicone-coated glass tubes of 5-mm internal diameter. Agarose (Industrie Biologique Française S.A., Gennevilliers, France) was used as the supporting medium. The separating medium of 0.8% agarose in 0.1 M potassium phosphate (pH 7.1) was melted, poured into the electrophoresis tubes to a height of 50 mm, and allowed to cool to form a solid gel. Samples (0.2 ml) of purified virus were mixed with melted 0.3% agarose, applied to the tops of the separating gels, and allowed to cool. Electrophoresis was carried out under 0.1 M potassium phosphate buffer (pH 7.1) at a current of 4 ma/gel for 9.5 hours ( $4^{\circ}$ ). The gels were then removed from the supporting tubes and fixed for 12 hours in 20% sulfosalicylic acid. The virus was visualized by staining with nigrosin, as described by Uriel (1964). Photographs of the stained gels were made on Polaroid transparencies, and the transparencies were scanned with a Spinco Analytrol densitometer. The densitometer tracings obtained are depicted in Figure 4.4.

Amino acid composition analyses of Mengo viral proteins (Chapter 3) have shown that acidic residues predominate over basic residues by a factor of about 2 to 1. At neutral pH, the acidic residues would carry a negative charge; therefore, one would predict that, at pH's close to neutrality, the net overall charge on L-, M-, and S-Mengo virions would be negative. Electrophoresis of whole virus on agarose gels



has shown this to be the case. The finding that L-Mengo virions have less net charge than either M- or S-Mengo virions is in agreement with the results of the dextran sulfate density gradient sedimentation experiment, which suggest that, of the three types, L-Mengo virions have the largest binding capacity for dextran sulfate molecules.

The absorbance - temperature profiles for the Mengo variants

Bachrach (1964;1965) used absorbance-temperature measurements to follow the degradation of foot-and-mouth disease virus (FMDV) and the release of its RNA component; and from such measurements was able to make inferences about the structure of the virion. It was hoped, therefore, that similar studies of the Mengo virus variants and their RNA's might reveal some structural differences among them.

The instrumental assembly for monitoring the "melting" behavior (i.e. the absorbance changes accompanying changes in temperature) of L-, M-, and S-Mengo viruses and their isolated ribonucleates consisted of a Beckman DB-G spectrophotometer, a "T<sub>m</sub>-analyzer" temperature programmer, and a 10" recorder (Beckman Instruments Inc., Fullerton, Calif.). The rate of temperature increase for all samples was 0.7°/min, and absorbance changes were followed at a wavelength of either 260 mμ (whole virus) or 258 mμ (viral RNA).

Chromatographically purified virus was used in these experiments; the virus being collected from the appropriate column fractions by high-speed centrifugation and resuspended in 0.10 M potassium phosphate (pH 7.1) to give an absorbance



Figure 4.5. Ultraviolet absorption photographs taken at 4-min intervals during the sedimentation of L-Mengo RNA. 52,640 rpm, 20°, 0.10 M potassium phosphate (pH 7.1).





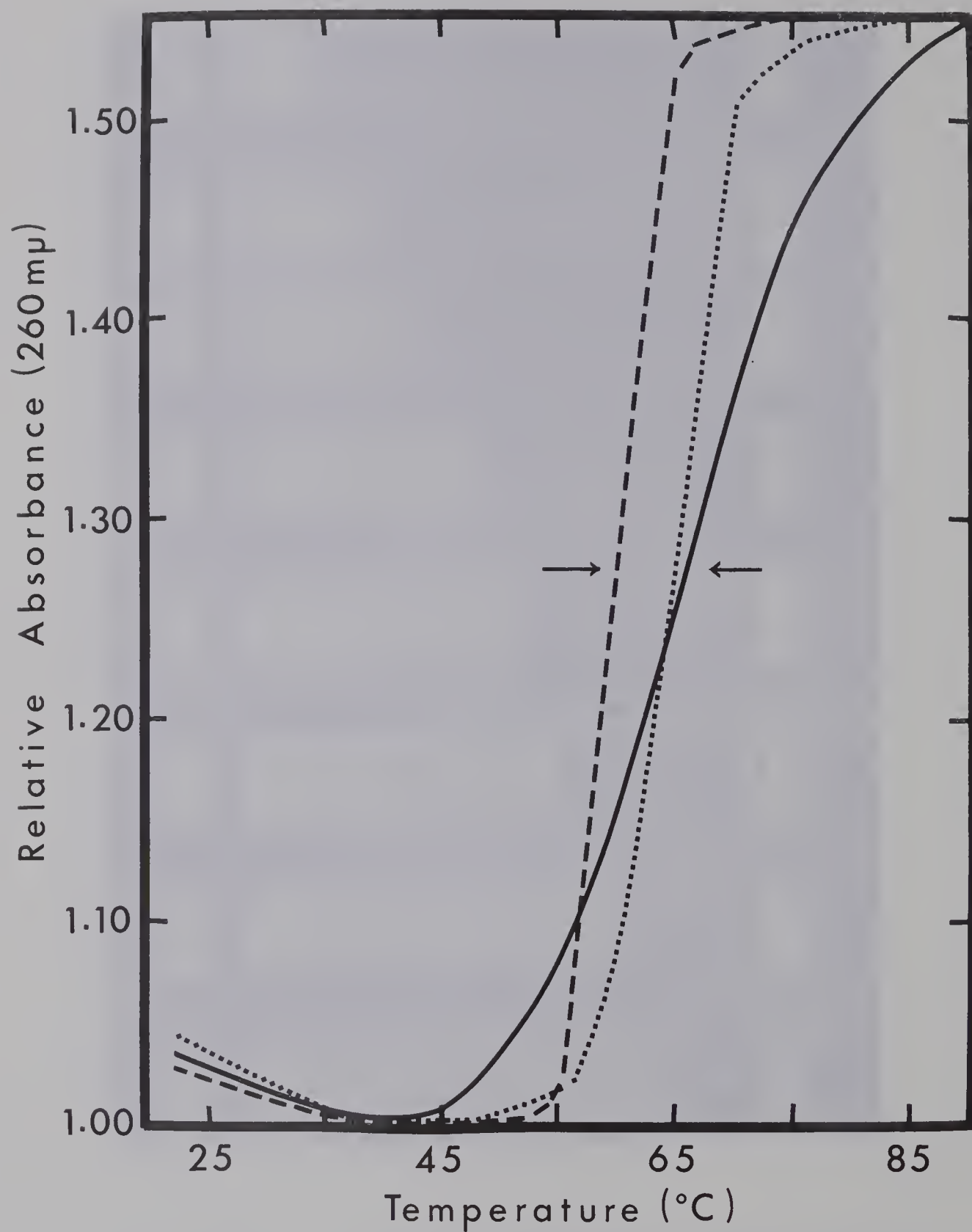


Figure 4.6. Melting curves for the Mengo virus variants in 0.10 M potassium phosphate (pH 7.1).

— = L-Mengo  
 - - - = M-Mengo  
 ..... = S-Mengo



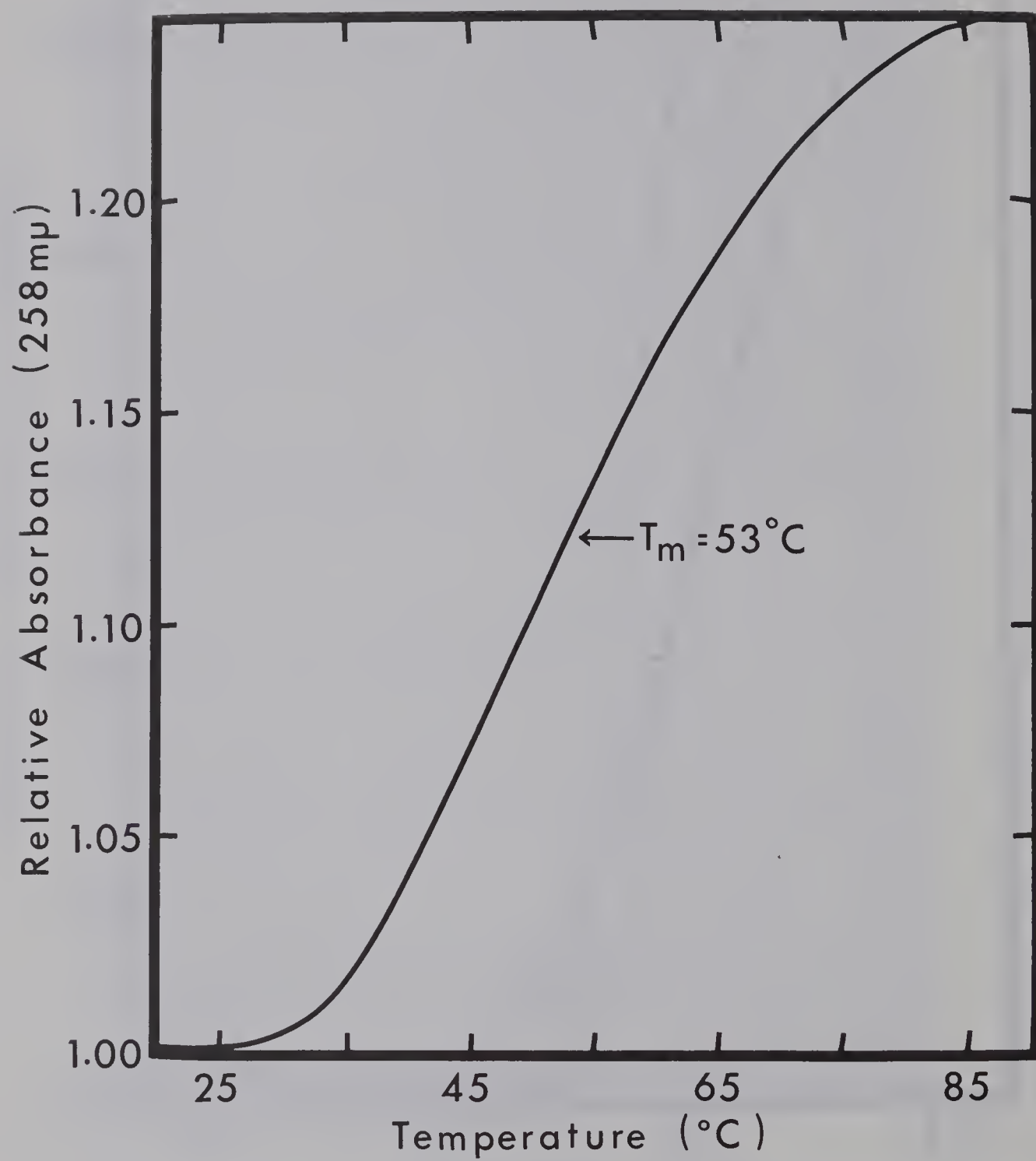


Figure 4.7. Melting curve for phenol-extracted Mengo RNA in 0.10 M potassium phosphate (pH 7.1).





Table 4.1

Melting Characteristics of the Mengo Variants  
and of Mengo RNA

Species	T <sub>m</sub>	Temperature range over which 90% of the hyperchromic change occurred	Net hyperchromicity (A <sub>90°</sub> /A <sub>25°</sub> )
L-Mengo	66	25	1.53
M-Mengo	60	5	1.54
S-Mengo	65	10	1.52
Mengo RNA*	53	48	1.24

\* No differences could be detected among the RNA's isolated from the three variants.

reading of approximately 0.3 at 260 m $\mu$ . It was found that the use of buffers of higher phosphate molarities caused precipitation of viral material at temperatures higher than 65°. Such precipitation prevented the measurement of maximum hyperchromicity.

For purposes of comparison, viral RNA was prepared as described in Chapter 3, except that all solutions used in the procedure were made up in 0.10 M potassium phosphate (pH 7.1). The change in buffer did not alter the sedimentation characteristics of the viral RNA, as is shown by Figure 4.5. Thus, the melting curves recorded for viral RNA's reflected the conformational changes occurring in intact molecules.

The characteristic melting curves for the Mengo virus variants are depicted in Figure 4.6, and a comparison of the features of these curves is presented in Table 4.1. The melting curve typical of ribonucleates isolated from L-, M-, or S-Mengo virus is shown in Figure 4.7 and described in Table 4.1. The hyperchromism observed upon heating the virus particles or the viral RNA's was real, and did not arise from light scattering - the absorbance increase at wavelengths of 260 m $\mu$  or 280 m $\mu$  was always much greater than that at non-absorbing wavelengths (340 m $\mu$ ). If light scattering had been a factor, one would have expected the change in absorbance at 340 m $\mu$  to exceed that at 260 m $\mu$  because the turbidity of a scattering solution varies as the fourth power of the wavelength of the incident light (Oster, 1948).





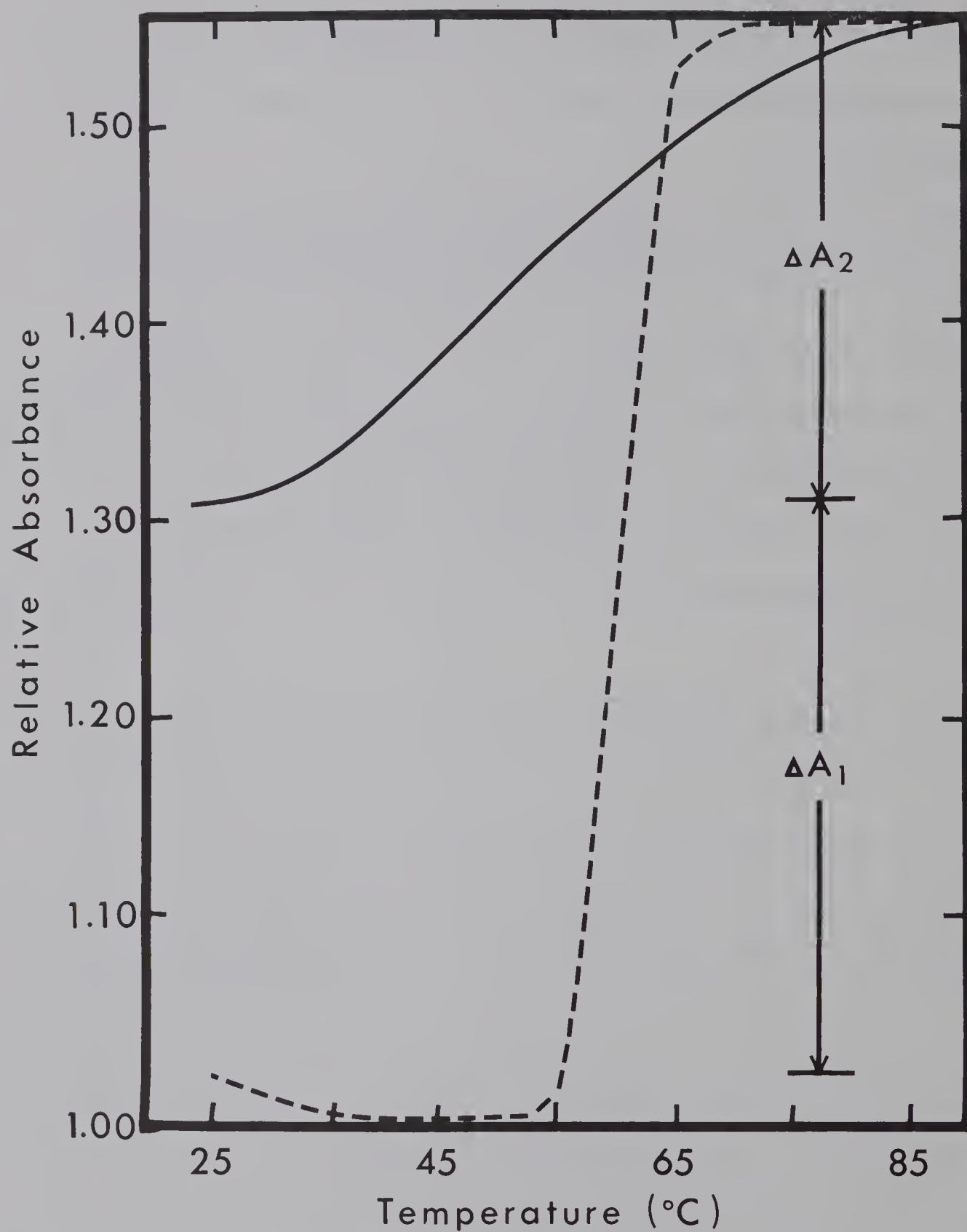


Figure 4.8. Comparative melting curves for M-Mengo virus (---) and phenol-extracted M-Mengo RNA (—), in 0.10 M potassium phosphate (pH 7.1). Relative hyperchromicities illustrate the tight packing of RNA within the virus particle (see text).



Although the melting profiles and  $T_m$ 's were found to be characteristic for each of the Mengo variants, a feature common to all three was resistance to hyperchromic change until the temperature reached about  $50^\circ$ . Assuming that all, or nearly all, of the absorbance at  $260\text{ m}\mu$  is attributable to the viral RNA, the resistance to hyperchromic change indicates stabilization of the conformation of the RNA within the virus particle by the protein capsid (the  $T_m$  of isolated RNA is  $53^\circ$ ).

A second feature common to the three virus melting profiles is a small but distinct hypochromism (2-3%) which accompanies the increase in temperature from  $20^\circ$  to  $45^\circ$ . Since the formation of hydrophobic bonds is an endothermic process (Kauzmann, 1959), this initial hypochromism may reflect a conformational rearrangement in the virions involving increased hydrophobic interactions between (a) the nitrogenous bases in the ribonucleates; and/or, (b) apolar components of the ribonucleates and those of the protein capsid.

A composite of the melting curves for M-Mengo virus and phenol-extracted M-Mengo RNA is presented in Figure 4.8, and shows that the hyperchromicity accompanying the temperature increase from  $25^\circ$  to  $90^\circ$  is much greater for the whole virus ( $\sim 52\%$ ) than for the isolated RNA ( $\sim 24\%$ ). Since the absorbance change for virus particles was measured at  $260\text{ m}\mu$ , one may assume that the observed hyperchromicity reflects the conformational change in the viral RNA alone, the protein component making no significant contribution. Thus, the 52% hyperchromicity ( $\Delta A_1 + \Delta A_2$ ) corresponds to the change in RNA conformation from a highly compact, highly intramolecularly



hydrogen- and hydrophobically-bonded structure within the virus capsid to a completely random structure with minimal intramolecular interactions in solution at  $90^{\circ}$ . The 24% hyperchromicity ( $\Delta A_2$ ) observed for the isolated RNA corresponds to the conformational change from an interacting random coil with some secondary and tertiary structure at  $25^{\circ}$  to a non-interacting chain at  $90^{\circ}$ . The absorbance change  $\Delta A_1$  is, therefore, indicative of the decrease in base-stacking and hydrogen-bonding which occurs upon release of the RNA from the virus particle into solution. The radius of gyration of Mengo RNA within the virus particle has been estimated to be about  $40 \text{ \AA}$ , while that of Mengo RNA in solution at  $25^{\circ}$  is about  $300 \text{ \AA}$  (Appendix, section 10). The substantial increase in this parameter upon removal of the RNA from the capsid implies the unstacking of base chromophores and, therefore, increased absorbance.

Colter et al. (1964a) demonstrated that crude pools of the M-variant of Mengo virus undergo a dramatic and irreversible loss in infectivity during brief incubation at pH 6.0-6.4. This loss of infectivity is much smaller for S-Mengo, and is negligible for L-Mengo. Campbell (1965) has postulated that at the low pH, the M-Mengo capsid "loosens", becoming permeable to nucleases present in the crude preparation. These nucleases then destroy the integrity of the viral genomes. Comparison of the melting curves for L-, M-, and S-Mengo virions at pH's 7.1 and 6.2 gives some support to this premise. When L-Mengo or S-Mengo virions were pre-incubated (60 min,  $25^{\circ}$ ) in 0.10 M potassium phosphate at pH









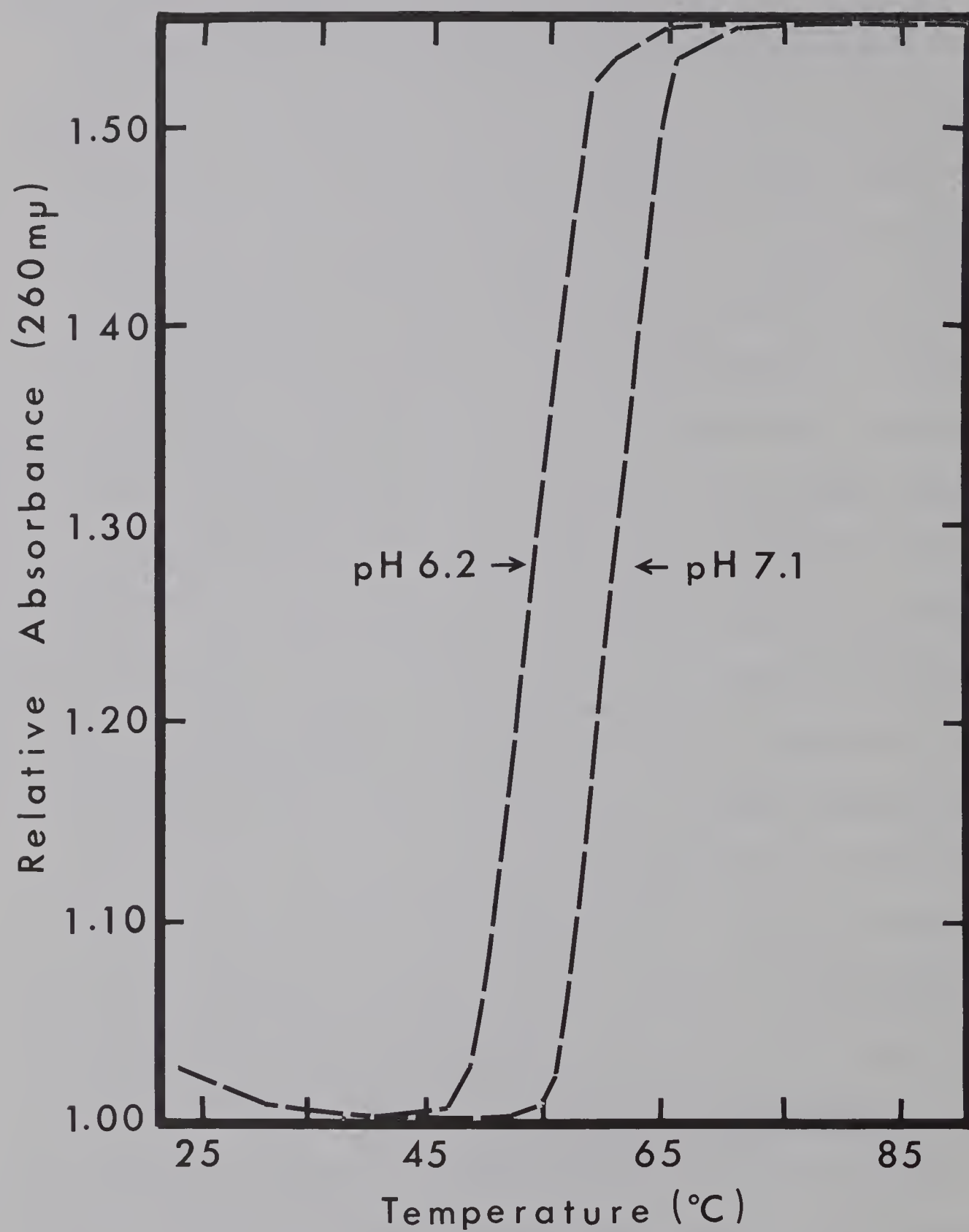


Figure 4.9. The effect of pH on the melting curve of M-Mengo virus (0.10 M potassium phosphate).

6.2, and melted in this buffer, absorbance-temperature curves identical to those observed at pH 7.1 were obtained. However, in the case of M-Mengo virions, the  $T_m$  was found to decrease from  $60^\circ$  at pH 7.1 to  $55^\circ$  at pH 6.2 (Figure 4.9). The protein capsid of the M-variant seems clearly to become more heat-labile when the pH is lowered.

Bachrach (1965) observed a remarkable stabilizing effect of magnesium ions on the secondary structure of FMDV-RNA in solution. He reported that the  $T_m$  of this ribonucleate in 0.02 M sodium phosphate (pH 7.5) increased from  $54^\circ$  to  $77^\circ$  when  $10^{-3}$  M  $Mg^{++}$  was added. The stabilizing effect of this divalent cation was confirmed by a comparison of the melting curves of phenol-extracted Mengo virus RNA in 0.10 M potassium phosphate (pH 7.1) in the absence and the presence of  $10^{-3}$  M  $MgCl_2$ . The addition of  $MgCl_2$  was found to increase the  $T_m$  from  $53^\circ$  to  $58^\circ$ . The fact that a higher concentration of salt was present during the melting of Mengo RNA than was employed by Bachrach in his studies of FMDV-RNA may explain the more dramatic effect of magnesium ions in the latter system. Divalent magnesium stabilizes RNA secondary structure by suppressing the negative charges in the phosphate backbone (Penniston and Doty, 1963); monovalent cations also have the same effect, but are not as efficient (Gesteland and Boedtker, 1964).

#### The total particle:infectious particle ratios for the Mengo variants

Numerous samples of column-purified virus were titrated by the plaque assay method, and their absorbances at





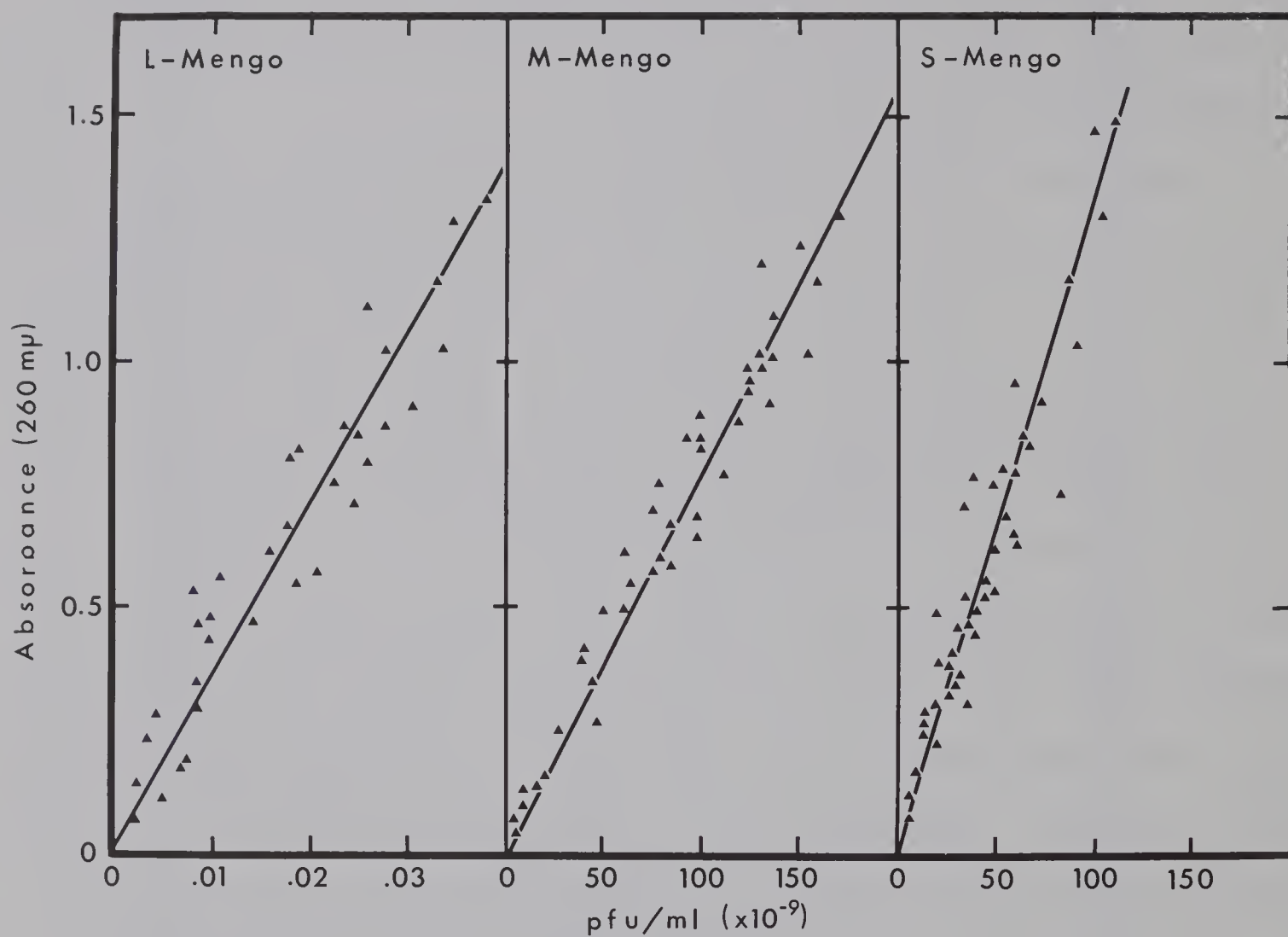


Figure 4.10. Relationships between absorbance and plaque-forming units for highly purified preparations of L-, M-, and S-Mengo viruses.





Table 4.2

Total:Infectious Particle Ratios for the  
Mengo Virus Variants

Variant	Calculated	Experimental
L-Mengo	3450	1500
M-Mengo	76	50
S-Mengo	113	60

260 m $\mu$  measured spectrophotometrically. A correlation of these data is presented in Figure 4.10. Assuming that absorbance is directly proportional to the total concentration of virus particles, it is clear that the total:infectious particle ratios are different for the L-, M-, and S-Mengo variants. By combining these data with the extinction coefficient for the Mengo virion ( $E_{260\text{m}\mu}^{1\%} = 76.3$ ; Chapter 3), the numerical values for the total:infectious particle ratios were calculated for each variant (see Appendix, section 11). These values are listed in Table 4.2.

The total:infectious particle ratios were also measured directly by particle counting in the electron microscope, using the spray-droplet technique of Backus and Williams (1950). Column-purified virus was dialyzed overnight against 0.05 M ammonium acetate (pH 8.0) and the number of pfu present was estimated from the absorbance at 260m $\mu$ , using the data of Figure 4.10. Samples were then diluted in deionized water to appropriate concentrations and mixed with aliquots of a suspension of 88-m $\mu$  latex particles (Run no. LS-040A; Dow Chemical Co., Midland, Mich.) of known concentration to give a total volume of 1 ml. To reduce clumping tendencies of virus and latex particles, 0.02 ml of a 1% solution of bovine plasma albumin (Mann Research Laboratories, New York, N. Y.) was added. The concentration of latex particles had been predetermined from dry weight measurements as outlined by Pinteric and Taylor (1962). The virus-latex mixtures, containing about  $10^{11}$  particles/ml of each, were sprayed onto formvar-coated, 200 mesh gold grids with a spray-mounting device (Ernest F.

Table 4.3  
Specific Infectivities of the  
Mengo Virus Variants\*

Variant	pfu/g ( $\times 10^{12}$ )	pfu/A <sub>260</sub> unit <sup>†</sup> ( $\times 10^{10}$ )
L-Mengo	0.21	0.28
M-Mengo	9.5	12.8
S-Mengo	6.4	7.5

\* Based upon the calculated values for the total:infectious particle ratios (Table 4.2).

<sup>†</sup>A<sub>260</sub> units = measured absorbance at 260 mμ (1 cm light path) x volume (ml).

Fullam, Inc., Schenectady, N. Y.). After drying, the grids were shadowed with palladium and strengthened with carbon. Particles in single droplets were photographed by Dr. T. Yamamoto of the Microbiology Department, University of Alberta, using a Phillips EM200 electron microscope. Enumeration of particles appearing on developed films was done with the aid of a Nikon microcomparator. The best experimental values for the total:infectious particle ratios are summarized in Table 4.2, and compare reasonably well with the calculated values.

These results demonstrate that there are real differences in the relative infectivities of preparations of L-, M-, and S-Mengo virus particles. These differences do not arise during the purification procedure because the recovery of infectious virus was found to be approximately equivalent for each of the variants (Chapter 1). The specific infectivities, in terms of pfu/g virus particles and of pfu/A<sub>260</sub> unit for the Mengo variants are listed in Table 4.3.

Estimated values of total:infectious particle ratios for other encephalomyocarditis viruses vary over a wide range. For example, the ratio for Mengo virus, strain 37A, was found to be 5 (Homma and Graham, 1963), for EMC virus the ratio was reported to be 10 (Faulkner et al., 1961), and for ME virus, it was estimated to be 4000 (Rueckert and Schäfer, 1965). Thus, for encephalomyocarditis viruses, the total:infectious particle ratio varies markedly among members of the group, and among different strains of the same virus.





### Discussion

That L-Mengo virions differ from M- or S-Mengo virions with respect to surface features has been demonstrated by hydroxylapatite chromatography. Burness (1967) has shown that a small-plaque variant of EMC virus is eluted from brushite (calcium phosphate) by higher phosphate buffer concentrations than is a large-plaque variant, and has suggested a correlation between elution behavior and plaque size. A similar situation has been observed in the case of the Mengo variants. S-Mengo and M-Mengo (small-plaque variants) elute from hydroxylapatite (hydroxylated calcium phosphate) at higher phosphate concentrations than does L-Mengo. However, direct correlation of elution behavior with plaque size is not possible for the L-, M-, and S-Mengo variants. Colter et al. (1964b) have shown that plaque size under regular agar overlay is determined by the relative affinities of the Mengo variants for an anionic "agar inhibitor" which, when attached to the virus particle, blocks virus-cell interaction. L-Mengo, having a lower net negative charge than M- or S-Mengo (see below), elutes at lower phosphate concentrations (Figure 4.1; 4.2); however, L-Mengo also has a lower affinity for the anionic "agar inhibitor". Elution of the Mengo variants from hydroxylapatite seems to depend upon the net surface charge on the virion, whereas plaque size depends upon the presence or absence of specific attachment sites for the "agar inhibitor".

The results of agarose gel electrophoresis of the Mengo



variants have shown that L-, M-, and S-Mengo particles are negatively charged at pH 7.1 and that, of the three, L-Mengo has the smallest net negative charge. This feature of the L-Mengo virus particle may be the cause of its slower uptake by mouse L-929 cells. Colter et al. (1964a) have shown that maximum irreversible attachment of M- or S-Mengo to a monolayer of L-929 cells is achieved in a 20 min incubation period at 37°; whereas attachment of L-Mengo is not complete before 60 min. Cohn and Parks (1967) have reported that pinocytosis in mouse macrophage cells is more effectively stimulated by anionic proteins than by neutral or cationic ones. Dales (1962) has shown that encephalomyocarditis virus particles enter susceptible cells by a process closely resembling pinocytosis. It is possible that measurement of the rate of irreversible attachment of Mengo virus to mouse L-929 cells is in fact a measurement of the rate of pinocytosis of virus particles. If such is the case, then the less anionic L-Mengo particles might be expected to enter the cells more slowly than do M- or S-Mengo particles.

The distinctive melting profiles observed for the L-, M-, and S-Mengo virions indicate that the latter differ with respect to interactions between the subunits of which their respective capsids are constructed. This in turn implies that there are distinctive amino acid sequences in the polypeptide chains of which the capsid subunits of each of the three variants is composed. M-Mengo virus particles have a lower  $T_m$  than do L- or S-Mengo particles, and are the only ones to exhibit decreased heat stability at pH 6.2. The

Table 4.4

Burst Sizes of the Mengo Variants in L-cells

Variant	Total particles/ infectious particles	Burst size	
		pfu/cell*	total particles/ cell <sup>†</sup>
L-Mengo	3450	220	759,000
M-Mengo	76	1050	79,800
S-Mengo	113	420	47,500

\*Taken from the data of Campbell (1961).

<sup>†</sup>Based upon the calculated values for the total:infectious particle ratios (Table 4.2).



observed lability of the M-variant supports the mechanism proposed for its inactivation at pH 6.2 (Colter et al., 1964a; Campbell, 1965), - namely that at the low pH, its protein capsid becomes permeable to nucleases which destroy the integrity of the genetic material. The relative fragility might also be related to the hypothesis that of the three variants, M-Mengo is most rapidly uncoated in the infected cell. Campbell (1965) has found that the eclipse phase of viral development is about 30% shorter for M-Mengo than for S- or L-Mengo (4.5 hours as compared to 5.5-6 hours). The short eclipse period might be due to more rapid uncoating of M-Mengo RNA.

The L-Mengo variant has been shown to be the most lethal of the three for laboratory mice (Colter et al., 1965), but was also the best interferon-inducing variant (Campbell and Colter, 1967). One would have expected a highly virulent virus to induce little interferon (see Ho, 1964). L-Mengo does, however, have the largest total:infectious particle ratio, and also the largest burst size in terms of total particles (Table 4.4). Whether only non-infectious particles induce interferon, or whether all virus particles are inducers, L-Mengo would be expected to be a better inducer than either M- or S-Mengo. This does not, of course, explain the high virulence of the L-variant.



## SUMMARY AND DISCUSSION

L-, M-, and S-Mengo virus particles have been highly purified and subjected to physical and chemical examination. No significant differences were detected among the three with respect to either size, shape, and hydrodynamic parameters, or to ultraviolet absorption and optical rotatory dispersion spectra. Moreover, ribonucleates isolated from the three variant particles were found to be essentially identical in molecular weights and base compositions; and the isolated proteins were shown to be very similar in amino acid compositions and to produce similar banding patterns when subjected to electrophoresis on polyacrylamide gels. These results emphasize that, in the case of the three Mengo variants, the dramatic biological differences which have been observed (Campbell, 1965) reflect very small structural differences among them.

Certain of the experiments summarized in this thesis did, however, reveal structural differences among the L-, M-, and S-Mengo virions, - differences which can conceivably be correlated with some of their divergent biological properties.

1. In the mouse, L-Mengo induces the production of more interferon per pfu of challenge virus than does either M- or S-Mengo (Campbell and Colter, 1967), even though L-Mengo is the most virulent of the three (Colter et al., 1965). As a general rule, avirulent strains of viruses have been found to be more efficient inducers of interferon production than their virulent counterparts (see reviews by Ho, 1964; Wagner, 1965).





The atypical behavior of L-Mengo may be explicable in the light of the observation that the progeny virus population produced as a result of infection of mouse cells with this variant contains a very high proportion of non-infectious particles (Chapter 4). It is conceivable that only non-infectious particles are capable of inducing cells to synthesize interferon, the infectious particles causing rapid impairment of the cellular synthetic machinery. If such is the case, then of the three variants, L-Mengo would be expected to be the most efficient inducer of interferon synthesis.

2. The M-Mengo variant is rapidly and irreversibly inactivated when the pH of a clarified cell lysate is lowered from 7.6 to 6.2 (Colter et al., 1964a). The postulated mechanism for this inactivation is that at the lower pH, the capsid of the M-Mengo virion (but not those of the L- and S-Mengo virions) becomes permeable to ribonucleases present in the lysate, and that these enzymes destroy the integrity of the viral genome. The observation that the M-variant is more heat-labile at pH 6.2 than at pH 7.1 (Chapter 4) is compatible with this hypothesis (the  $T_m$  for M-Mengo was reduced by  $5^{\circ}$  when the pH was lowered from 7.1 to 6.2, while no such effect was observed with either L-, or S-Mengo). The relative fragility of the M-Mengo capsid may also be directly related to the relatively short latent period observed for this variant during one-cycle growth in cultured mouse cells (Campbell, 1965). The shorter latent period suggests that the M-Mengo genome may be uncoated more rapidly in the cell than are those





of L- and S-Mengo.

3. That the L-Mengo virion carries a smaller net negative charge on its surface than do the M- and S-virions has been demonstrated by agarose gel electrophoresis and dextran sulfate density gradient centrifugation, and it is tempting to correlate this fact with the observation that, of the three variants, L-Mengo attaches most slowly to cultured L-929 cells (Colter et al., 1964a). However, the attachment process may involve specific interactions between complementary sites on the virion and on the cell membrane by some combination of hydrogen, hydrophobic, electrostatic and/or covalent bonding. If this is the case, the overall net charge on the virus particle may be of minimal importance in determining the rate of virus-cell interaction.

The availability of methods for producing and purifying milligram amounts of Mengo virus particles should make it possible to obtain a comprehensive structural description of the Mengo virion. However, there are two problems which must be solved before further studies can be done. First, it has been found that column-purified virus, stored in phosphate buffer at  $-20^{\circ}$ , is not stable for more than a few days. In order to stockpile the quantities of virus necessary for future experiments, a method for storing purified virus without degradation must be found. Second, viral protein preparations obtained thus far were found to be insoluble in common aqueous salt solutions. Chemical and physical analyses of the individual Mengo polypeptides must await the development of procedures for their isolation or modification which will



increase their solubility. Once these difficulties have been overcome, there are several aspects of Mengo virion structure which will become amenable to investigation.

1. The number of different polypeptides comprising the virus capsid (believed to be four from the results of polyacrylamide gel electrophoresis as reported in Chapter 3) could be verified by chemical analysis of the number of N-terminal amino acids.

2. The capsid polypeptides could be resolved by preparative polyacrylamide gel electrophoresis (Rueckert and Duesberg, 1966), and their physical characteristics investigated by optical and ultracentrifugal methods. "Fingerprinting" of peptides obtained after partial hydrolysis of the viral proteins (see Canfield, 1963) should indicate the extent of the differences in composition among those from L-, M-, and S-Mengo. Molecular weights of the proteins could be estimated from rates of migration in polyacrylamide gels containing sodium dodecyl sulfate (Schapiro et al., 1967). From information obtained from these examinations of the protein components, it should be possible to draw certain conclusions concerning structural features of the virus capsid. For example, does there exist a small, basic polypeptide which is intimately associated with the RNA in the interior of the virion? Also, what are the numbers of physical and chemical subunits, and how are these related? The answer to the latter question would require, in addition to precise information regarding the number and molecular weights of the polypeptides, x-ray diffraction data to establish the number of physical subunits







in the capsid of the intact virion.

3. Techniques have been worked out for analyzing the times of appearance and the functions of poliovirus-specific proteins during the intracellular phase of the viral growth cycle (Summers et al., 1965; Maizel et al., 1967). Application of these techniques to the Mengo virus-L-cell system could yield interesting information about the non-capsid viral proteins. Perhaps differences among these proteins are responsible for some of the biological differences among the L-, M-, and S-Mengo variants. The study of intracellular development might also shed some light upon the construction of the viral capsid - what are the steps involved in assembly? What is the sequence of insertion of the different capsid proteins? Are there virus-specific proteins which have a morphopoietic (i.e. shape-specifying) function?

4. The availability of highly purified virus should also make it possible to investigate the nature of the binding sites on the surface of the virion which are responsible for attachment to the membrane of a susceptible cell. It should be possible to selectively modify amino acid residues on the surface without destroying the integrity of the virus particle, and to examine the ability of the modified virions to interact with cells. Chemical modification studies might also be informative in investigating the antigenic properties of the Mengo virion (i.e. the nature of the antigenic determinants and the antibody-combining sites). Tillotson and Lerner (1966) have, for example, reported that mild periodate oxidation of poliovirus particles resulted in loss of



infectivity. This suggests that poliovirus particles contain essential capsid carbohydrate. Is such the case with the encephalomyocarditis viruses?



# BIBLIOGRAPHY

- Amako, K., and Dales, S. (1967). *Virology* 32, 184.
- Andrewes, C., and Pereira, H. G. (1967). *In* *Viruses of Vertebrates*, 2nd ed., p. 31. Baillière, Tindall, and Cassal, London.
- Armstrong, J., Myers, D., Verpoorte, J., and Edsall, J. T. (1966). *J. Biol. Chem.* 241, 5137.
- Bachrach, H. L. (1964). *J. Mol. Biol.* 8, 348.
- Bachrach, H. L. (1965). *Virology* 25, 532.
- Backus, R. C., and Williams, R. C. (1950). *J. Appl. Phys.* 21, 11.
- Baltimore, D., and Franklin, R. M. (1963). *J. Biol. Chem.* 238, 3395.
- Beavan, G. H., and Holliday, E. R. (1952). *Adv. Protein Chem.* 7, 319.
- Beavan, G. H., Holliday, E. R., and Johnson, E. A. (1955). *In* *The Nucleic Acids*. *Edited by* E. Chargaff and J. N. Davidson. Vol. 1, p. 513. Academic Press, New York.
- Bengtsson, S., Philipson, L., Persson, H., and Laurent, T. C. (1964). *Virology* 24, 617.
- Billeter, M. A., and Weissman, C. (1966). *In* *Procedures in Nucleic Acid Research*. *Edited by* G. L. Cantoni and D. R. Davies, p. 498. Harper and Row, New York.
- Brown, F., Cartwright, B., and Stewart, D. L. (1963). *J. Gen. Microbiol.* 31, 179.
- Burness, A. T. H. (1967). *J. Virol.* 1, 308.
- Burness, A. T. H., Vizoso, A. D., and Clothier, F. W. (1963). *Nature* 197, 177.
- Burness, A. T. H., and Walter, D. S. (1967). *Nature* 215, 1350.
- Campbell, J. B. (1965). Ph.D. thesis, University of Alberta, Edmonton.
- Campbell, J. B., and Colter, J. S. (1967a). *Virology* 32, 69.
- Campbell, J. B., and Colter, J. S. (1967b). *Canad. J. Microbiol.* 13, 931.
- Canfield, R. E. (1963). *J. Biol. Chem.* 238, 2691.





- Casals, J. (1963). *Nature* 200, 329.
- Caspar, D. L. D. (1965). *In* Viral and Rickettsial Infections of Man. Edited by F. L. Horsfall and I. Tamm. 4th ed., p. 51. J. B. Lippincott, Philadelphia.
- Chrambach, A., Reisfeld, R. A., Wycoff, M., and Zaccari, J. (1967). *Anal. Biochem.* 20, 150.
- Cohen, C., and Szent-Györgyi, A. G. (1957). *J. Am. Chem. Soc.* 79, 248.
- Cohen, S. S., and Stanley, W. M. (1942). *J. Biol. Chem.* 144, 589.
- Cohn, E. J., and Edsall, J. T. (1943). *In* Proteins, Amino Acids and Peptides. Ch. 16. Reinhold, New York.
- Cohn, Z. A., and Parks, E. (1967). *J. Exp. Med.* 125, 213.
- Colter, J. S., Bird, H. H., Moyer, A. W., and Brown, R. A. (1957). *Nature* 179, 859.
- Colter, J. S., Campbell, J. B., and Hatch, L. R. (1965). *J. Cell. Comp. Physiol.* 65, 229.
- Colter, J. S., Davies, M. A., and Campbell, J. B. (1964a). *Virology* 24, 474.
- Colter, J. S., Davies, M. A., and Campbell, J. B. (1964b). *Virology* 24, 578.
- Craighead, J. E. (1965). *Proc. Soc. Exp. Biol. Med.* 119, 408.
- Craighead, J. E. (1966a). *Am. J. Path.* 48, 333.
- Craighead, J. E. (1966b). *Am. J. Path.* 48, 375.
- Dales, S., and Franklin, R. M. (1962). *J. Cell Biol.* 14, 281.
- Davis, B. J. (1964). *Ann. N. Y. Acad. Sci.* 121, 404.
- Day, L. A. (1966). *J. Mol. Biol.* 15, 395.
- Dick, G. W. A. (1948). *Brit. J. Exp. Path.* 29, 559.
- Dick, G. W. A. (1949). *J. Immunol.* 62, 375.
- Dick, G. W. A., Best, A. M., Haddow, A. J., and Smithburn, K. C. (1948a). *Lancet* 255, 286.
- Dick, G. W. A., Smithburn, K. C., and Haddow, A. J. (1948b). *Brit. J. Exp. Path.* 29, 547.
- Dickman, S. R. (1958). *Science* 127, 1392.



- Dulbecco, R., and Vogt, M. (1954). J. Exp. Med. 119, 408.
- Eagle, H. (1959). Science 130, 432.
- Earle, W. R. (1943). J. Nat. Cancer Inst. 4, 165.
- Edelstein, S. J., and Schachman, H. K. (1967). J. Biol. Chem. 242, 306.
- Ellem, K. A. O., and Colter, J. S. (1961). Virology 15, 340.
- Enger, M. D., Stubbs, E. A., Mitra, S., and Kaesberg, P. (1963). Proc. Nat. Acad. Sci., Wash. 49, 857.
- Farnham, A. E. (1965). Virology 27, 73.
- Fasman, G. D. (1963). In Methods in Enzymology. Edited by S. P. Colowick and N. O. Kaplan. Vol. 6, p. 928, Academic Press, New York.
- Faulkner, P., Martin, E. M., Sved, S., Valentine, R. C., and Work, T. S. (1961). Biochem. J. 80, 597.
- Finch, J. T., and Klug, A. (1959). Nature 183, 1709.
- Finch, J. T., and Klug, A. (1966). J. Mol. Biol. 15, 344.
- Fraenkel-Conrat, H., and Williams, R. C. (1955). Proc. Nat. Acad. Sci., Wash. 41, 698.
- Franklin, R. M. (1962). J. Cell Biol. 12, 1.
- Franklin, R. M., Wecker, E., and Henry, C. (1959). Virology 7, 220.
- Gajdusek, C. (1955). Pediatrics 16, 819.
- Gauntt, C. J., and Lockhart, R. Z. (1968). J. Virol. 2, 567.
- Gesteland, R. F., and Boedtke, H. (1964). J. Mol. Biol. 8, 496.
- Goodheart, C. R. (1967). J. Mol. Biol. 23, 183.
- Goodwin, T. W., and Morton, R. A. (1946). Biochem. J. 40, 628.
- Gray, M. W., and Lane, B. G. (1967). Biochim. Biophys. Acta 134, 243.
- Grossberg, S. E., Lwoff, M., and Lwoff, A. (1966). J. Bacteriol. 92, 1473.
- Hanks, J. H., and Wallace, R. E. (1949). Proc. Soc. Exp. Biol. Med. 71, 196.







- Harris, J. I., and Hindley, J. (1965). J. Mol. Biol. 13, 894.
- Hausen, P., and Schäfer, W. (1962). Z. Naturforsch. 17b, 15.
- Helwig, F. C., and Schmidt, E. C. H. (1945). Science 102, 31.
- Hinz, R. W., Barski, G., and Bernhard, W. (1962). Exp. Cell Res. 26, 571.
- Ho, M. (1964). Bacteriol. Rev. 28, 367.
- Homma, M., and Graham, A. F. (1963). J. Cell. Comp. Physiol. 62, 179.
- Homma, M., and Graham, A. F. (1965). J. Bacteriol. 89, 64.
- Horton, E., Liu, S.-L., Martin, E. M., and Work, T. S. (1966). J. Mol. Biol. 15, 62.
- Hudson, L., Gray, M. W., and Lane, B. G. (1965). Biochemistry 4, 2009.
- Huppert, J., and Saunders, F. K. (1958). Nature 182, 515.
- Jirgensons, B. (1966). J. Biol. Chem. 241, 147.
- Joklik, W. K. (1965). Prog. Med. Virol. 7, 44.
- Jungeblut, C. W. (1958). In Handbuch der Virusforschung. Edited by C. Hallauer and K. F. Meyer. Vol. 4, p. 459. Springer-Verlag, Vienna.
- Jungeblut, C. W., and Dalldorf, G. (1943). Am. J. Pub. Health 33, 169.
- Jungeblut, C. W., and Sanders, M. (1940). J. Exp. Med. 72, 407.
- Kaighn, M. E., Moscarello, M. A., and Fuerst, C. R. (1964). Virology 23, 183.
- Kaiser, A. D. (1966). J. Gen. Physiol. 49, 171.
- Kauzmann, W. (1959). Adv. Protein Chem. 14, 1.
- Kay, C. M., and Oikawa, K. (1966). Biochemistry 5, 213.
- Klug, A., Longley, W., and Leberman, R. (1966). J. Mol. Biol. 15, 315.
- Lauffer, M. A., and Bendet, I. J. (1954). Adv. Virus Res. 2, 275.
- Levin, O. (1962). In Methods in Enzymology. Edited by S. P. Colowick and N. O. Kaplan. Vol. 5, p. 28. Academic Press, New York.



- Levintow, L., and Darnell, J. E. (1960). J. Biol. Chem. 235, 70.
- Longsworth, L. G. (1937). J. Am. Chem. Soc. 59, 1483.
- Maizel, J. V. (1963). Biochem. Biophys. Res. Comm. 13, 483.
- Maizel, J. V., Phillips, B. A., and Summers, D. F. (1967). Virology 32, 692.
- Markham, R. (1962). Adv. Virus Res. 9, 264.
- Martin, R. G., and Ames, B. N. (1961). J. Biol. Chem. 236, 1372.
- Mayer, V., Slávik, I., and Libíková, H. (1967). Acta Virol. 11, 407.
- Meselson, M., Stahl, F. W., and Vinograd, J. (1957). Proc. Nat. Acad. Sci., Wash. 43, 581.
- Mitra, S., Enger, M. D., and Kaesberg, P. (1963). Proc. Nat. Acad. Sci., Wash. 50, 68.
- Möller, W. (1964). Proc. Nat. Acad. Sci., Wash. 51, 501.
- Montagnier, L., and Sanders, F. K. (1963). Nature 199, 664.
- Moore, S. (1963). J. Biol. Chem. 238, 235.
- Moore, S., and Stein, W. H. (1963). In Methods in Enzymology. Edited by S. P. Colowick and N. O. Kaplan. Vol. 6, p. 819. Academic Press, New York.
- Moscarello, M. A., and Kaighn, M. E. (1964). Biochim. Biophys. Acta 90, 161.
- Murnane, T. C., Craighead, J. E., Mondragon, H., and Shelokov, A. (1960). Science 131, 498.
- Oster, G. (1948). Chem. Rev. 43, 319.
- Ozaki, H., Diwan, A. R., Takizawa, M., and Melnick, J. L. (1965). J. Bacteriol. 89, 603.
- Penniston, J. T., and Doty, P. (1963). Biopolymers 1, 145.
- Pickels, E. G. (1942). Chem. Rev. 30, 340.
- Pinteric, L., and Taylor, J. (1962). Virology 18, 359.
- Roberts, W. K., Newman, J. F. E., and Rueckert, R. R. (1966). J. Mol. Biol. 15, 92.
- Rueckert, R. R. (1965). Virology 26, 345.





Rueckert, R. R., and Duesberg, P. H. (1966). J. Mol. Biol. 17, 490.

Rueckert, R. R., and Schäfer, W. (1965). Virology 26, 333.

Sanford, K. K., Earle, W. R., and Likely, G. D. (1948). J. Nat. Cancer Inst. 9, 229.

Sarkar, P., and Doty, P. (1966). Proc. Nat. Acad. Sci., Wash. 55, 981.

Schachman, H. K. (1957). In Methods in Enzymology. Edited by S. P. Colowick and N. O. Kaplan. Vol. 4, p. 69. Academic Press, New York.

Schachman, H. K. (1959). In Ultracentrifugation in Biochemistry. Academic Press, New York.

Schaffer, F. L., and Frommhagen, L. H. (1965). Virology 25, 662.

Schaffer, F. L., Moore, H. F., and Schwerdt, C. E. (1960). Virology 10, 530.

Schaffer, F. L., and Schwerdt, C. E. (1959). Adv. Virus Res. 6, 159.

Schapiro, A., Vinuela, E., and Maizel, J. V. (1967). Biochem. Biophys. Res. Comm. 28, 815.

Scheraga, H. A., and Mandelkern, L. (1953). J. Am. Chem. Soc. 75, 179.

Schwerdt, C. E. (1957). Special Publication, N. Y. Acad. Sci. 5, 157.

Schwerdt, C. E., and Schaffer, F. L. (1955). Ann. N. Y. Acad. Sci. 61, 740.

Schwert, G. W. (1951). J. Biol. Chem. 190, 799.

Simmons, N. S., and Blout, E. R. (1960). Biophys. J. 1, 55.

Stanley, W. M. Jr., and Bock, R. M. (1965). Biochemistry 4, 1302.

Strauss, J. H., and Sinsheimer, R. L. (1963). J. Mol. Biol. 7, 43.

Summers, D. F., Maizel, J. V., and Darnell, J. E. (1965). Proc. Nat. Acad. Sci., Wash. 54, 505.

Svedberg, T., and Eriksson-Quensel, I. B. (1936). Nature 137, 400.

Svedberg, T., and Pedersen, K. O. (1940). In The Ultracentrifuge. Clarendon Press, Oxford.





- Tanford, C. (1961). In Physical Chemistry of Macromolecules. p. 306. J. Wiley and Sons, New York.
- Tillotson, J. R., and Lerner, A. M. (1966). Proc. Nat. Acad. Sci., Wash. 56, 1143.
- Tovell, D., and Colter, J. S. (1968). Canad. J. Biochem. In press.
- Uriel, J. (1964). In Immuno-electrophoretic Analysis. Edited by P. Grabar and P. Burtin, p. 30. Elsevier, Amsterdam.
- Vande Woude, G. F., and Bachrach, H. L. (1968). Arch. ges. Virusforsch. 23, 353.
- Vizoso, A. D., and Hay, R. (1964). Nature 204, 56.
- Wagner, R. R. (1965). Am. J. Med. 38, 726.
- Warburg, O., and Christian, W. (1941). Biochem. Z. 310, 384.
- Warren, J. (1965). In Viral and Rickettsial Infections of Man. Edited by F. L. Horsfall and I. Tamm. 4th ed., p. 562. J. B. Lippincott, Philadelphia.
- Warren, J., Smadel, J. E., and Russ, S. B. (1949). J. Immunol. 62, 387.
- Weil, M., Warren, J., Breeze, S. S., Russ, S. B., and Jeffries, H. (1952). J. Bacteriol. 63, 99.
- Wolfe, F. H., and Kay, C. M. (1967). Biochemistry 6, 2853.
- Yang, J.-T. (1967). In Poly- $\alpha$ -Amino Acids. Edited by G. D. Fasman, p. 239. Marcel Dekker, New York.



## APPENDIX

### 1. The Möller method for the estimation of diffusion coefficients

The equations for a homogeneous boundary diffusing in a centrifugal field are (Svedberg and Pedersen, 1940):

$$D = \frac{\bar{u}^2(1 - S \omega^2 t)}{4y^2 t} \quad (1)$$

$$\frac{c}{c_0} = \frac{1}{2} \left[ 1 - \frac{2}{\sqrt{\pi}} \int_0^y e^{-y^2} dy \right] \quad (2)$$

In equation (1),  $\bar{u}$  is the mean experimental distance in cm at a time  $t$  from a level in the boundary where the concentration ratio  $\frac{c}{c_0}$  is 0.5, to two equidistant levels with concentration ratios determined by equation (2). For a definite value of  $\frac{c}{c_0}$ , the factor  $y$  (the solution of the probability integral  $\int_0^y e^{-y^2} dy$ ) can be found in tables of probability functions. For example, if  $\frac{c}{c_0} = 0.2(0.8)$ , equation (2) becomes  $0.8 = 0.5 - \frac{1}{\sqrt{\pi}} \int_0^y e^{-y^2} dy$ ;  $0.2 = 0.5 - \frac{1}{\sqrt{\pi}} \int_0^y e^{-y^2} dy$ , and, solving gives  $y = \pm 0.3541$ .

Thus, for  $\frac{c}{c_0} = 0.2(0.8)$ ,  $\frac{1}{4y^2} = 0.7060$ .

Similarly, for  $\frac{c}{c_0} = 0.3(0.7)$ ,  $\frac{1}{4y^2} = 1.8183$ .

The influence of a centrifugal field on the diffusion process is given by the factor  $(1 - S \omega^2 t)$ , in which  $S$  is the sedimentation coefficient of the particle under the conditions of the low-speed centrifugation,  $\omega$  is the angular velocity, and  $t$  is the time from the start of the run. In our experiments, the value of  $S$  was approximated by using the intrinsic sedimentation coefficient calculated in the usual fashion.





The experimental procedure involved a two-phase operation of the analytical ultracentrifuge: a short initial run at high speed to establish a solvent-solution boundary, followed by a long run at low speed. The boundary was photographed at intervals during centrifugation by employing the ultraviolet absorption optical system. Graphical representations of the boundary spreading during the low-speed phase were obtained from the photographs by using an analytical densitometer.

Corresponding values of  $\bar{u}$  lying on opposite sides of the centroid were determined directly from the densitometer tracings. This was achieved by drawing two horizontal lines through the plateau areas adjacent to the boundary. From the measured vertical distance between these lines, the 0.5, 0.2(0.8), and 0.3(0.7) points were estimated.

The diffusion coefficient was obtained from a plot of  $1/4y^2 \left[ \bar{u}^2 (1 - S \omega^2 t) \right]$  vs  $t$ ,  $D$  being given by the slope of the curve. Correction for temperature and salt effects (see Schachman, 1957) gave the standardized diffusion coefficient,  $D_{20,w}$ . An advantage of the Möller method was that the values obtained for  $D_{20,w}$  could be regarded as intrinsic (that is, independent of concentration) because the amounts of virus or RNA required were very small (about  $1 \times 10^{-5}$  g virus, or  $3 \times 10^{-6}$  g RNA).

## 2. Estimation of $\bar{v}$ for Mengo virus particles

The partial specific volume of the virion may be calculated from the  $\bar{v}$  values of its constituent protein and ribonucleate components according to the equation:

$$\bar{v}_{\text{virion}} = \bar{v}_{\text{protein}} \times w_{\text{protein}} + \bar{v}_{\text{RNA}} \times w_{\text{RNA}} \quad (3)$$



where  $w_{\text{protein}}$  and  $w_{\text{RNA}}$  are the weight concentrations of protein and RNA in the virus. Such a calculation assumes that the virion is composed solely of protein and RNA.

The  $\bar{v}$  of the viral protein was estimated to be 0.731 ml/g (Chapter 3), and the  $\bar{v}_{\text{RNA}}$  value was assumed to be 0.53 ml/g (Kay and Oikawa, 1966).

The percentage composition of the Mengo virion was determined by three independent methods. A modification of the method of Warburg and Christian (1941), using the relative absorbances of the virion at 260 and 280 m $\mu$  (Chapter 3) gave a value for the weight percentage of RNA of 24%. From the molecular weights of the virion ( $8.3 \times 10^6$ ) and the viral RNA ( $1.74 \times 10^6$ ) as determined by hydrodynamic methods, the percentage RNA is 21%. Schaffer and Schwerdt (1959) suggested a method of determining the percentage of RNA in poliovirus from the phosphorus content of the RNA and the extinction coefficient of the whole virus. From the base ratios of Mengo virus RNA (Chapter 3), the percentage by weight of phosphorus was calculated to be 9.6%. Assuming a molar extinction coefficient of 10,000 for phosphorus in RNA, and using the measured extinction coefficient for Mengo virus of 76.3 (Chapter 3), the percentage by weight of RNA in the virus was calculated to be 24.6%. Thus, the best average value for the composition of the Mengo virus virion is 23.2% RNA and 76.8% protein. Substituting these values in equation (3) gave  $\bar{v}_{\text{virion}} = 0.684$  ml/g.





### 3. Calculation of molecular (particle) weight

Having determined the hydrodynamic parameters  $S_{20,w}^0$ ,  $D_{20,w}^0$ , and  $\bar{v}$ , the particle weight of Mengo virus and the molecular weight of the viral RNA were calculated from the Svedberg equation (Svedberg and Pedersen, 1940);

$$M = \frac{RTS}{D(1-\bar{v}\rho)} \quad (4)$$

where R is the ideal gas constant ( $8.314 \times 10^7$  erg/mole-degree), T is the standard temperature ( $293^\circ\text{K}$ ),  $\rho$  is the density of water at  $293^\circ\text{K}$ , S is the intrinsic sedimentation coefficient (sec), D is the intrinsic diffusion coefficient ( $\text{cm}^2/\text{sec}$ ), and  $\bar{v}$  is the partial specific volume (ml/g). The value of the molecular weight, M, calculated is that of the anhydrous species.

### 4. The diameter of the Mengo virus particle in solution

The hydrated diameter of the virion was calculated from the experimentally determined value for its diffusion coefficient.

(a) From Stokes' Law:

$$r = \frac{RT}{6\pi\eta ND} \quad (5)$$

In this expression, r is the hydrated particle radius (cm),  $\eta$  is the viscosity of water at  $293^\circ\text{K}$  (centipoise), and N is Avogadro's number ( $6.024 \times 10^{23}$ ).

(b) Alternatively, an empirical relationship devised by Markham (1962) was used:

$$2r = \frac{4.258 \times 10^{-13}}{D} \quad (6)$$





The diameters calculated from equations (5) and (6) were  $29.04 \times 10^{-7}$  cm and  $28.97 \times 10^{-7}$  cm, respectively.

5. Calculation of the water of hydration of the Mengo virus particle in solution

(a) Volume of hydrated particles per mole =  $\frac{4}{3} \pi r^3 N$   
(where  $r$  is the radius of the hydrated particle)

Volume of one mole of dry virus =  $M\bar{v}$

Volume of water of hydration per mole of virus =  
 $\frac{4}{3} \pi r^3 N - M\bar{v}$

Volume of water of hydration per gram of dry  
virus =  $\frac{\frac{4}{3} \pi r^3 N - M\bar{v}}{M}$

Weight of water of hydration per gram of dry  
virus =  $\left( \frac{\frac{4}{3} \pi r^3 N - M\bar{v}}{M} \right) \rho$

Substituting in this expression gave a value of 0.228 g water per g dry virus.

(b) Since the anhydrous virus particle is a sphere (as shown in electron micrographs), the observed frictional ratio for the particle in solution involves only a hydration factor [i.e.  $(f/f_0)_{\text{obs}} = (f/f_0)_{\text{hyd}}$ , see section 7]. Oncley (1941) has given an expression relating frictional ratio to weight of water of hydration:

$$\left( \frac{f}{f_0} \right)_{\text{hyd}} = \left( 1 + \frac{w}{\bar{v} \rho} \right)^{1/3} \quad (7)$$

Using a value of 1.10 for the frictional ratio (section 7),  
 $w = 0.231$  g water per g dry virus.



## 6. Calculation of the diameter of the anhydrous virus particle

Volume of water per gram dry virus = 0.2299 ml (section 5)

Volume of water per mole dry virus = 0.2299 M  
 $= \frac{4}{3} \pi N (r^3 - r_a^3)$ , where  $r_a$  is the radius of the anhydrous particle.

Thus,  $0.2299 M = \frac{4}{3} \pi N (r^3 - r_a^3)$ .

Since  $r = 14.50 \times 10^{-7}$  cm (section 4),  $r_a = 13.2 \times 10^{-7}$  cm.

The calculated diameter of the anhydrous particle is, therefore, 26.4 mμ.

## 7. Calculation of the frictional ratio of the virus particle

(a) The frictional coefficient of the hydrodynamic particle is given by either of the following expressions (see Armstrong et al., 1966):

$$f = \frac{k_B T}{D} \quad (8)$$

( $k_B$  is the Boltzmann constant,  $1.38 \times 10^{-16}$  erg/deg)

$$f = \frac{M(1 - \bar{v} \rho)}{NS} \quad (9)$$

Substituting in equation (8),  $f = 2.751 \times 10^{-7}$ ; substituting in equation (9),  $f = 2.755 \times 10^{-7}$ .

The frictional coefficient of the anhydrous sphere is given by the expression:

$$f_o = 6 \pi \eta \left( \frac{3 M \bar{v}}{4 \pi N} \right)^{1/3} \quad (10)$$

From this expression,  $f_o$  for the Mengo virus particle was calculated to be  $2.503 \times 10^{-7}$ .

Therefore, the frictional ratio,  $\frac{f}{f_o} = \frac{2.753 \times 10^{-7}}{2.503 \times 10^{-7}} = 1.100$ .







(b) Svedberg and Pedersen (1940) have given equations permitting calculation of  $f/f_o$  from S and D (equation [11]), or from S and M (equation [12]):

$$\frac{f}{f_o} = 10^{-8} \left( \frac{1 - \bar{v} \rho}{D^2 S \bar{v}} \right)^{1/3} \quad (11)$$

$$\frac{f}{f_o} = 1.19 \times 10^{-15} \left( \frac{M^{2/3} (1 - \bar{v} \rho)}{S \bar{v}^{1/3}} \right) \quad (12)$$

Substitution of the appropriate values in either of these equations gave  $f/f_o = 1.096$ .

#### 8. Shape of the Mengo virus particle in solution

The frictional ratio is generally assumed to be composed of two terms, an asymmetry term for the anhydrous particle, and a hydration term (see Schachman, 1959). That is,

$$\left( \frac{f}{f_o} \right)_{\text{observed}} = \left( \frac{f}{f_o} \right)_{\text{asym.}} \times \left( \frac{f}{f_o} \right)_{\text{hyd.}} \quad (13)$$

Since electron micrographs have shown that the anhydrous virus particle is essentially spherical,

$$\left( \frac{f}{f_o} \right)_{\text{observed}} = \left( \frac{f}{f_o} \right)_{\text{hyd.}} = 1.10 \quad (14)$$

A frictional ratio of 1.10 for the hydrated virus corresponds to a  $\beta$ -value (Scheraga and Mandelkern, 1953) of  $2.15 \times 10^6$  for an equivalent prolate ellipsoid of revolution or  $2.13 \times 10^6$  for an oblate ellipsoid. These values in turn indicate an axial ratio of 2/1 to 3/1 for the Mengo virus particle in solution (see the tabulation in Schachman, 1959). Thus, the hydrodynamic particle can be considered to be spherical.



9. Estimation of the  $\alpha$ -helical content of Mengo virus protein

From ultraviolet optical rotatory dispersion data, the magnitude of the Cotton trough at 233  $m\mu$  has been used as an index of helical content for Mengo virus protein in situ. The relationship employed was given by Yang (1967):

$$\text{Fraction helix} = \frac{[m']_{233m\mu} + 2000}{-13,000} \quad (15)$$

In this expression,  $[m']$  is the reduced mean residue rotation of the protein, which in turn is defined by:

$$[m']_{\lambda} = \left( \frac{3}{n^2 + 2} \right) \left( \frac{MRW}{100} \right) [\alpha]_{\lambda} \quad (16)$$

where  $n$  is the refractive index of the medium, MRW is the mean residue weight for the protein, and  $[\alpha]$  is the specific rotation in degrees. The refractive index dispersion data has been tabulated by Fasman (1963). From amino acid composition analysis (Chapter 3), the MRW for Mengo virus protein was calculated to be 112.

$$\text{Thus, } [m']_{233-234m\mu} = -2520$$

and  $\% \alpha\text{-helix} = 4\%$ .

10. Calculation of the radius of gyration of Mengo virus RNA

(a) In the virion:

$$\text{Volume of the virus particle} = \frac{4}{3} \pi r^3$$

Assuming a radius of 145  $\text{\AA}$  for the virion in solution (see section 4), its volume is  $12.15 \times 10^6 \text{\AA}^3$ .

Volume of RNA in the virus particle:

$$\text{Wt.\% RNA} = 23; \text{ Wt.\% protein} = 77 \text{ (section 2).}$$





$$\begin{aligned}\text{Volume \% RNA} &= \frac{\text{Wt.\%RNA} \times \bar{v}_{\text{RNA}}}{(\text{Wt.\%RNA} \times \bar{v}_{\text{RNA}}) + (\text{Wt.\% protein} \times \bar{v}_{\text{protein}})} \\ &= \frac{23 \times 0.53}{(23 \times 0.53) + (77 \times 0.73)} = 18\%\end{aligned}$$

Therefore, the volume of the RNA "core" =  $0.18 (12.15 \times 10^6)$   
 $= 2.19 \times 10^6 \text{ \AA}^3$

Radius of the RNA in the virus particle:

$$\begin{aligned}r_{\text{RNA}} &= \sqrt[3]{\frac{\text{Volume of RNA}}{4/3 \pi}} \\ &= 52.3 \text{ \AA}\end{aligned}$$

The radius of gyration for a sphere of radius  $r$  is given by:

$$R_G^2 = \frac{3}{5} r^2 \quad (17)$$

(Tanford, 1961)

From this expression, and using  $r = r_{\text{RNA}}$ , the radius of gyration of the RNA within the Mengo virion was calculated to be  $40.5 \text{ \AA}$ .

(b) In solution ( $25^\circ$ ,  $0.10 \text{ M K}^+$ ):

Assuming a random coil model, Strauss and Sinsheimer (1963) have proposed an approximate relationship between molecular weight and radius of gyration for bacteriophage RNA's:

$$3.0 < \frac{\sqrt{M}}{R_G} < 6.0 \quad (18)$$

Mengo viral RNA, with a molecular weight of  $1.74 \times 10^6$  daltons (Chapter 3), would be expected to have a radius of gyration of  $220\text{--}440 \text{ \AA}$  in solution.





11. Calculation of total:infectious particle ratios for the Mengo virus variants

Assuming a molecular weight for the Mengo virion of  $8.32 \times 10^7$  daltons, the weight of an individual virus particle is equal to  $1.38 \times 10^{-17}$  g.

The extinction coefficient,  $E_{260m\mu}^{1\%}$ , for Mengo virus particles has a value of 76.3; that is, 1 ml of a solution containing 10 mg of virus has an absorbance at 260 m $\mu$  of 76.3 (Chapter 3).

Now, 10 mg virus =  $\frac{10^{-2}}{1.38 \times 10^{-17}} = 7.25 \times 10^{14}$  particles.

And, the concentrations of infectious virus which would give an absorbance of 76.3 at 260 m $\mu$  are: L-Mengo,  $2.1 \times 10^{10}$  pfu/ml; M-Mengo,  $9.5 \times 10^{11}$  pfu/ml; and S-Mengo,  $6.4 \times 10^{11}$  pfu/ml (from Figure 4.10).

Therefore, the total:infectious particle ratios for the Mengo variants are:

$$\text{L-Mengo} = \frac{7.25 \times 10^{14}}{2.1 \times 10^{10}} = 3450$$

$$\text{M-Mengo} = \frac{7.25 \times 10^{14}}{9.5 \times 10^{11}} = 76$$

$$\text{S-Mengo} = \frac{7.25 \times 10^{14}}{6.4 \times 10^{11}} = 113$$





**B29907**